A Trial of Quantified Evaluation According to the Style Characteristics of Historical Artifacts

Through the Form Analysis of Wood Carving of Shrine and Temple
February 2021

WANG   JIAN

Graduate School of Engineering

CHIBA UNIVERSITY

A Trial of Quantified Evaluation According to the Style Characteristics of Historical Artifacts

Through the Form Analysis of Wood Carving of Shrine and Temple
February 2021

WANG　JIAN

Graduate School of Engineering

CHIBA UNIVERSITY

CONTENTS

Chapter 1
Introduction

Chapter 1. Introduction

1.1 Background

1.1.1 Wood Carving in Edo Period

Wood carving Decoration is considered as an important part of Japanese architecture in Edo Period [1]. Since the Azuchi-Momoyama period, the number of shrines, temples, palaces, and other architectures decorated with wood sculptures has increased. In the early Edo period, the Tokugawa Shogunate(徳川幕府) started a series of construction activities of temples in the Kanto region, such as Nikko Toshogu Shrine(日光東照宮), Kunozan Toshogu Shrine（久能山東照宮）, and Rinnoji Daiyuin（輪王寺大猷院）. The need for the wood carving of architectural decoration increased with these construction activities, and the elaborate wood carvings became one of the main features of Edo-era architecture. As the Shogunate entrusted the construction and restoration of the temples and shrines to the construction groups of the Edo region, the carvers(彫物大工) have also branched out from the traditional construction worker as a special type to produce wood decorations in the architectures and gradually diverged into different styles [2]. In the middle of the Edo period, the number of the carving styles and sculptors increased, and wood carvings became widespread in the local temples, houses, and other buildings in the countryside [3]. Even today, a large number of beautiful wood carvings from the Edo period remain in the shrines and temples in the Kanto region.

Over the past four years, observation of sculptural forms, 3D digital model collection, and style analysis of Edo-period wood carving decorations in various shrine and temples in Chiba Prefecture have been conducted by the collaborative investigation with Design Culture Laboratory. Through these investigations, the research value of clarifying the excellence of these wood sculptures of temples and shrines and the style design knowledge hidden in the sculptures was convinced.

The research target of this study focuses on the wood carvings of Takeshi Ihachiro Nobuyoshi (武志伊八郎信由) and Goto Rihei Tachibana Yoshimitsu (後藤利兵衛橘義光), two famous carvers who were active in the Kanto region and mainly in Chiba Prefecture, during the mid to late Edo period. They were well known for their wood carvings with high perfection, and their works were widely spread in the Chiba and Kanto regions. Takeshi Ihachi was best known for his dynamic sculptures of waves, which could be easily distinguished from the wave carvings of other sculptors [4]. Goto Yoshimitsu belonged to the Edo Goto style (江戸後藤流) and was best known for his exquisitely detailed wood carvings of dragons [5]. According to the observation of the wood carvings, the previous research, and the opinions of relevant experts, it is confirmed that although the masters of these two great carvers belonged to the same Murai Style and they were active in a similar time of the Edo period, there are apparent differences in the style characteristics of their works.

Studies on the carvings of Ihachi and Yoshimitsu have tended to be carried out separately for each carver. Because of the strong regional character of the objects they carved, there have been few studies that have attempted to compare them objectively and compare the characteristics of their forms. Furthermore, most of the previous research on the works of the two carvers focuses on the relevant period background, the semantic meaning represented by the shapes and the cultural or religious connotations, and the style analysis of the wood carvings focused on the categorization of the Theory of Style(様式論).

1.1.2 Proliferation of carvers and popularization of wood carving

Carve(彫物大工) is also known as the wood sculptor (彫刻師), or woodcarver(木彫師). The term "彫物大工" was first used in a record in 1636 in the "Catalogue of the Records of Nikkosan Toshogu Daigonken (日光山東照大権原様御造営目録)"[6]. Before 1636, the names of carvers were usually recorded in the category of the Great Buddha

Group (大仏組)，leaded by the Buddhist carving masters. After the construction of Nikkosan Toshogu, the carvers of the Kanto region called Takamatsu Style (高松家，the successors of Murai Style(村井家))and the Izumi Style(和泉家), took turns as the leader of professional carvers (彫物大工棟梁) working for the Shogunate in the Edo period, in charge of the production and repair of wood carving decorations in Tokugawa relic temples and shrines. According to the Tokyo Museum collection of " Master-Apprentice Relationship of Takeshi Family and Goto Family(彫工左氏後藤氏世系図)" organized by Ito Ryuichi[6], the Waizumi Style has been concentrated in the construction activities of the Shogunate. At the same time, Takamatsu Style and Shimamura Style(島村家，a branch of the Murai Style) began to expand the number of disciples from the middle of the Edo period. A part of the members of Takamatsu Style differentiated into the Goto(後藤家), Ishikawa（石川家）, Komatsu（小松家）and other styles that were very active in the late Edo period. The carvers of these styles were not only involved in the Shogunate's construction projects but also expanded their business to the other areas of the Kanto region, such as Chiba, Saitama, and Kanagawa. The local people of these areas raised money through donations and entrusted carvers to create wood carving decorations for the local temples and shrines and the religious ritual objects such as Dashi(山車) and Mikoshi（神輿）．As a result, the wood carving decorations were no longer simply a symbol of the power and wealth of the Shogunate but also became a part of the regional cultural facilities that served the people for worship and entertainment.

Among the great carvers of the Kanto region who were active during the middle and late Edo period, the first Takashi Ichihachiro Nobuyoshi and the first Goto Rihei Tachibana Yoshimitsu are considered to be the most famous carvers in Chiba Prefecture. Even these days, the two carvers' works are still popular in Chiba Prefecture. There are not only research and exhibition of their wood carvings in the

local museums but also local fan associations such as 'Ihachi-kai(伊八会)' and '彫工の里・千倉会'. The works of the two sculptors have become the important cultural relics of Chiba Prefecture.

1.1.3 Background of Ihachiro and Yoshimitsu

The sculptural styles of Takeshi Ihachi and Goto Yoshimitsu were influenced by the Shimamura and Goto style when they were under the training of carving as the disciples. Therefore, it is necessary to clarify their affiliation and career history in the genealogy of Edo-era Kanto sculptors to understand and analyze their sculptural styles. According to the " Master-Apprentice Relationship of Takeshi Family and Goto Family ", their positions are shown in Figure 1-1.

左甚五郎
左乗吉
乗顕
乗俊
正俊
俊元

村井家　島村家

和泉家

高松家
邦教

石川家　小沢家　根本家　竹井家

後藤家　徳章　頼直
邦教門人　正網　頼品
名人ナリ　徳章門人　正常
正網次男　正響
小松家　正常門人　正網
名人ナリ　正響門人　常俊
正網門人

義光
常俊門人

圓哲
俊元男
俊実
圓哲門人
貞亮
俊実門人

信由
貞亮門人
名人ナリ

武志家
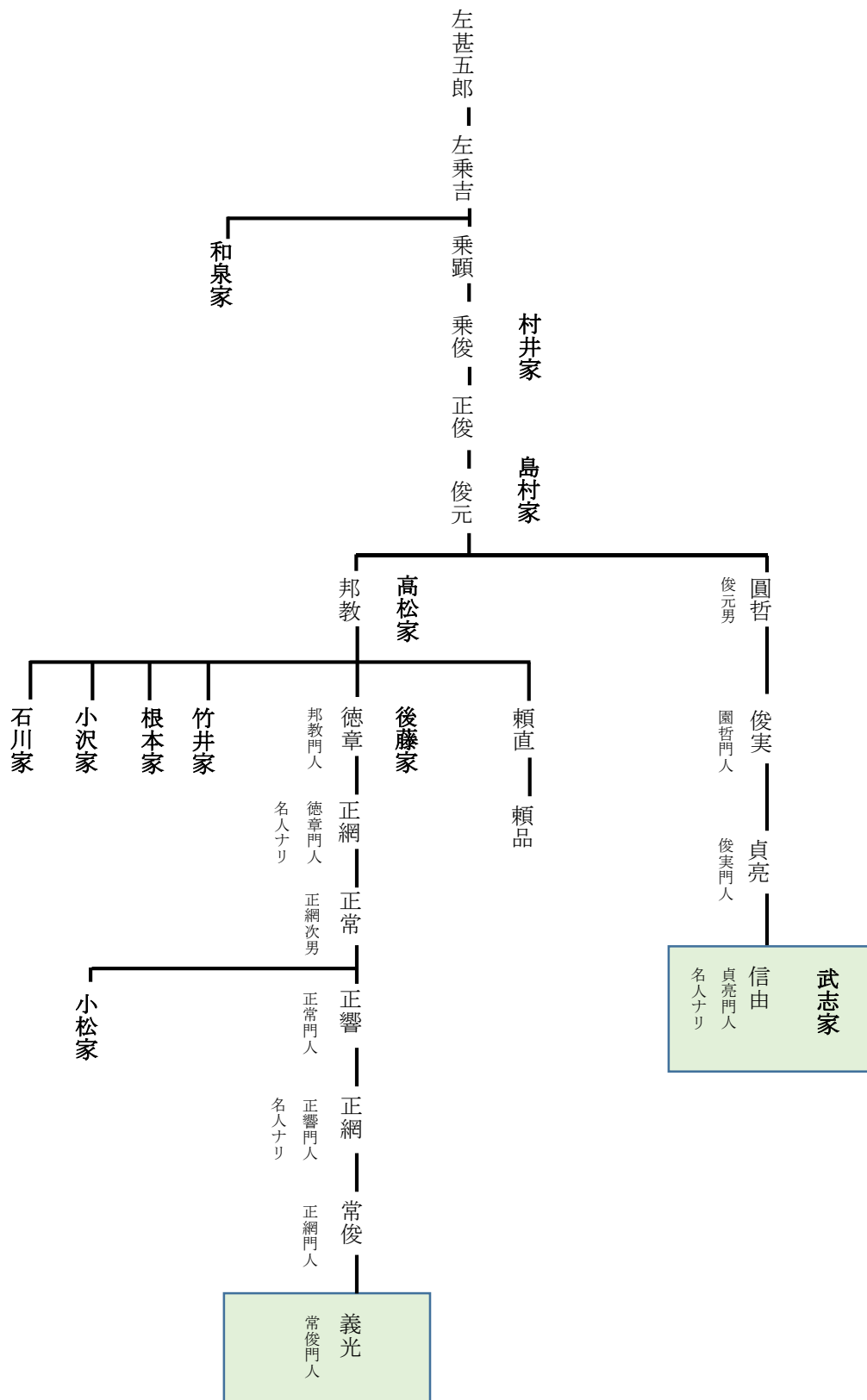
Figure 1-1. Master-Apprentice Relationship of Takeshi Family and Goto Family

Figure 1-2. Ihachi's Wave Sculpture

Figure 1-3. Yoshimitsu's Dragon Sculpture

Background of Takeshi Ihachi

Takeshi Ichihachiro Nobuyuki (1751 - 1824) was born in Shimoutsumi Village, Nagasaka-gun, Awanokuni (安房国長狭郡下打墨村) (Utsumi, Kamogawa-shi, Chiba), and followed carver Shimamura Ryuemon Sadao(島村右衛門貞亮) from Uenuki-mura, Eisumi-gun, Kazusanokuni (上総国夷隅郡植野村) in his 10s. At the age of 23, he started his career as a carver sculpting the wood decorations in the ancestral hall of Kyoninji Temple (鏡忍寺) (Kamogawa City, Chiba Prefecture). As his carving technique matured, he became famous for his unique wave forms and waves combined various subjects such as dragons, cranes, rhinoceroses, rabbits, and jewels to create a unique style. According to the comments in previous research, the evaluation of the uniqueness of Ihachi's wave sculptures is mainly attributed to the fact that although waves are difficult to depict due to their ever-changing forms, Takeshi Ihachi succeeded in capturing the "transient form" and "dynamic sense of change" of the waves（Figure 1-2）, and expressed his unique style of wave modeling[7]. His wave relief located in Gyoganji (行元寺)(Izumi City, Chiba Prefecture) is considered to be the original reference that inspired Katsushika Hokusai to create his famous painting "Kanagawaokinamiura(神奈川沖浪裏)".

Background of Goto Yoshimitsu

Goto Riheie Tachibana Yoshimitsu (1815-1902) was born in Kita Asayi Village,

Asayi-gun, Awanokuni(安房国朝夷郡北朝夷村) (Kitaasayi,Chikura-machi, Minamibousou-shi, Chiba), and his father was also a carver. In 1837, he went to Edo and became a disciple of the Goto Style sculpting master, Tsunetoshi (常俊), and inherited the Goto surname later. Even though he and Ihachi were both called the "three craftsmen of the Awa"[8], there are fewer early studies on Yoshimitsu Goto than Ihachi. According to the comments of current wooden sculptures and sculptors, Yoshimitsu's works reveal his solid basic sculptural skills and artistic accomplishment. In some commentaries on Japanese architectural history and sculpture, it has been pointed out that most of the decorative wooden sculptures of the Edo period were based on a single range of materials and expressions and lacked a sense of whimsy and human expression[9]. Compared to the creative wave forms in the works of Ihachi Takeshi, the works of Yoshimitsu may appear to follow more traditional and conservative themes and compositions, which may be one of the reasons why his influence is slightly lower than that of Ihachi Takeshi. However, for sculptural technique, Yoshimitsu's works, which inherited the Goto Style from the late Edo period to the early Meiji period, are highly finished with a full range of overall shapes and a large amount of sufficient detail (Figure 1-3). It fully reflects the evolution of architectural wood carvings from the flat, shallow relief style of the Azuchi-Momoyama period to a three-dimensional sculptural style with a sense of real volume.

In art creation and design, "innovation" and "tradition" are two topics that seem to be contradictory yet always being discussed. In the eyes of the general public, "innovation" with unconventional ideas and styles could often attract more attention. However, for professional designers involved in creative and design activities for years, "innovation" is always a challenging task, and imitating "tradition" is usually the first thing most newcomers need to do at the initial stage. In an interview with Casper Konefal, a Senior Concept Artist at Bioware two years ago, he talked about

the "innovation" in concept design cautiously: "Most of the "innovation" is processed little by little, and depends on years of repetition and exploration of existing themes by the designer or artist. A solid foundation in painting and sculpting skills and a good understanding of anatomy, mechanical design, and other related fields are the necessary soil for "innovation". While we marvel at the unconventional concept designs on Artstation, we actually didn't know how many failed attempts at innovation they have destroyed behind the scenes. And if we carefully analyzed these designs, it could be found many elements of past classical design" The different appeal of Ihachi Takeshi's and Yoshimitsu Goto's work seems to echo this statement. Takeshi Ihachi's sculptures demonstrate, which is more intuitive and easy to understand. Still, this innovation could not be achieved his studies on Shimamura's sculpting skills and years of careful observation and consideration of the waves, animals and other natural objects. Goto Yoshimitsu, on the other hand, is more inclined to the innovation of sculptural techniques for Japanese wood carvings, based on the full understanding and mastery of the traditional skills of the previous generation. His "innovation" focused on the sculpting technique to enhance the feeling of mass and volume in traditional relief sculptures. When we read about art history, we sometimes take for granted the distinction between different periods of art styles in a disjunctive manner, such as "Hellenistic sculpture" or "Roman sculpture". However, in the actual development and transformation of art, there is often no clear-cut in the evolution of the art style, and stylistic innovation is often a slow and gradual process that takes over several generations. This kind of innovation is even slower and often not perceived or understood by the average viewer. Still, this challenging improvement may have been one of the driving forces behind the gradual evolution of traditional Japanese architectural wood sculpture from 2D flatness to truly three-dimensional feeling. This tendency for Takeshi Ihachi and Goto

Yoshimitsu to differ in their representational approaches may also reflect the value of studying the comparative styles of the two sculptors' works.

1.2 Methods in the Previous Research

In previous studies of Japanese architecture, wood carvings for decorations, also known as Miyabori(宮彫り), were often described as an accessory to the architecture. While in most of the art history of Japanese sculpture, the study of Buddhist statues occupies a more predominant role. Therefore the research of wood carvings for architectural decoration is naturally influenced by analysis methods of Buddhist art. Among the previous research on wooden architectural sculpture in the Kanto region in the Edo period, three types of research are representative: a study of the genealogy and background of the groups of carvers, a method of categorizing and documenting the stylistic features of wooden sculpture, and a pictorial research method of interpreting the religious and cultural meanings represented in wooden sculpture.

Among these research methods, the genealogical arrangement of the carver in history helps to clarify the relationship between the carving styles. It provides essential reference information to grasp the changing of architectural wood carving styles and the historical environmental factors behind them. The other two research methods are also the main research methods in the study of Buddhist art. The theory of style is a method to create a database by classifying the themes and the main components of the sculptures. The researchers could estimate the author and the date of the sculpture and identify the anonymous artifacts by discussing the similarities of the style characteristics in the sculpture according to the database. For example, for an anonymous dragon relief to be identified, we could take photos to record the style features like the shapes of the eyes, nose, whiskers, horns, scales, claws, tail and pearls. Then the similarities between these features with author-identified dragon

reliefs were compared. After collecting and analyzing information on a considerable amount of sculptural objects with this method, a database with catalogs of style features belonging to different sculpting styles could be established. And the other method called iconography tends to rely on information from canonical documents related to the theme of the sculpture or the historical context that could explain the religious meaning of the sculpture. For example, based on old geographic histories and historical records of the village, the researcher could found the belief in the dragon gods of the Boso region and the Tsunami disaster from the Pacific Ocean could be the motives to build the dragon and wave status. In some study of the conservation and restoration of cultural artifacts, methods of the theory of style and iconography were also used to analyze the background of the sculpting styles and the sculptors.

In this research, the variation of the styles of wave relief in the Edo period according to the theory of style were simply cataloged. Then the basic concepts of computer graphics in 3D scanning digital models and style design principles to extract and analyze the relationship between the three-dimensional composition of the basic stylistic elements were used. The style characteristics of wood carvings and compared the difference between the two carvers' works were visualized and quantify. The aim of this research is to provide technical support for the preservation, restoration, and identification of traditional wood carvings.

1.3 Thesis Structure

Chapter 1: This chapter briefly introduced the background of Takeshi Ihachi and Goto Yoshimitsu, their place in the genealogy of Edo carving styles, and the two sculptors' representative works. Briefly summarized the analysis methods used in the previous research and this study.

Chapter 2: This chapter provided the background description of the two groups of four sculptures and the reports of the direct observations on the sculptures. Combined with the observation, the evolution of the sculptural techniques of waves and dragons in the Edo period was reviewed.

Chapter 3: This chapter briefly explains the style design process of simplying complex natural forms into polyhedral to the primary 3-dimensional composition of the form. According to this process, style characteristics of the sculptures were extracted from the 3D scanned digital models of Ihachi and Yoshimitsu's wood carvings.

Chapter 4: This chapter explained the similarity in the forms of the wood carving in the rough carving period and the low-resolution polygon model of the wood carving. A method was approached for visualizing and quantifying the orientations of all polygons of the sculptural form by mapping the facet normal vectors of the polygons to a unit sphere and plotting the density of the endpoints of the vectors in the color spectrum.

Chapter 5: In this chapter, the surface orientation distribution of 2 groups of sculptures using the method of normal vector unit spheres approached in chapter 4 were visualized and quantitatively evaluated. The results were validated by the dendrogram clustering to the endpoints of facet normal vectors on the unit sphere.

Chapter 6: According to the conclusions of the observations in Chapters 2 and 3 and the results of the quantitative assessment in Chapter 5, this chapter discussed how the orientations of the surfaces on the sculpture might affect the mass and volume of the form and the reasons for the differences in the face distribution in the models of Takeshi Ihachi and Goto Yoshimitsu.

Chapter 7: This chapter described the conclusions of the studies.

Reference:

1. 伊藤延男，文化庁講座　日本の建築 4　近世 I，第一法規出版株式会社，1973，230-233

2. 伊東龍一，関東の彫物大工の系譜と幕府彫物大工棟梁高松家，日本建築学会計画系論文報告集，420，1991.2，71-72

3. 伊東龍一，「彫物大工の活動と工夫、彫物の未来」（若林純，　社寺の装飾彫刻　関東編・下の序言，　日貿出版社，2015，5）

4. 片岡栄，名工波の伊八、そして北斎，文芸社，2016，185

5. 稲垣祥三：南総の彫工初代後藤義光 2，コアブックス，3－5，2013.11

6. 大河直躬，東照宮，鹿島研究所出版会，1970，83－85

7. 片岡栄，名工波の伊八、そして北斎，文芸社，2016，185

8. 佐藤輝夫：彫刻師 後藤利兵衛橘義光，館山市文化財保護協会会報 7・8 号

9. 伊藤延男，文化庁講座　日本の建築 4　近世 I，第一法規出版株式会社，1973，240

Chapter 2

Direct Observation of Wood Carvings

Chapter 2. Direct Observation of Wood Carvings

From 2016 to 2020, a series of observations, 3d form measurements and collections of architectural wood carvings of Takeshi Ihachi and Goto Yoshimitsu preserved in Chiba and Kanagawa prefectures were conducted. Morphological analysis to the wood carvings were applied according to the comments of the researchers specializing in art history and active sculptors' intuitive impressions of the sculpture. Based on the results of 3d scanning data and direct observation, two groups of wood carvings were selected to analyze the main style characteristics and style differences in the sculptures of Takeshi Ihachi and Goto Yoshimitsu, as well as the similarities between different works of the same sculptor.

The two groups include:

(1) The wave shape in the sculpture "Tenryu and Chiryu(天龍と地龍)" (by Takeshi Ihachi) pent roof of Fudoudo hall（不動堂）, Oyama-ji Temple（大山寺）, and the center of the sculpture "Hyakutai no Ryu(百態の龍)" (by Yoshimitsu Goto) on the ceiling of the worship hall(拝殿) of Tsuruya Hachimangu（鶴谷八幡宮）.

(2) The heads of the Kibana lions（木鼻獅子） of Fudouido, Oyama-ji Temple (by Takeshi Ihachi) and in the main shrine of Zenrin-ji Temple（禅林寺）(Yoshimitsu Goto).

2.1 Dragons of sky and earth in Fudodo Oyamaji.

Figure 2-1. Dragons of sky and earth

The Fudodo hall of Oyamaji Temple, located on Mount Takakura(高倉山) near the suburbs of Kamogawa City, is presumed to be built in the late Edo period (1802). According to the inscription on the reverse side of the wood carving on the pent roof, the wood carvings of Fudoudo hall were completed in 1803. The Fudoudo Hall of Oyama-ji Temple was influenced by the tendency of heavy decoration on the temples and shrines in the Kanto region of the Edo period. The relief on the pent roof was named "Dragons of sky and earth(天龍と地龍, Figure 2-1). On both sides of the earth dragon are the wave carvings, which are Ihachi's representative sculptures.
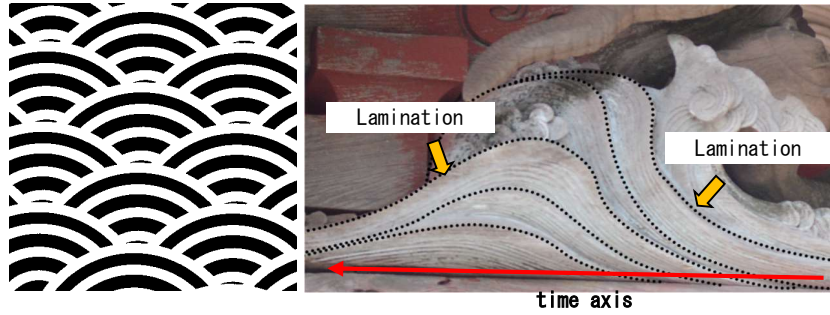
Figure 2-2. Painting of Dragon face

Figure 2-3. Seigaiha Pattern and the wave form

The forms of the dragon and wave are expressed in a cartoon-like style. This cartoonish expression is due to Ihachi's consideration of emphasizing the basic characteristics of the dragon and waves and exaggeratedly reconstructing them. Ihachi's exaggeration is similar to the expression in traditional Japanese and Chinese paintings of dragons (Figure. 2-2). The forehead, eyeballs, and other parts of the dragon's face are consciously enlarged and protruded. The shape of the waves has been simplified into a shape similar to the traditional pattern of "Seigaiha(青海波)" (Figure. 2-3). The body of the dragon tends to omit the dynamic transformation of the muscles with the movement of the body. The basic shape of the dragon's body becomes flat and tubular, which emphasizes the contour lines of the body. As a result, the contours are easy to read, and the fluidity of the curves is emphasized. But the realistic three-dimensional representation of the dragon's body as a living creature, especially its tail, is missing, which makes the form in a two-dimensional expression.

Also, the waves show a tendency of lamination in form. The thick, plate-like waves proceed along the right and left directions on both sides of the dragon's body. Multiple wave layers were arranged along the right to left direction, which represents the time axis of the movement of the wave. By the movement of the viewer's sight along the time axis, the temporal change of the waves was expressed by the lamination of the layers. This wave form with the hidden time axis is an original expression that doesn't

Figure. 2-4 Wave form in the early Edo period Nikko Toshogu Shrine (left), Naritasan Shinkakuji

Figure 2-5.　Spoondrift painting

exist in the work of Takeshi Ihachi's master or the other carvers of the same period in the Kanto area.

2.2 Evaluation of the sculptural techniques of wave reliefs

The shallow reliefs in the Momoyama period were considered to be a 3-dimensional transformation of the paintings used to decorate the interior of the architecture since the Kamakura period. For example, the themes and patterns of architectural carvings in the Momoyama and early Edo periods were similar to those of screen paintings of the same period. The maturation of the techniques of "Taka niku carving(高肉彫り)" in goldsmith carving and "maru carving（丸彫り）" in stone

and wood carving since the Momoyama period is one of the reasons why architectural decorations were transformed from 2D to 2.5D and even to 3D.

The change from 2D to 2.5D and even to 3D can also be seen in the wave reliefs. Reliefs in Figure 4 are the relief decoration "flying dragon on the wave(波に飛龍)" of Nikko Toshogu Shrine, which was built in the early Edo period, and the relief of wave and dragons in Shinsyoji Temple(新勝寺) of Naritasan(成田山)(Figure. 2-4). The wave form in the early Edo period was close to a combination of multiple slender bands that emphasize the shape of the curves in the waves, and the spoon drifts in realistic style as the detailed parts could also be observed in the wave form. Since the form of the wave was flat, the carver used blue paint on the background and white/gold paint to trace the contour lines of the wave. The colorful paints enhanced the 3D visual effect of relief, but also makes the wave carvings of this period still have strong characteristics of the 2D painting. According to the historical records, during the construction of Nikko Toshogu Shrine, painters of Kano Style(狩野派), including Kano Tanuki(狩野探幽), participated in the production of decoration sculptures and provided 2D drawings for the sculptures as a reference. Thus, wave carvings of this period still have expression methods similar to the wave paintings and patterns.

Among the paintings and patterns of waves in the Japanese Middle Ages, there are two general types of wave shapes: the abstract pattern "Seigaiha" with semi-circular curves, and the wave-crest patterns in a relatively realistic style (Figure 2-5). The origin of the name of " Seigaiha " was derived from the Gagaku(雅楽). According to the records of "Kenreimonen Ukyou no Daibusyu(建礼門院右京大夫集)", Tairano Koremori(平維盛) and Fujiwara Tsunemune(藤原経宗) performed the dance of the

Figure 2-6. Wave Relief of Shimamura Entetsu

Gagaku Seigaiha in front of the hall of Hokkeji Temple(法華寺). Then the wave pattern with multiple semi-circular was named Seigaiha, because it resembles the vibration of the robe and sleeves of the dancer like the surging waves [2].

In the wave relief sculptures made by Shimamura Entetsu(島村圓鉄) from the mid-Edo period, it could be found that a form of the lamination of multiple semi-circular, which is similar to the pattern Seigaiha has gradually appeared in the wave reliefs. However, at this time, the three-dimensionality of the reliefs was still relatively weak and needed to be reinforced with lacquer (Figure. 2-6).

For Takeshi Ihachi, the expression of the waves has been further developed. By comparing Ihachi's wave forms in different periods, it was confirmed that the evolution of this expression was a gradual and continuous process of exploration. In the early 20th generation of Ihachi's works, such as the reliefs of Kyoninji(鏡忍寺) and Atago Shrine(愛宕神社) (Figure 7), the wave form was similar to the Style of

Figure 2-7.   Wave Form in Ihachi's 20s

Figure 2-8.   Wave Form in Ihachi's 30s

Figure 2-9.   Wave Form in Ihachi's 40s‐50s

Shimamura Entetsu, consisting of multiple curved slender bands and spoon drifts. In the works of his 30s, such as the reliefs in the Main Hall（本殿）of Shinganji Temple(心厳寺) and the Main Hall of Chofukuji Temple(長福寺) (Fig. 2-8), the slender bands turned into the laminating semi-circles of pattern Seigaiha, and the thickness of the waves gradually increased from the original shallow relief into the 2.5D forms with thickness and actual volume. The amount of geometric curved

Figure 2-10. Central Part of "Dragons in a Hundrad Styles"

grooves on the wave also increased. In the reliefs made after his mid-40s, such as the "Dragon on the wave(波に龍)" of Chizoji(智蔵寺) and the private collection "Rhino on the wave(波に犀)" (Figure. 2-9), the density of the curved grooves increased further. But the thickness of the shape became shallow, and the details of the spoon drifts appeared again. The overall composition of the relief became graphical, with a good visual perspective depth in the front view of the relief.

2.3 Dragon in a hundred styles Relief in Tsuruya Hachimangu

Tsurutani Hachimangu Shrine is considered to be the main shrine of the ancient Awa Shrine, and the main hall was built in 1721 and destroyed by the fire in the 1850s. The restoration of the shrine in the Bunkyu era (1861-1864). During the restoration, people raised the money and commissioned the local carver Goto Yoshimitsu to create a group of woodcarving dragons on the ceiling in 1866, named "Dragons in

a hundred styles(百態の龍)."

The group of woodcarving dragons consists of a large relief of a curly dragon(団龍) in the ceiling's center (Figure. 2-10), surrounded by 54 small dragon reliefs. Due to the different degrees of completion of the small dragon reliefs, they were possibly made by the other carvers in Yoshimitsu's workshop.

In Yoshimitsu's dragon sculptures, a rigorous attitude in pursuit of a high level of perfection in his work and a steady sculpting ability due to training under the tutelage of Goto Style sculptors could be observed. From the static tension in these sculptures, we could observe Yoshimitsu's skillful depiction of the dragon's face and the muscles with the movement of the body. Even though it is a relief, the work has a strong three-dimensional visual effect of the mass in the sculpture.

2.4 Evolution of the mass and volume in the Relief

As mentioned in section 2.2, the mass of the wood carvings changed from shallow relief carvings to the real three-dimensional shapes with the development of the sculpting skills during the Momoyama and Edo periods. In the early Edo period, the manufacture of the dragon reliefs, such as the "Dragon on the wave" of the Nikko

Figure 2-11. Dragon Relief of Nikkotoushogu

Figure 2-12. Dragon Relief of Nishikano Shrine

Figure 2-13. The form of dragon's rolling Tail

Toshogu Shrine (Figure 2-11), usually followed the "Yosegi Zukuri" technique [4].

The carver used multiple thin wood panels to create the individual parts of the sculpture and then matching them together with the background layer. Therefore, the carving of the dragons in this period usually only produced the external outline. Details such as the undulating muscles and scales were simplified or omitted. The carver would use lacquer in different colors to paint out the details, just like the method applied to the wave carvings to enhance the visual three-dimensionality of the relief.

By the late Edo period, carving techniques of Goto Style had matured to naturally depict the muscular changes of the dragon due to the distortion of its body. In the reliefs of the early Edo period, the dragon's body appears to be thin and flat. While with the development of the carving techniques, in Yoshimitsu's works such as the relief of Tsuruya Hachimangu and the Nishikana Shrine(西叶神社) (Figure. 2-12), the body of the dragon has a realistic mass and volume. In particular, the dragon's coiled tail enhanced the three-dimensional effect of the relief by its real volume and the way it extends out from the edge of the square composition of the relief. According to the field survey, this tail shape repeatedly appeared in Yoshimitsu's multiple works as a representative form. (Figure 2-13)

Figure 2-14. Kibana Lion of Fudodo Oyamaji

2.5 Kibana Lion of Fudodo Oyamaji by Ihachi

The wooden Kibana lion and the wooden Kibana elephant are decorated on the left and right side of the sculpture "Dragons of Sky and Earth" in Fudodo Hall of Oyamaji, which were both made by Ihachi Takeshi. The shape of the Kibana lion tends to be flattened in the forehead, cheeks, and mouth area. The transition between the front view and the side view is relatively rigid, which makes the overall shape of the head in a hexagonal cubic shape. The outline of the lion's mouth, the edges of the eyebrows and eyes, and the jawline's edge are close to geometrical curves (Figure. 2-14). This method of simplifying the organic shapes into geometric curves could also be found in the contour lines of Ihachi's wave reliefs.

Figure 2-15. Kibana Lion of Zenrinji

2.6 Kibana Lion of Zenrinji by Yoshimitsu

Zenrinji Temple(禅林寺)is located in Yokohama. The wood carvings on the pent roof and the kibana decorations are considered to be created in Kae Period (1848-1855). The overall shape of this Kibana is more rounded (Figure 2-15), with a more curved forehead, cheeks, and forearm shape that tends to emphasize the volume of the lion's muscles. Compared to Ihachi Takeshi, the transition between primary surfaces is more rounded and soft, closer to the animal's natural form. The shape of the lion's hair shows a conscious expression of the dynamic sense of the hair flowing in the wind.

Reference

1. An architectural decoration. In Chinese and Japanese architecture, a decorative plate attached to the lower part of a gable with a metal or wooden plug, called a six-leaf, on either side of the lower part or inside the lower part of a gable to conceal the ends of the purlins and girders.

2. 高橋昌明，別冊太陽　平清盛（源氏物語と平家のひとびと），平凡社，2011

3. 伊東龍一，彫物大工の活動と工夫、彫物の未来（若林純，社寺の装飾彫刻・関東編下），日貿出版社，2015,8

4. Yosegi Zukiri is a method of piecing together several pieces of wood to create a sculptural form.

Chapter 3

Abstracting Style Characteristics from Polygon Models

Chapter 3. Abstracting Style Characteristics from Polygon Models

3.1 Composition of Geometrical Features in the Style

According to the theory of composition in Western art, the silhouette and the composition of the geometrical features (such as sphere and cubic) is one of the
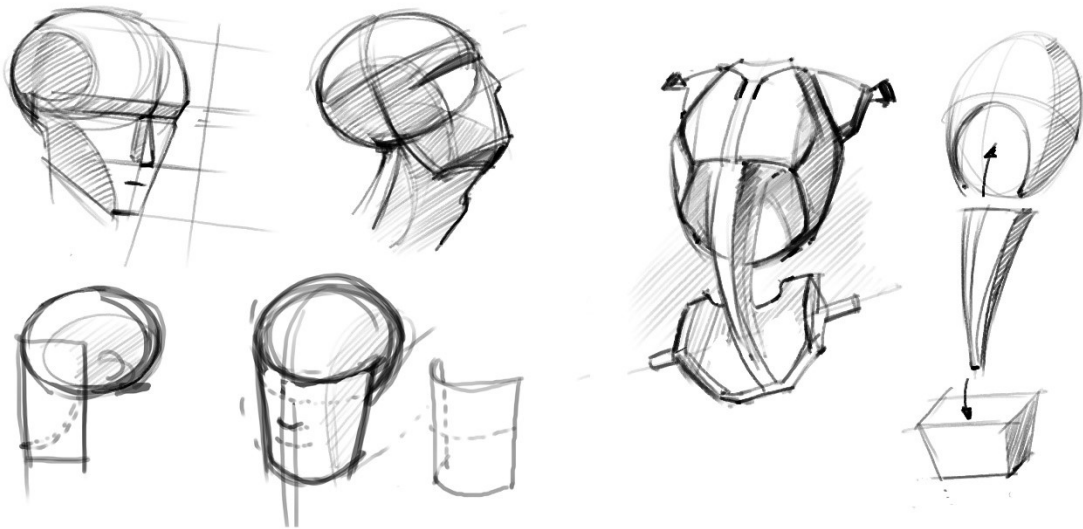

Figure 3-1. Abstract Composition of Human Body

important factors that influence the balance of a complex organic form. For the designers and artists, it is a common method to create the compositional relationship of the geometric features in the early stage of the work. It is a quick way to grasp and develop the initial form at the beginning of the design. I the study of the art anatomy, the human's head and body are usually abstracted into a combination of spheres and cubes to help beginners grasp the primary characteristics and the proportion of the shape of the body (Figure 31) [1]. In the early 20th century, artists like De Stijl, Piet Mondrian and Vassily Kandinsky also apply abstract geometric features in their artworks [2]. Till today, this concept of constructivism is commonly used in industrial product design and the concept art of film and games. The American concept artist
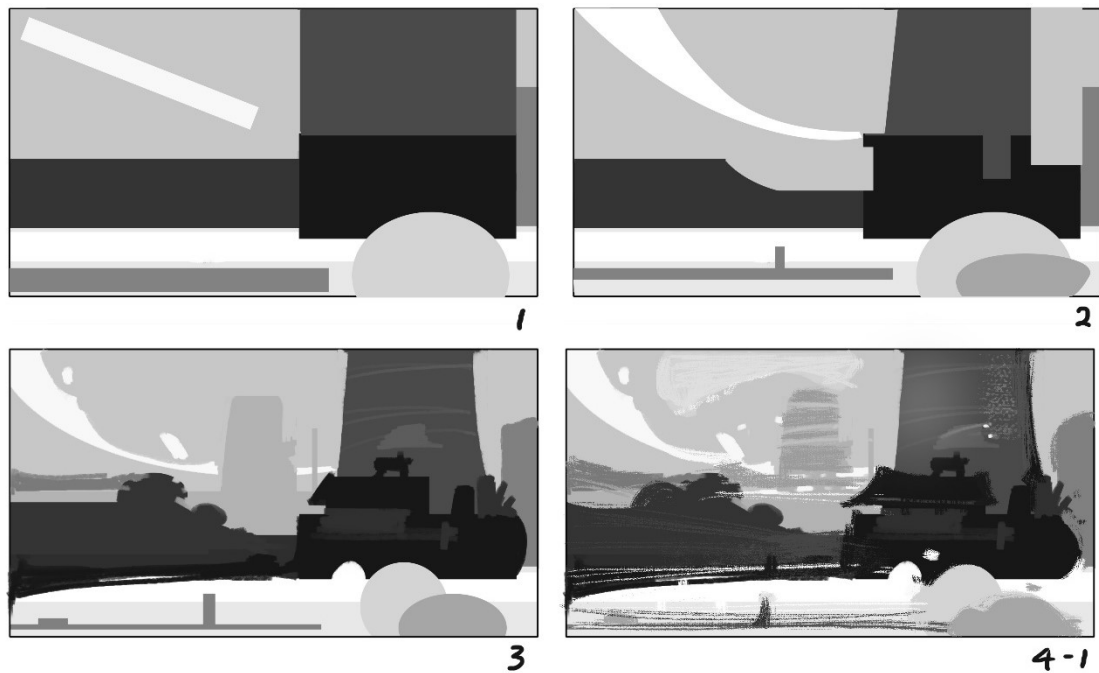
Figure 3-2. Abstract Composition of Thumbnails

Robuch Lafore referred to this concept as "the beauty of abstract reality" [3]. Figure 3-2-1 is the combination of the geometrical features that represent the composition of the illustration. Based on this composition, the painter could gradually break the silhouette and add the details to transform the geometrical composition into an illustration. But no matter how the details variate, the balance of the illustration is mainly determined by the geometrical composition.

In the case of temple and shrine wood carving, it is also important to extract multiple geometrical features from the form of the sculptures to interpret the "style" of the sculpture through the compositional relationships. In the Edo period, books and tools of western painting were imported with the development of the foreign trades, which influenced the workflow of Japanese painters and sculptors. In the "Early Guide to Sketching(略画早指南)", Katsushika Hokusai introduced the method of using a compass to draw the basic forms of the waves and lions (Figure 3-3).

Figure 3-3. Ryakuga Hayaoshie: Draw with compass

Besides, since the themes of the wood carvings mainly focused on the natural scenes, animals and historical or fantasy stories, the forms of the carvings usually consisted of a large number of organic surfaces and details. According to this complex

of the forms, it became generally difficult to evaluate the original form of the woodcarving quantitatively. Therefore, the concept of extracting the geometrical composition from the complex organic form was applied into the analysis method in this study.

Furthermore, CAD software's functions to detect geometrical features in the 3D form are mainly designed for the reverse engineering of industrial products, which have regular geometrical shapes that could be easily measured quantitively. But for the "Wave", "Dragon" and "Lion" woodcarvings, which were made by the chisels and human crafts, it became an challenge to leave the task of detecting the geometrical features entirely to the automatic calculation of the software. In detecting, it is necesseary to choose the type of geometrical features to be detected and the detecting areas on the 3D form. This process depends on the result of the direct observation and other geometrical elements, such as the curvature spectrum and the contour lines that could be automatically generated in the software as the reference to improve the accuracy.

3.2 Style Characteristics of Ihachi and Yoshimitsu's Sculptures

The 3D polygon models of Ihachi and Yoshimitsu's sculptures were created for the detecting analysis. Techniques for creating 3D forms from realistic objects have developed into various methods. Till now, the popular methods include laser scanning and photogrammetry. Laser scanning could provide an extremely high-resolution 3D form, but also requires the object to be scannable very closely and from almost 360° directions. In many cases, the carvings were placed in high positions in the temples and shrines that could not be separated from the architectures for the reason of preservation and frangibility. These conditions make it difficult to use a 3D scanning instrument for the measurement. Therefore, the original high-resolution 3D polygon mesh models were generated in Autodesk Remake from photographs taken from

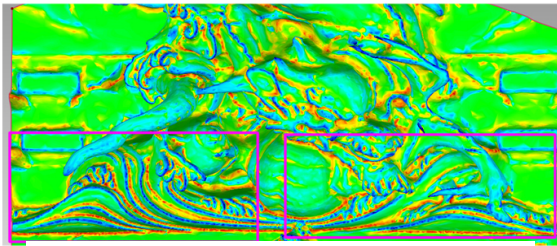different perspectives by digital cameras.
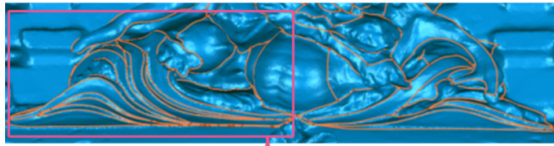

Figure 3-4. Curvature Map of Ihachi's wave

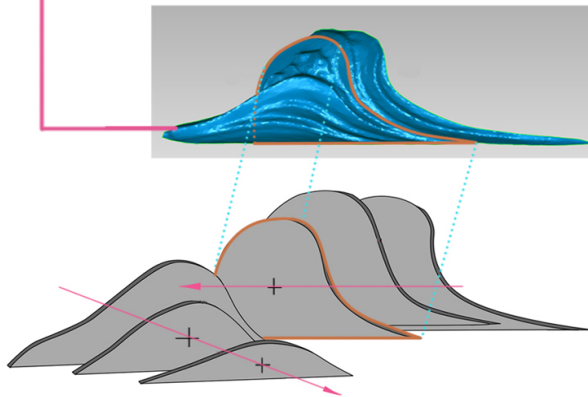Figure 3-6. Feature Lines of Wave

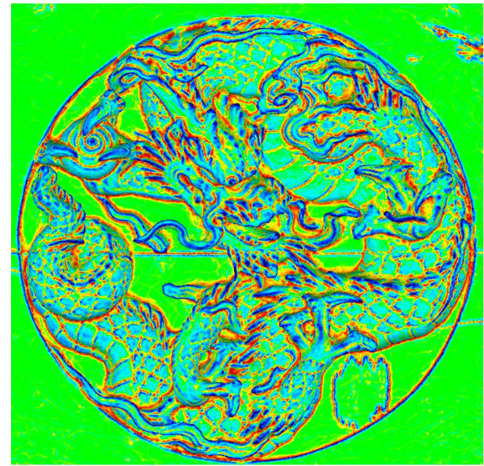Figure 3-7 Replacing the wave with Planes

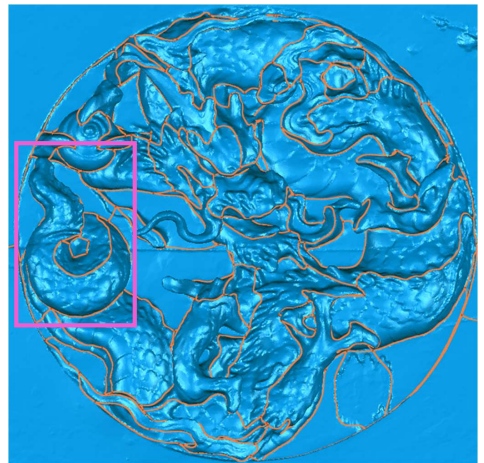Figure 3-5. Curvature Map of Dragon

Figure 3-8. Feature Lines of Dragon

In order to confirm the characteristics of the whole form intuitively, the curvature spectrum map (Figure. 3-4, Figure. 3-5) of the entire polygon mesh was created in Geomagic Studio [4], and the highly convex regions (blue regions) and highly concave regions with sharp valley-like edges and grooves (red regions) were detected. In the highly convex and concave area, curves were generated to represent the boundaries where the highest curvature exists in each form. The curvature spectrum maps and the high-curvature curves could be used as references to detect the geometrical features.

3.2.1 Curvature Spectrum and Feature lines of wave and dragon tail

(1) **High-Curvature Curves and Definition of Laminated Layers in "Ihachi Wave**
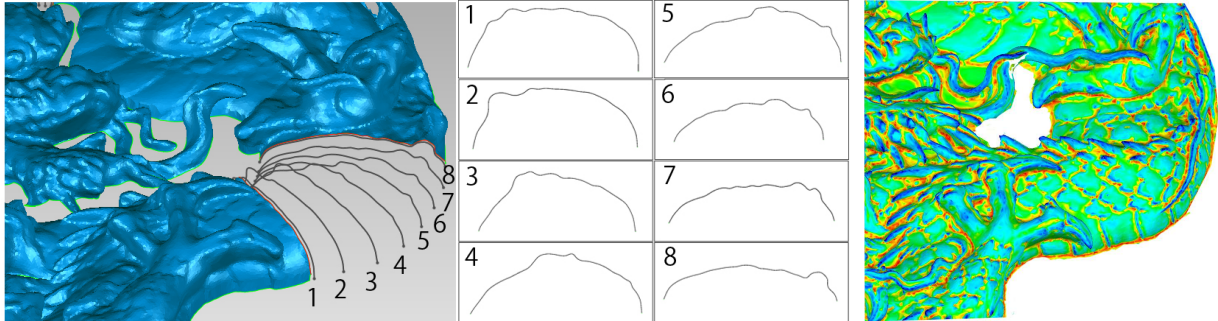

Figure 3-9. Cross Sections
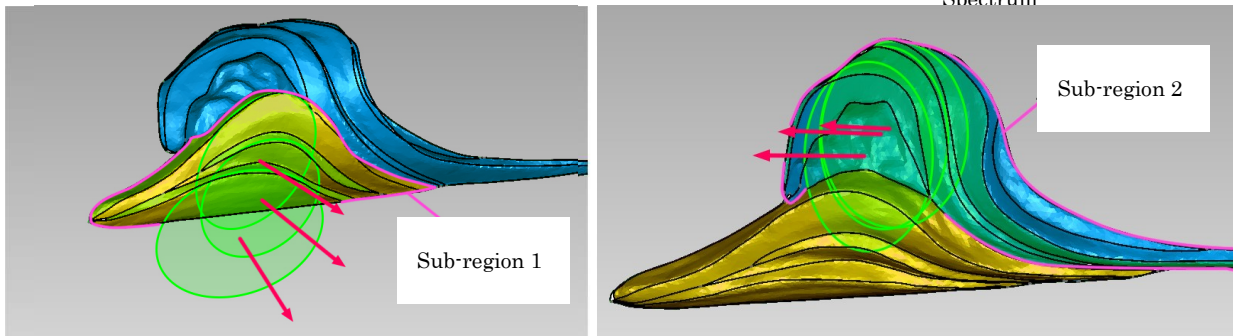

Figure 3-10. Curvature Spectrum

Figure 11. Orientations of Circle Features in the Wave Form

In the 3D form of "Dragons of sky and earth", the high-curvature curves were generated on the silhouette of the dragon placed in the center of the wood carving and the contour line and the curved grooves of the wave forms on the left and right sides by the dragon body (in the pink frame of Figure. 3-4). In the front view of this wave form (Figure 3-6), the combination of the contour lines is similar to a 2.5-dimensional wireframe of the wave. As mentioned in Chapter 2, this method of expressing the three-dimensional sense of the relief by layering waves can be understood as transforming a traditional Japanese pattern called Seigaiha into 2.5-dimensional relief. As the Seigaiha pattern could be divided into multiple semi-circles, it is possible to decompose Ihachi's wave form into a lamination of layers with the same thickness. Each of the layers is a flat plate in a similar wave-form silhouette, which could be

considered as being cut out along the high-curvature curves. This small flat plate was defined as a laminated layer and the "axis" that represents the normal direction of the laminated layers as the "lamination axis(Pink arrow in Figure 3-7)".

(2) **High-Curvature Curves of Yoshimitsu's Dragon Tail**

According to the conclusion of the observation in Chapter 2, the dragon's coiling tail in Yoshimitsu's "Dragons in a hundred styles" is a representative form that could be observed in Yoshimitsu's multiple reliefs (in the pink frame of Figure 3-5). In the curvature spectrum of the tail, a large amount of the high-curvature areas as the contour of the grooves could observed, which represent scales, distributed over the surfaces of the tail. But these high-curvature areas do not have the same strong influence on the overall shape as the edges and grooves in Ihachi's Wave. These high-curvature areas of the scale's grooves are different from the high-curvature curves generated from the tail's silhouettes (Orange curves in the pink frame, Figure 3-8), which might influence the primary shape of the tail.

In other words, the basic form of tail would not change even without these high-curvature areas of the scale grooves. But for Ihachi's wave form, the whole form will corrupt if any of the high-curvature curves were deleted. This difference in the influence of the high-curvature areas and curves indicates that the high-curvature curve is an essential element to define the shape of the surfaces in Ihachi's wave form, but for Yoshimitsu's dragon tail, the scale grooves are only the auxiliary curves to enhance the three-dimensional sense of the form.

We used planes to crosscut the form of the dragon's body to confirm how the curvature of the surface changes. According to the result in Figure 3-9, it could be notice that the cross-sections of the dragon's body appear to be in the arch shape. In the curvature spectrum of this area, most of the areas are in light blue (Figure 3-10), which indicates that the surface of the dragon body bends in nearly constant convex
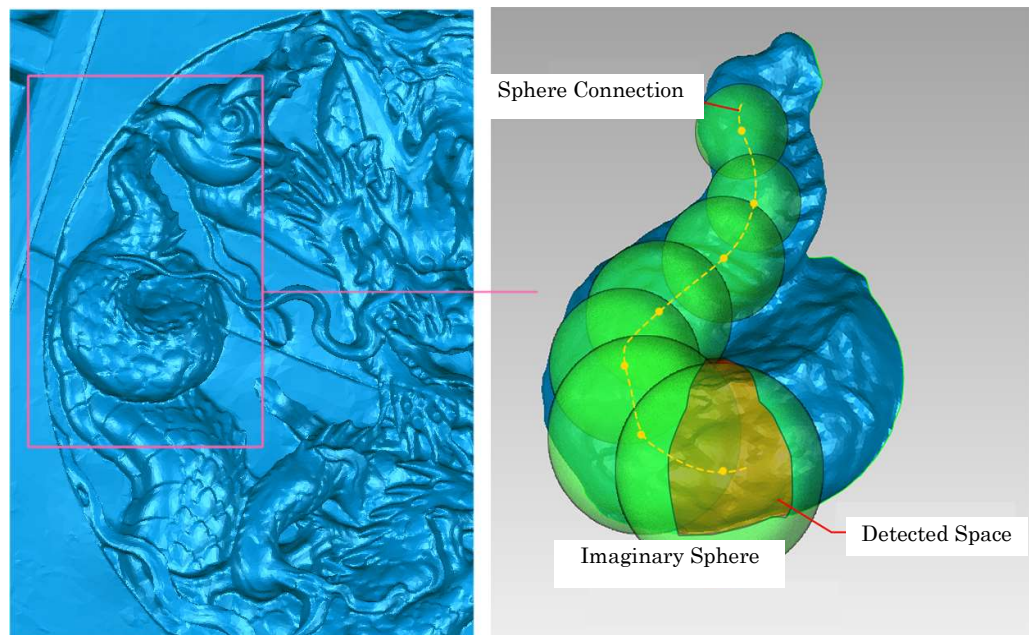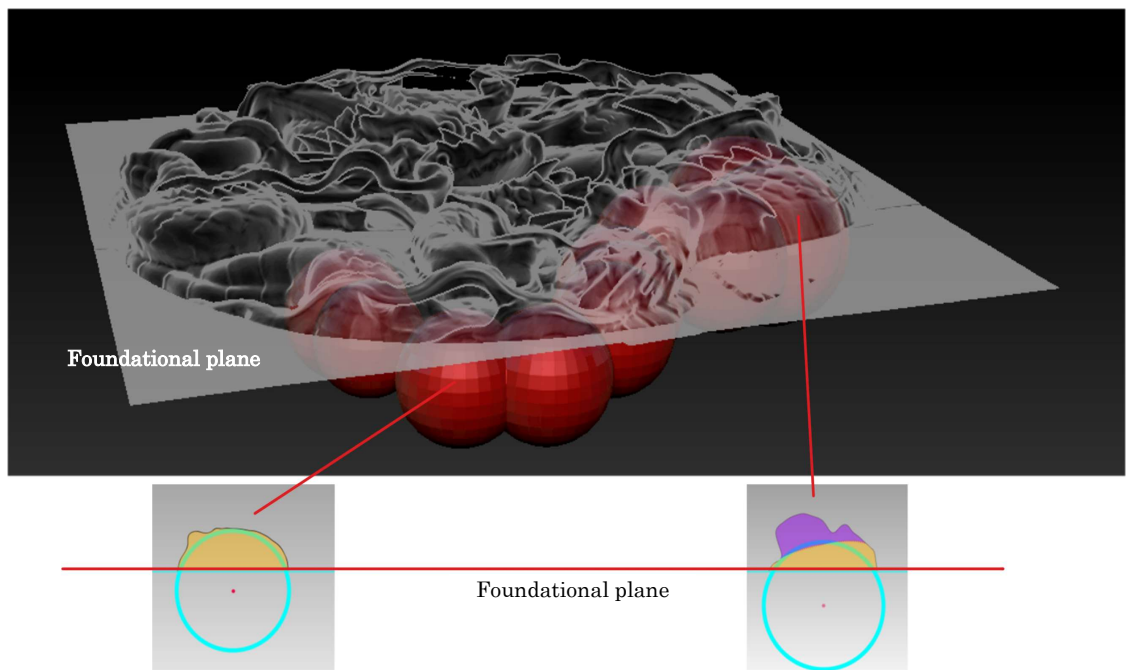
Figure 3-12. Connection of Imaginary Spheres

Figure 3-13. Relationship of Sphere features and the foundation plane

curvatures. Therefore, the forms of the body and the tail are cylindrical [5]. This makes Yoshimitsu's "dragon" a strong reality of the muscular tensity.

3.2.2 Style Characteristics of wave and dragon tail

In this section, the author attempt to explain the geometric meaning of the composition of the wave by the "laminated layer" defined in the previous section.

For the form of the dragon's tail, there are no high-curvature curves as seen in the case of the wave that was directly framing the shape of the dragon, but the contours of the scales give the impression of a living being's bulge (cylindrical or spherical) to the entire form of the dragon. According to the arched crosssections and the constant curvature of the dragon's body and tail, this bulge can be re-expressed with geometric features such as cylinders, circles and spheres. In this paper, the author focused on the form of the dragon's tail and defined a circle feature inscribed on the cross-section of the dragon's tail. Then the circle was used as the largest cross-section to create a sphere feature. The combination of multiple sphere features inscribed the dragon's tail could represent the inner volume and mass of the form.

(1) Definition of the direction of the laminated layer that constitutes the wave form

In the recomposition of wave form by the laminating layers defined in the previous section, it was confirmed that the normal directions of the laminating layers concentrate in several specific directions. In this section, the analyse focused on the wave form on the left side of the dragon analyzed in section 3.2.1.(1)

In this wave form, it was confirmed that there are two "lamination axis" defined in section 3.2.1.(1). The whole form of the Wave as the main region and each of the regions composed according to one of the two differently lamination axes was defined as a sub-region(Pink framed regions in Figure 3-11).

Now the wave form is divided into several laminating layers for each sub-region, and the lamination axis is highlighted in Figure 3-11. Circle features inscribed to each high-curvature curves in Figure 3-11 were detected to define a representative orientation for each layer. These circle features are detected by the Fitting Statistics

evaluation method [6], and the normal direction of the circular features is indicated by the pink arrows in Figure 3-11.

By comparing Figure 3-11 with the photos of the real wood carving of the wave, the dynamic movement of the wave and a dramatic proceeding of the wave, which is expressed by the arrangement of the laminating layers staggered one by one were perceived. This dramatic effect of the laminating layers might provide an attractive and exciting entertainment space for the local people who lived near the temple in the Edo period.

(2) Relationship between the connection of the virtual spheres in the tail of the dragon and its form

As described in the previous section, the arch-shaped cross-section of the body of Yoshimitsu's dragon shows that the body of the dragon can be simplified and approximated by a cylinder. Furthermore, it indicates that the form of the dragon's body and tail could be recomposed by a series of the inscribed sphere features with diameters matching the thickness of the dragon's body (Figure 3-12). The lines that connect the centers of these spherical features could be considered as a skeletal frame at the center of the dragon's body.

When observing the skeletal frame composed of these spheres together with the foundation plane (the lowest plane in the relief, shown in Figure 3-13) of the entire sculpture, it was confirmed that the skeletal frame and the lower parts of the sphere features sunk underneath the foundation plane. This visual volume is different from the regular forms of the reliefs in the early and middle Edo period that the form of the dragon's body is directly squashed into a flattene shape to fit the thickness limitation of the relief. But for Yoshimitsu' dragon relief, the arc-shaped cross-section of the body and the position of the connecting sphere features seem to have been designed consciously in such a way to give the viewers an image of the entire dragon body
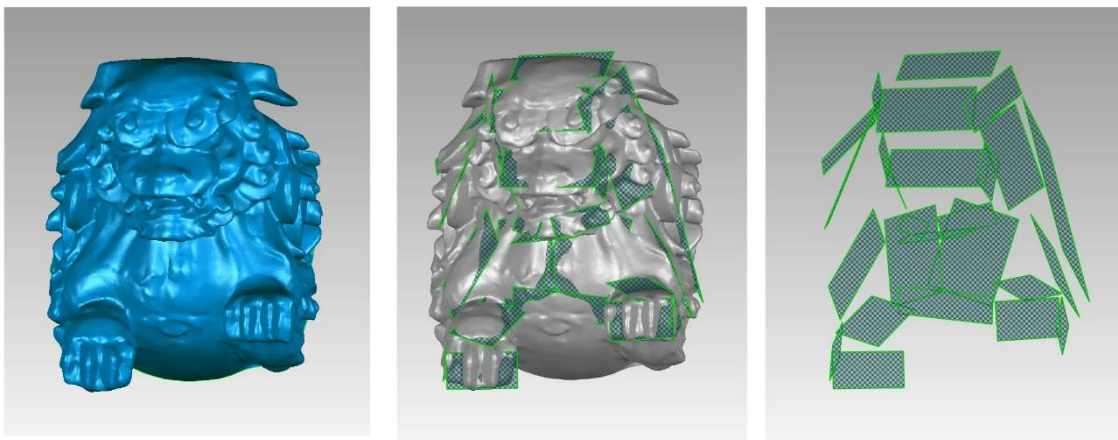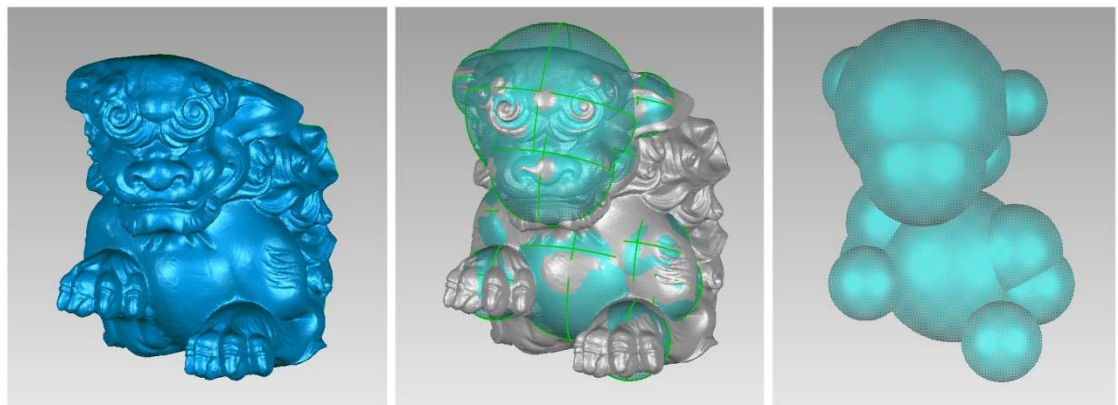
Figure 3-14. Curvature Spectrums of Kibana Lions
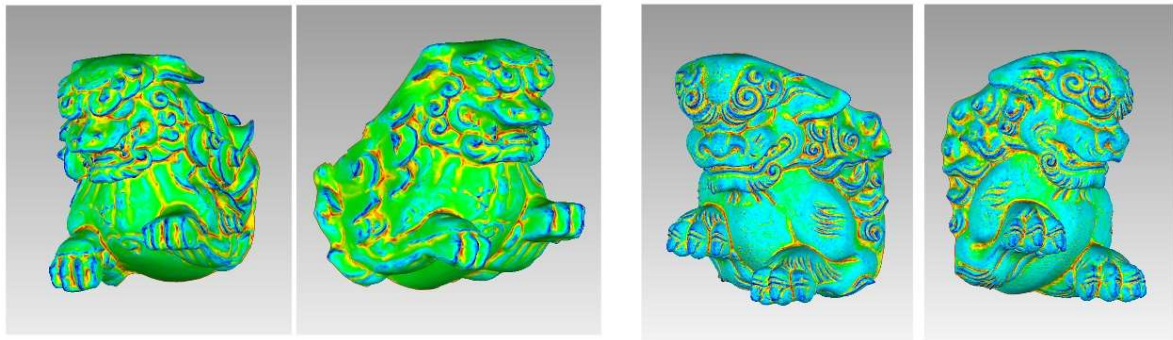
(a) Ihachi's Kibana Lions

(b) Yoshimitsu's Kibana Lions

Figure 3-15. Style Characteristics of Kibana Lions

sinking into the foundation plane and only the upper part of the dragon's body remains uppon the foundation plane (Figure 3-13). This sculptural technique enhanced the three-dimensional sense of the relief.

According to the latent composition of the geometrical features in Ihachi's wave and Yoshimitsu's dragon tail, the "laminating layers" and the "connecting spheres" were defined as the style characteristics of the wave form and the dragon form.

3.2.3 Style Characteristics of Kibana Lions

From the curvature distribution map (Figure 3-14), it could be observed that the areas of high curvature of the two wooden-nosed lions are concentrated in the hair flow, the mouth and the marginal areas of the nose and eyes. However, in terms of the color distribution of curvature on the surface of the overall shape, the large green area in the shape of Ihachi Takeshi indicates that there are many relatively flat areas in the form, and the whole form has a strong sense of blockiness. In contrast, the light blue area in Yoshimitsu Goto's model is significantly larger than the green area, indicating that the surface with lower convex curvature has a higher proportion than that of Ihachi Takeshi's model, and the overall shape has a stronger sense of sphericity.

Based on the above curvature distributions, the planar features for the Ihachi Takeshi model and the spherical features for the Yoshimitsu Goto model were extracted. The composition of the sphere features are shown in Figure 3-15, which is similar to the connecting spheres of the dragon tail.
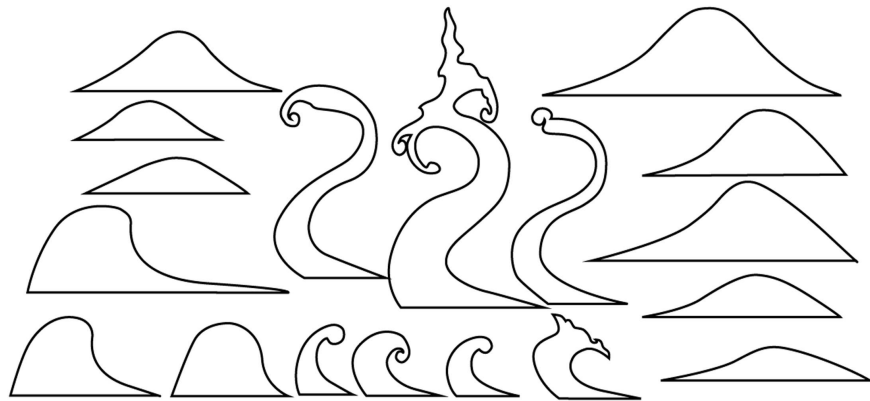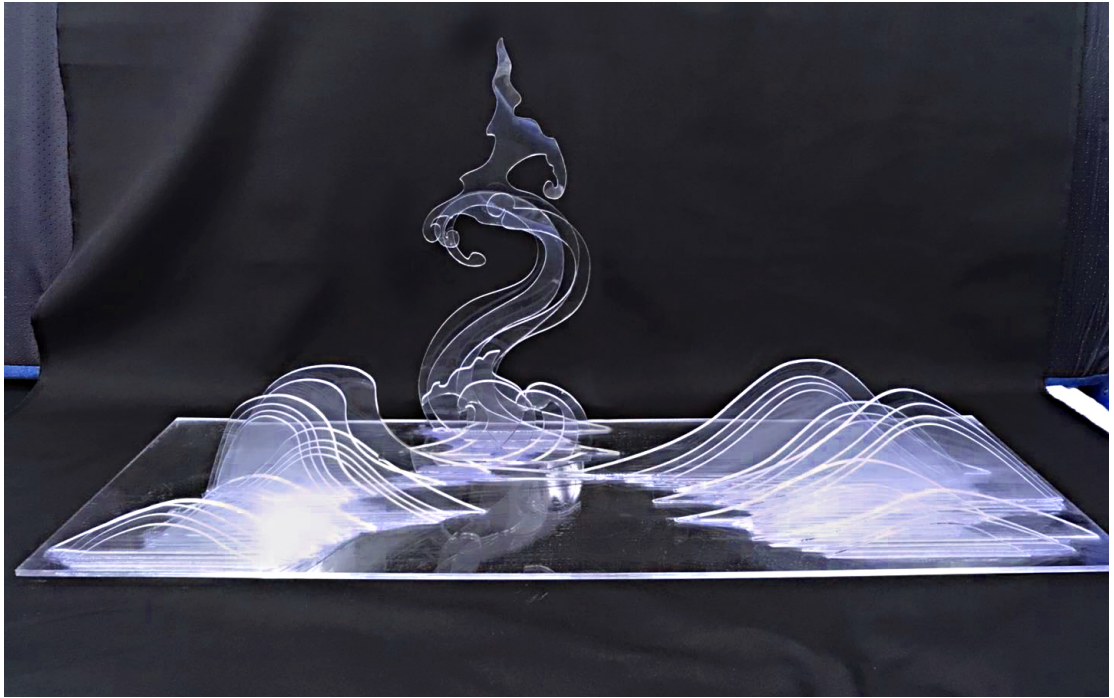
Fig. 3-16 Ihachi's wave form recomposed with acrylic laminated layers

3.3 Creation of explanatory models for the exhibition

Although the differences in the styles of the works between Ihachi and Yoshimitsu were rarely evaluated in the previous research, many local researchers and amateurs of the temple and shrine sculpture delighted in a further study of the latent sculpting knowledge in the works of both sculptures. The local museum staffs also expect to convey the latent sculpting knowledge to the viewers. Therefore, at the exhibition
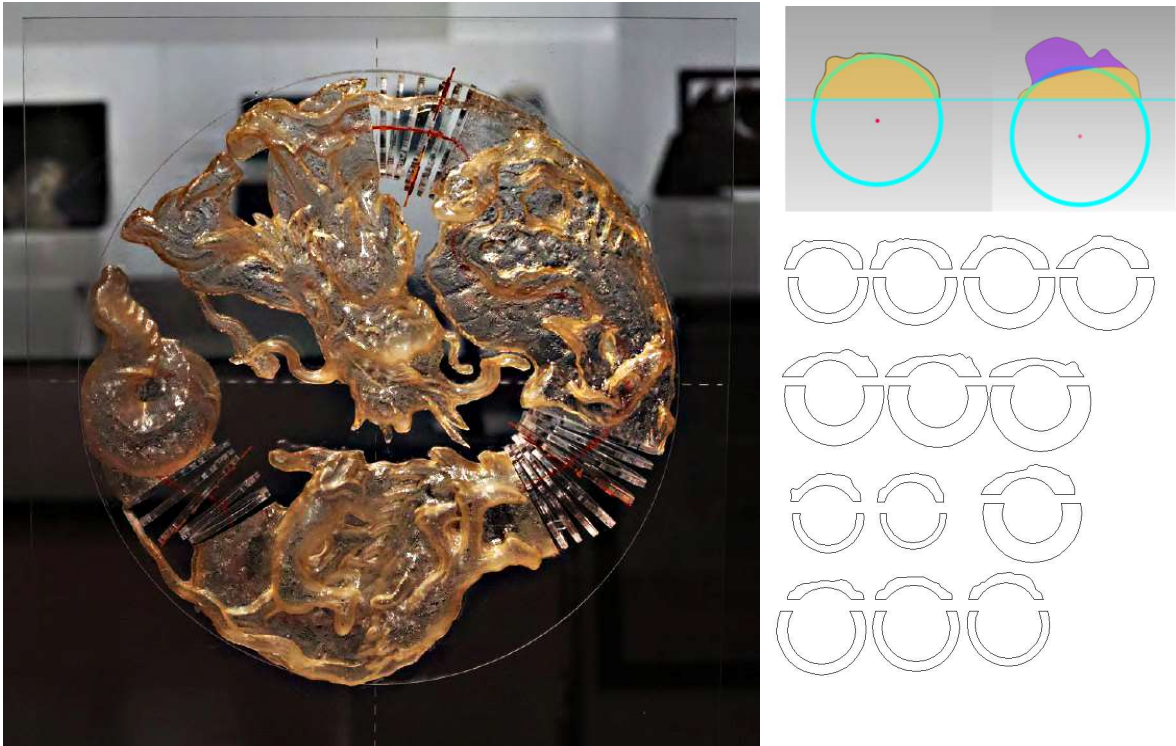
Figure 3-17   Style recomposition model for the characteristics of the dragon body

"Watching Ihachi and Yoshimitsu in 3D(3D で観る伊八と義光)" held from February 25 to March 26, 2017 at Kamogawa Folk History Museum（鴨川郷土資料館）in Kamogawa, Chiba Prefecture, the forms of Ihachi's "Wave" and Yoshimitsu's "Dragon" with the geometrical features were recomposed and two 'style recomposition models' were created to exhibite and convey the concept of the two models. These models emphasize the visualization and the explanation of the style characteristics of Ihachi's laminating layers and Yoshimitsu's connecting spheres that were analyzed in this chapter.

For the model of Ihachi's "wave" shown in Figure 3-16, the laser cutter were used to cut out multiple wave-form thin boards from 3 mm transparent acrylic board and arranged them at an equal interval on the base to reproduce the composition of the laminating layers. Each of the thin boards was oriented in the same direction and adhered to the transparent base. A green LED was placed underneath the base and
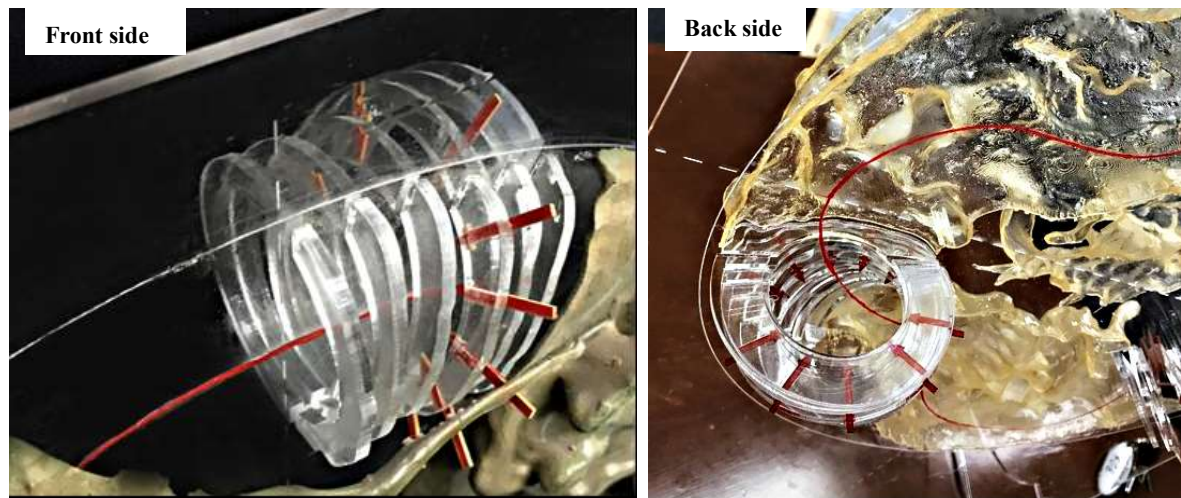
Figure 3-18. Parts of the Cross-section and the red arrows

reflected the green light to the thin boards' contours (Figure 3-19) to enhance the visual effect of the silhouette of the lamination.

For the model of Yoshimitsu's dragon shown in Figure 3-17, three parts of Yoshimitsu's dragon relief that shows a significant mass of the dragon's body were selected and cutted out the parts representing the shapes of the cross-sections of the body from a 3 mm transparent acrylic board. The shapes of the cross-sections referred to the circle feature with the same diameter as the sphere feature defined in the previous section. As shown in Figure 3-18, the parts of the dragon body created by the 3D printer and the parts of the cross-section circles representing the connecting spheres were aligned and placed on a transparent acrylic base plate. The red arrows on the part of the cross-section circle represent the normal directions of the surfaces of the dragon's body, and the red curve on the base shows the skeletal frame inside the dragon's body.

Along with the exhibition of these two models (Figure 3-19, 3-20), a presentation was also held for the public to explain the two sculptures' style characteristics and the differences between the styles of Ihachi and Yoshimitsu. Questionnaires were collected to investigate the audience's understanding of the contents of the
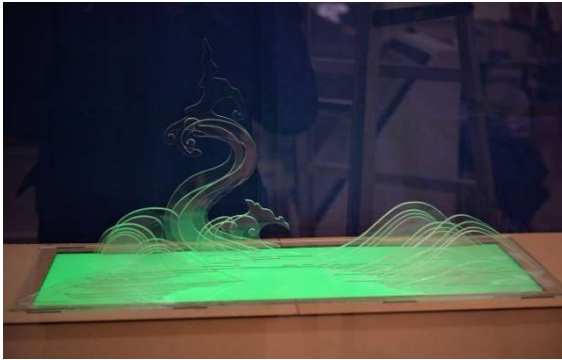
Figure 19 The wave model displayed in the exhibition

Figure. 20 Explaining Yoshimitsu's style to the audience using the recomposition model

presentation and the meaning of the two style recomposition models. There were 66 audiences submitted the questionnaires. According to the results shown in Table 1, 55 people (81.1%) answered that they could understand the style of the laminating layers of Ihachi's wave form, and 33 people (49.1%) answered that they could understand the connecting spheres of Yoshimitsu's dragon. The significant difference in the degree of understanding between the two forms shows that the style characteristic of Ihachi's Waves tended to be understood intuitively through the explanatory model, while the meaning of the circle feature and the skeletal frame shown by the red curve in Yoshimitsu's Dragons tended to be difficult to understand (Table 3-1). As introduced in Chapter 1, the concept of the connecting spheres and the skeletal frame is related to the evolution of the sculpting technique to express the volume and the mass of the sculptures, which requires some fundamental knowledge or experience of sculpting to understand in a short time. But the sculpting technique of the lamination layers is relatively easy to read and understand for viewers with no sculpting experience. This might be the reason that caused the difference in the degree of the understanding between the two carvers' style characteristics. A teenage viewer commented that he became interested in Chiba's historical shrine and temple sculpture through the models. This result suggested the possibility of inducing the views' interest in the latent sculpting knowledge of temple and shrine sculptures

Style characteristic			Positive Comments	Negative Comments	Unexpected Comments
The difference of Style Characteristic in Ihachi and Yoshimitsu	Ihachi	Lamination Layers of Wave form	• Ihachi's innovation of sculpting techniques • Exellent style design	• understood the meaning of the styl e characteristics by the presentation	• It has a unique artistic aesthetic that goes beyond the level of the carver. • Sensing space (the universe)
		Dynamic form of the Wave	• Ihachi's . • The Realities of Waves. • Impressive visual effect of the wave	• cannot understand tonly through the model.	
	Yoshimitsu	Skeleton Frames inside the form	• The awesomeness of three-dimensionality • Yoshimitsu's (reliable/stable) (sculpting)technique		• Delicacy of the Sculpture • Details.
		Muscle Mass of the Dragon's Body	• The reality of dragon. • The expression of the mass and volume are different from Ihachi		

through the style recomposition models.

Reference

1. George Bridgeman, Bridgman's complete guide to drawing from life, Sterling Pub Co Inc, 93-94, 2009

2. Susan Alyson Stein, Kandinsky and abstract stage composition: practice and theory, 1909–12, Art Journal, 43, 61-66, 1983

3. Robh Ruppel, Graphic L.A., Design Studio Press, 106-112, 2014

4. CAD software from 3D System, a toolbox for converting 3D scan data into highly accurate surfaces, polygons and native CAD models

5. 本川達雄, 生き物は円柱形, NHK 出版, 23－25, 2018

6. Fitting Statistics Evaluation Method: The minimum distances between all the vertices of a polygonal issue that make up a laminated layer and the feature boundary are calculated, and then the minimum distances between the vertices that are furthest from the outside and inside of the feature and the average of the minimum distances of all the vertices are statistically calculated. Since the subject of this study is a large sculpture with a height of more than 5 meters, it was not worthwhile to care about the accuracy of feature detection, and therefore, we adopted features whose average minimum distances were within 1 mm.

Chapter 4

Quantify the Style Characteristics with Polygon Mesh

Chapter 4. Quantify the Style Characteristics with Polygon Mesh

In Chapter 2 and Chapter 3, direct observation were conducted and the style characteristics were extracted from the works of Takeshi Ihachi and Goto Yoshimitsu. According to the direct observation of the two groups of forms, a significant difference was found between the modeling characteristics of Ihachi and Yoshimitsu. The features of the laminating layers in the wave form and the cubics consisting of plane features in the Kibana lion of Ihachi indicate that the large surfaces of Ihachi's form orient to several specific directions. In contrast, the connecting spheres in Yoshimitsu's dragon and Kibana lion show that the large surfaces tend to orient to directions in variety. In order to analyze the differences in the distribution of orientation of the surfaces in the works of the two carvers, a qualitative method based on the geometric characteristics of the surface of the decimated models to visualize and to compare the distribution of the directions that the main surfaces of the sculptures orient was propose.

4.1 Represent the composition relationship in rough sculpting with Decimated model

4.1.1 Simplification of the high-resolution model

In order to visualize and quantify the differences in orientations of surfaces on the sculptural forms which have the style characteristics analyzed in the previous chapters, it was necessary to translate the visual information of the style characteristics into geometric properties that can be quantitively evaluated in 3D digital models. In recent years, the technology of 3D scanning and reverse engineering has been developed to record the features of the scanning target directly

<div align="center">

(a) Original Model (200000 Polygons)   (b) Low-Poly Model (680 Polygons)

Figure 4-1. From Original to Low-Poly Model

</div>

and accurately. The basic geometric properties such as points, lines and surfaces can be described quantitatively in the polygonal mesh model of the wood carvings collected in the field survey provided the possibility for this translation.

However, the original models directly generated from 3D scanned point clouds are generally not suitable for direct quantitative analysis of the shapes. This is because the data of 3D scanned point clouds is usually very large, which makes the original models have an extremely high resolution of polygons, making a huge data load for quantitative analysis. Besides, the original models often have holes, self-intersecting polygons, and duplicated vertices caused by the unavoidable noise of the measurement can also interfere with the quantitative analysis. Therefore, the original model usually needs to be fixed (Appendix1-1, 2) and decimated (Appendix 1-3)into a more simple shape (Figure 4-1) with lower amount of polygons, which still retains the global geometrical to reduce the computing load and to repair the geometrical errors in the original model. This simplification could not only speed up the editing process but also emphasizes the essential style characteristics (such as the outer contour, proportion, and primary shapes and composition.) of the form to be analyzed [1].

（a）Rough carving   （b）Low-poly model

Figure 4-2. Similarity of Rough carving and Low-poly model of cat head

Figure 4-3 Chisel used in Rough Carving Process

The simplification of the polygon model usually has two approaches: vertex decimating and retopology [2]. Vertex decimating is a method of merging vertex of the polygons to transform a high-resolution polygon mesh model into another with much less polygons, edges and vertex[3]. Retopology overlays a new low-resolution polygon mesh with much less polygons, edges and vertex onto the original model. The new polygon mesh has a better tessellation of quad polygons and is easy to

topology.

The original models directly generated by point clouds before simplification and the models made by digital sculpting are generally called "original models" because of their extremely high resolution, which often exceeds hundreds of thousands of polygons. The simplified models that retain the primary geometrical features of the original model are called "decimated model". In recent years, the decimated model has been used in combination with texture maps for high-resolution static rendering. The number of polygons is generally around 10,000-25,000. The number of polygons used for dynamic rendering in games and animations through rig-bonding is several hundred to several thousand.

4.1.2 Similarity of the decimated model and the rough carving

The concept of simplifying forms to grasp the style characteristics in sculpting and painting is a common technique widely used in the early stages of style design to organize the primary composition relationships of the form. Since this polyhedra form of the sculpture or the painting is a simplification of a complex natural reference object and retains the primary geometrical properties, it usually has a similar form to the digital decimated model. The rough form of wood carving is an example of this similarity.

In previous carving workshops, the rough carving that would mainly determine the style of the sculpture was often completed by the experienced masters. In this stage, the rough carving focused on the composition of the primary form and was closer to polyhedral without details [4]. As shown in Figure 4-2-a, the rough carving of the cat's head is close to a geometric polyhedron shape. At this stage of carving, the carver usually uses a flat chisel (Figure 4-3) to carve a small flat plane after each cut. Through the combination of a large number of these small planes, the carver could establish a clear and simple form that is easy to modify and adjust quickly. Figure 4-

2-b shows a decimated model of a cat's head made in Zbrush. Comparing the rough carving of the cat's head with the decimated model, it could be seen that the small plane created with a flat chisel in the rough carving can be interpreted as a polygon in the decimated model.

Based on this form similarity between the wood carving at the rough carving stage and the decimated model of the polygon mesh model, the decimated model of the 3D scan of the wood carving was chose to use for the quantitative analysis of the shape. In order to describe the style characteristics of the decimated model quantitatively, it is necessary to select one or several essential geometrical properties of the polygon mesh model for quantifying such characteristics. A Polygon mesh usually consists of a number of triangles, quadrilaterals, or other simple convex polygons and other types of small planes. And a single Polygon consists of vertices, edges, faces, and the facet normal vector represents the direction that the face orients [5]. According to the definition of the polygon mesh, a polygon mesh in ASCII format consists of the geometric information used to define a polygon in a three-dimensional coordinate system, which includes three (corresponding to the triangular mesh) or four vertices (corresponding to the quadrilateral mesh) information of the XYZ axis coordinate and the facet normal information used to mark the orientation of the polygon. According to the style characteristics of Ihachi and Yoshimitsu, the specific direction of the surfaces in Ihachi's modeling and the non-specific orientation of the face in Yoshimitsu's modeling are the characteristics of one of the obvious differences between the two carvers' works. Accordingly, the facet normal vector that can quantitatively describe the orientation of each polygon in the decimated modeling was chose as a quantitative parameter to compare the differences of style characteristics between the two engravers.

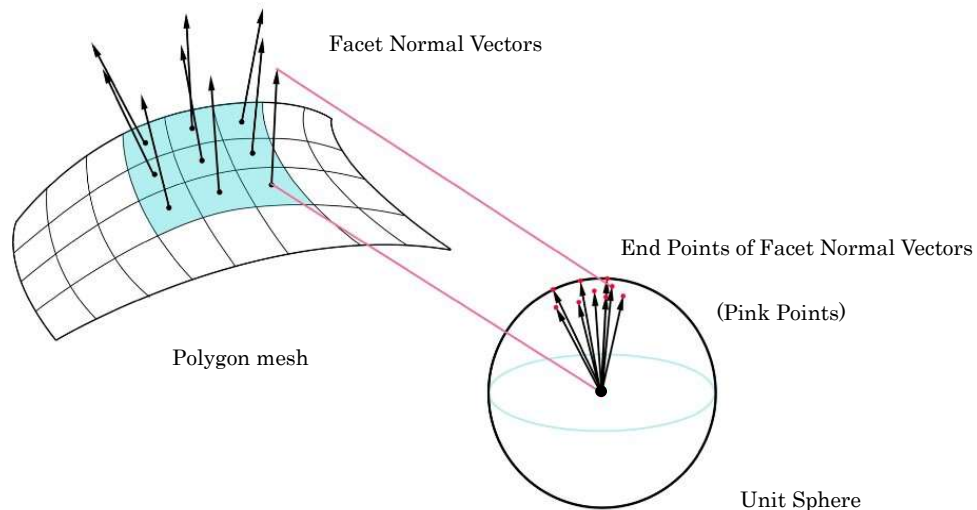## 4.2 Surface Orientations quantified with the Unit Normal Sphere

Figure 4-4. Mapping from Facet Normal Vectors to Unit Sphere

Our method uses facet normal vectors to visualize and quantify the distribution of the directions in which the primary surfaces of the sculpture are oriented. All 3D coordinate values of the facet normal vectors of the polygons from the STL-ASCII data of the polygon object were abstracted in R-studio [6](Appendix1-4). Then a mapping of normal vectors was defined from the polygon mesh to a unit sphere in Matlab[7]. In this mapping, every endpoint of the facet normal vector corresponds to a point on the unit sphere, while every starting point of the facet normal vector corresponds to the center of the unit sphere (Figure 4-4). Since each polygon responding to the facet normal vector is a regular triangle of the same size, the density of the endpoints on the unit sphere represents the concentration level of the normal vectors.
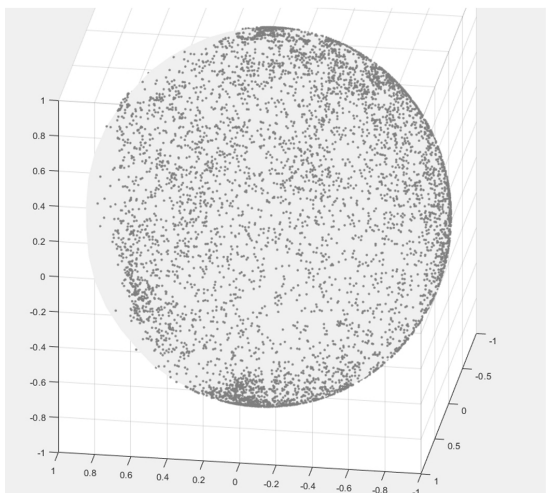
According to this method, the density distributions of the end points on the unit sphere of Ihachi's wave, Yoshimitsu's dragon tail and two Kibana lions were
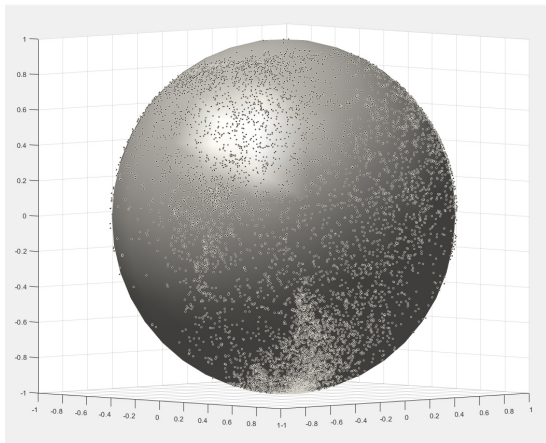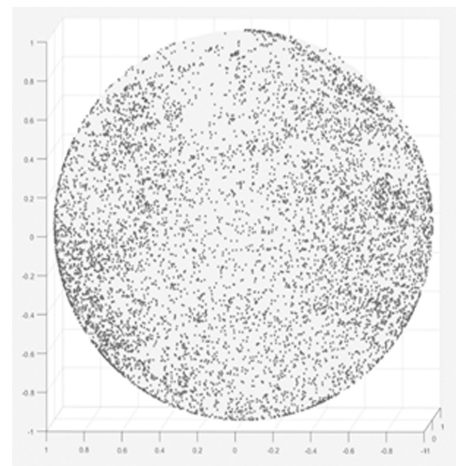
(a) Ihachi's wave
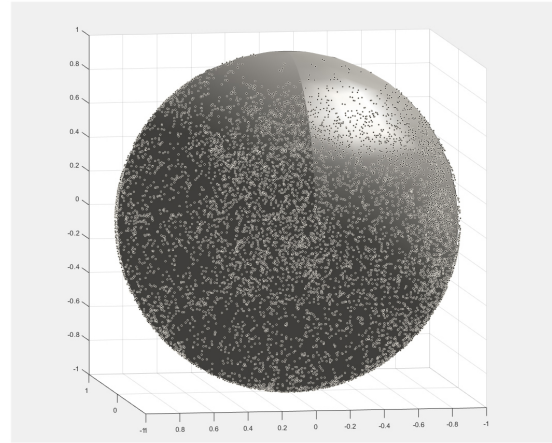
(b) Yoshimitsu's Dragon Tail

(c) Ihachi's Kibana Lion

(d) Yoshimitsu's Kibana Lion

Figure 4-5. Distribution of the end points of Ihachi and Yoshimitsu's forms on the unit sphere

generated (Figure 4-5) (Appendix1-5.1). From the density distributions, it could be observed that the end points of Ihachi's forms concentrate on specific areas with very high density, while the end points of Yoshimitsu's forms distribute with relatively similar densities on the unit sphere.

4.3 Visualize the variation of the distribution in color map

To make the distribution of endpoints on the surface of the unit sphere easier to observe, the Kernel density estimation [8] of the end points was calculated to generate the color map of the distribution on the unit sphere. Kernel density estimation is a

The number of endpoints (blue points on the yellow sphere) of the facet normal vectors was counted in every small cubic space (marked in red frames)
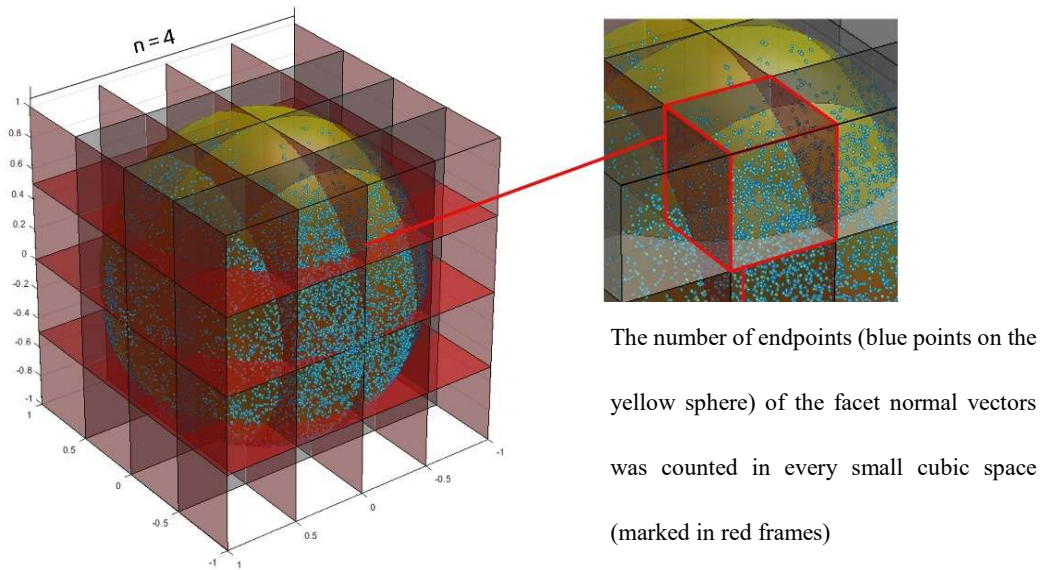
Figure 4-6. Counting the number of endpoints of the facet normal vectors in unit cubic spaces

by N-dimensional histogram

statistic method to estimate the probability density function of a random variable, such as the end point cloud in this study.

In this Kernel density estimation, Bruno Luong's N-dimensional Histogram algorithm [9] was used to divide the 3D space from -1 to 1 was divided into n^3 equal small cubic spaces (Figure 4-6), which is called 'Bins'. The number of bisections of the Axis X, Y, Z was defined as parameter *n*. Then the number of endpoints was counted in each bin (marked in a red frame on the right side of Figure 5). Figure 6 shows a case of quadrisection of the X, Y, Z axis when parameter n = 4 and the 3D space from -1 to 1 is divided into $4^3 = 64$ small cubic bins.

Since the end point cloud in this study is only distributed on the surface of the unit sphere, the area of the end points distributed on in each bin is not equal, which might causes errors between the results of the Kernel density estimation according to the numbers of the points in different bins. To correct the error between different bins, points distributing on the unit sphere with equal interval was generated as the density

reference of the distribution according to Atsushi Yamaji's GSS (Generalized Spiral Sets of points with uniform distribution on the unit sphere) generator code [10] (Appendix1-5.2). Euclidean coordinates of 1,000,000 Points with equal interval were generated as the reference points.

For each of the reference points, N-dimensional histogram with the same value of the parameter n was applied and the number of the points in each bin was counted. Since the reference points distribute with equal intervals on the unit sphere, the number of the reference points in the bins is in proportion to the areas of the spherical surfaces included in the bins. Thus the number of the reference points in each bin could be considered as the value to represent the differences of the spherical areas included different bins.

For Bin (form) is the number of the end points of the form in the bin, and Bin (ref) is the number of the reference points in the bin with the same parameter n and the same position in the coordinate, the error of the number of the end points in the bins caused by the differences of spherical areas was corrected as below:

Bin (correct) = Bin (form) / Bin (ref)

Bin (correct) for each bin was calculated as the corrected value of each bin and the Gaussian smoothing method using a weighted average of the number of the endpoints contained in the bin and its surrounding bins was adopted to smooth the transition between different density colors. The values after Gaussian smoothing was defined as the Kernel estimated density. Finally, all points were color-marked according to the density value. Larger density values were marked in higher color temperatures (approaching red); lower density values were marked in lower color temperatures (approaching blue). By this method, the density of the end points was plotted in the spectrum on the unit sphere (Appendix1-5.3).

The workflow of the method for generating a density distribution color map by

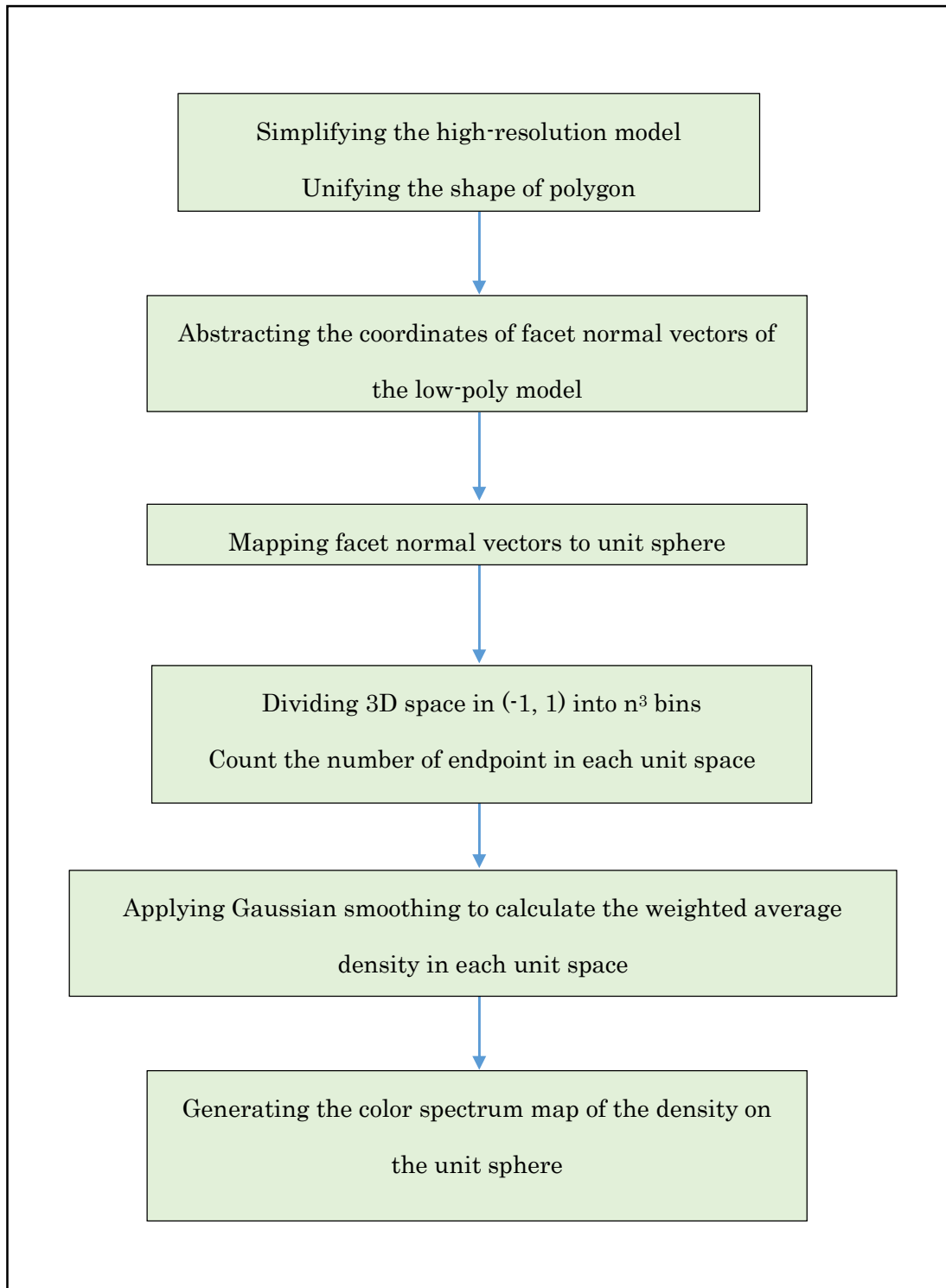mapping all facet normal vectors in the decimated model of the wood carving to a

Simplifying the high-resolution model

Unifying the shape of polygon

Abstracting the coordinates of facet normal vectors of

the low-poly model

Mapping facet normal vectors to unit sphere

Dividing 3D space in (-1, 1) into n^3 bins

Count the number of endpoint in each unit space

Applying Gaussian smoothing to calculate the weighted average

density in each unit space

Generating the color spectrum map of the density on

the unit sphere

Figure 4-7. Method Structure of Quantitative Analysis and Visualization of Orientation of Polygon mesh

unit normal sphere is shown in Figure 4-7.
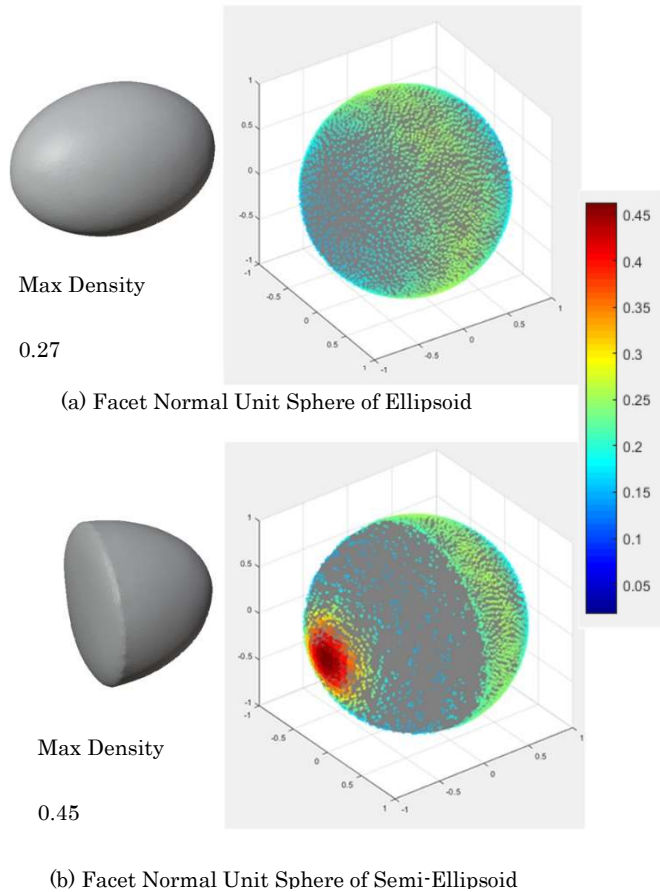
4.4 Validation example of the Unit Normal Sphere Method

Max Density

0.27

(a) Facet Normal Unit Sphere of Ellipsoid

Max Density

0.45

(b) Facet Normal Unit Sphere of Semi-Ellipsoid

Figure 4-8. Distribution of Facet Normal End points

on the Unit Spheres of Ellipsoid and Semi-Ellipsoid

Whether the normal vector unit sphere method would enable us to effectively quantify and visualize the overall face orientation of the model was tested with an ellipsoid and a semi-ellipsoid model. The left side of the y-axis of an ellipsoid were partially flattened and recreated a more uniform polygon mesh on both the ellipsoid and the semi-ellipsoid, unifying the two models with 10,000 polygons consisting of regular triangle polygons having identical side lengths. Direct observation of the two models shows that the surface orientation of the ellipsoid is relatively uniformly distributed, while the "squashed" side of the semi-ellipsoid reveals a distinct and specific orientation. All facet normal vectors of the polygon models were projected on the unit sphere, as shown in Figure 4-8. The facet normal endpoints of the ellipsoid tends to be uniformly distributed on the unit sphere and has a low density. In contrast, the semi-ellipsoid has a significant high-density red area on the squashed side, with significant orientation in a particular direction, consistent with the direct observation.

Reference

1. Marco Rossoni, Sara Gonizzi Barsanti, Retopology and Simplification of Reality-based Models for Finite Element Analysis, Computer-Aided Design & Applications, 17(3), 2020, 525-546

2. Schroeder, W.J.; Zarge, J.A.; Lorensen, WE.: Decimation of triangle meshes. ACM SIGGRAPH Computer Graphics, 26(2), 65_70, 1992.

3. Taime, A.; Saaidi, A.; Satori, K.: Comparative study of mesh simplication algorithms. In Lecture Notes in Electrical Engineering, 2016.

4. Fukue, K., The formation of the concept of a solid in Sculpture, Journal of Graphic Science of Japan 42, 57-62, 2008

5. Mario Botsch,　Polygon Mesh Processing, A K Peters/CRC Press ,15-16, 2011

6. R-Studio is an integrated development environment (IDE)for R, a programming language for statistical computing and graphics.

7. MATLAB is a multi-paradigm numerical computing environment and proprietary programming language developed by MathWorks

8. Artur Gramacki, Nonparametric Kernel Density Estimation and Its Computational Aspects, Springer, 25-27,2019

9. A Matlab cod package that provides the function to divide an N-dimensional area equally into n3 unit spaces (n is an input number defined by the user) and counts the number of the points in each unit zone. The result returns a histogram of the numbers of the points in each unit space. https://jp.mathworks.com/matlabcentral/fileexchange/23897-n-dimensional-histogram (Accessed August 30, 2020)

10. A. Yamaji, GSS Generator: A software to distribute many points with equal intervals on a unit sphere, Geoiformatics, vol.12, no.1, 3-12,2001

Chapter 5

Quantification of Ihachi and Yoshimitsu's Style Characteristics

Chapter 5. Quantification of Ihachi and Yoshimitsu's Style Characteristics

5.1 Simplification of the Polygon models

Decimated models with different numbers of polygons were created to compare the shapes of the decimated models with photographs of actual rough carving models in the same theme to produce a decimated model with a similar shape to the real rough carving models. Curvature spectrum map was used to check whether the decimated model retained the main geometrical characteristics of the original model.

5.1.1 Standard Deviation and RMS estimate of the comparsion between decimated model and original model

On the spectrum map, areas of high-concave curvature are marked in red, and areas of high-convex curvature are marked in blue. Shapes of the high-curvature areas of 3d models in different numbers of polygons were generated (A part of the results are listed in Figure 5-1) and the standard deviation and RMS (Root Mean Square) estimate of the shortest distance from the vertex of the decimated model to any point on the surface of the original model were generated to compare the geometrical differences (Figure 5-2). It was confirmed that the increasing rate of the standard deviation and RMS estimate grown faster with the increase of the decimation percentage, especially when the decimation percentage is above 90%. According to the standard deviation and RMS estimate, it was confirmed that the shapes of the high-curvature areas retained until the number of the polygons was below about 10000, when the decimation percentage is 90% - 91.7% (Figure 5-3).

5.1.2 Certificate the differences of the distribution color maps between decimated model and original model

The distributions of the ending points of the original high-resolution model and the

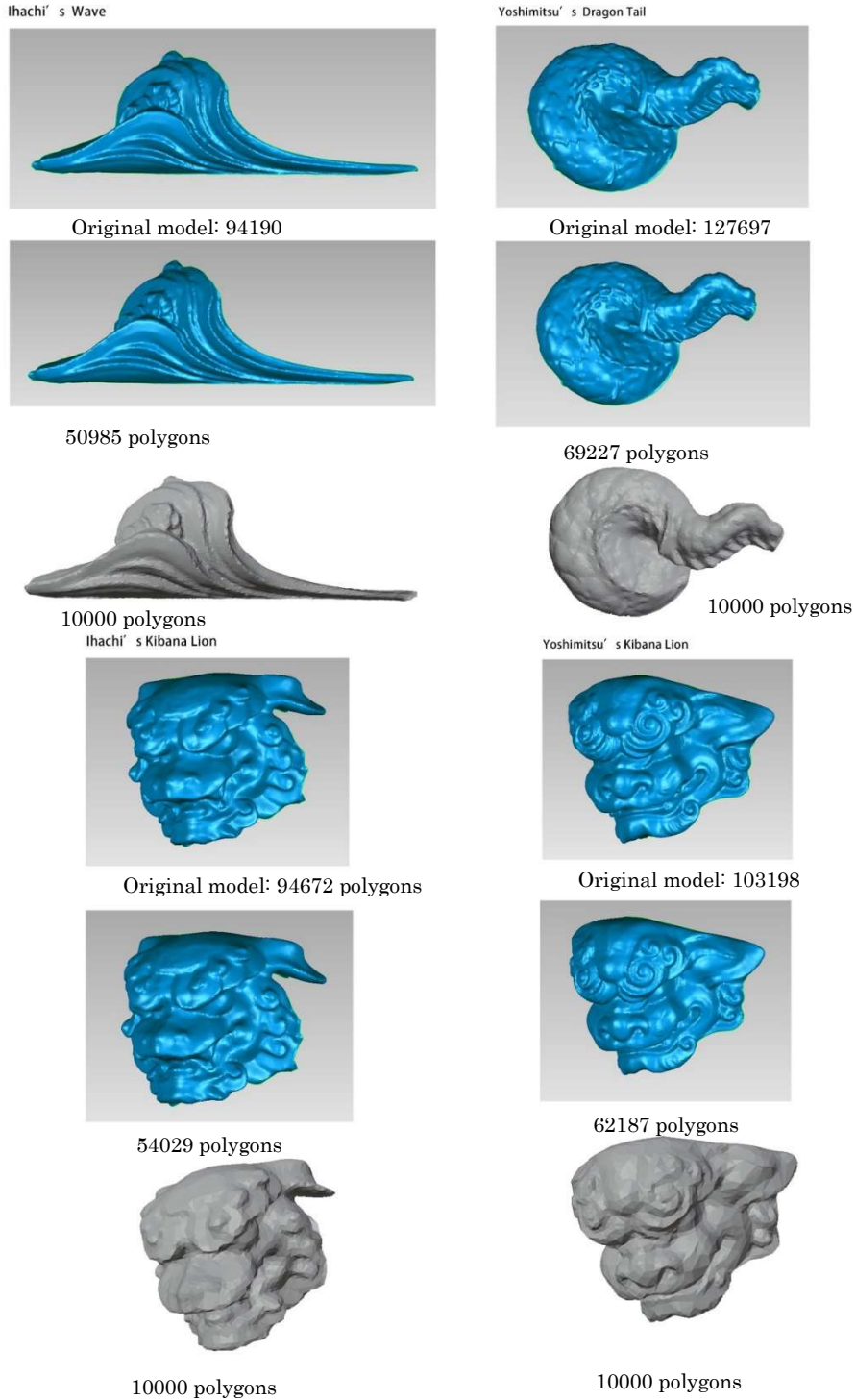decimated models with different numbers of polygons and the parameter n of n-

Ihachi's Wave

Original model: 94190

50985 polygons

10000 polygons

Ihachi's Kibana Lion

Original model: 94672 polygons

54029 polygons

10000 polygons

Yoshimitsu's Dragon Tail

Original model: 127697

69227 polygons

10000 polygons

Yoshimitsu's Kibana Lion

Original model: 103198

62187 polygons

10000 polygons

Figure 5-1. Original models and decimated models of the sculptures
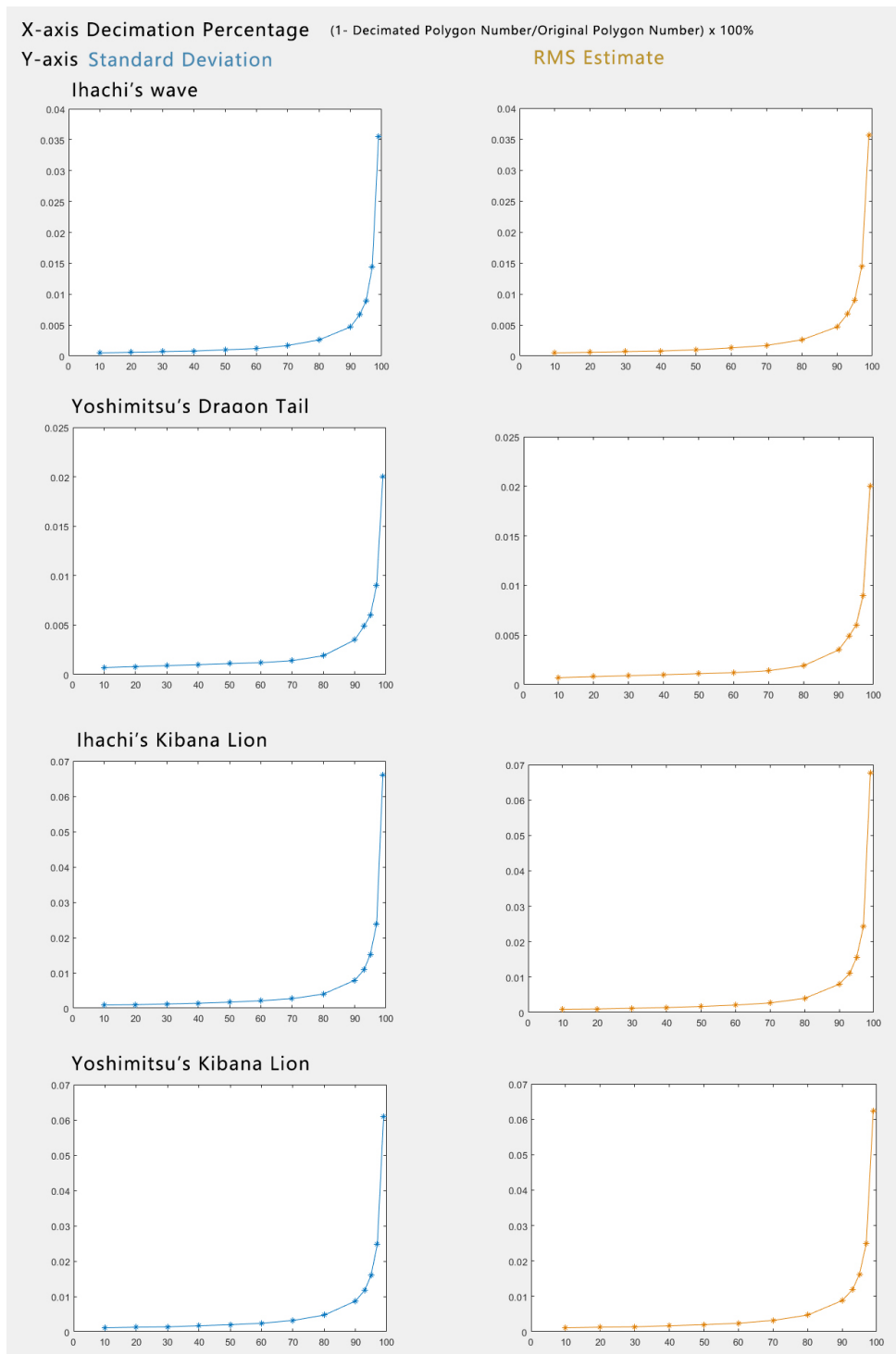
Figure 5-2. Standard Deviation and RMS Estimate of Decimated Models

dimensional histogram were compared. The results of the distributions of the two pairs of the sculpture forms are shown in Figure 5-3-1, Figure 5-3-2, Figure 5-3-3 and

103198 Polygons

62187 Polygons

10,000 Polygons
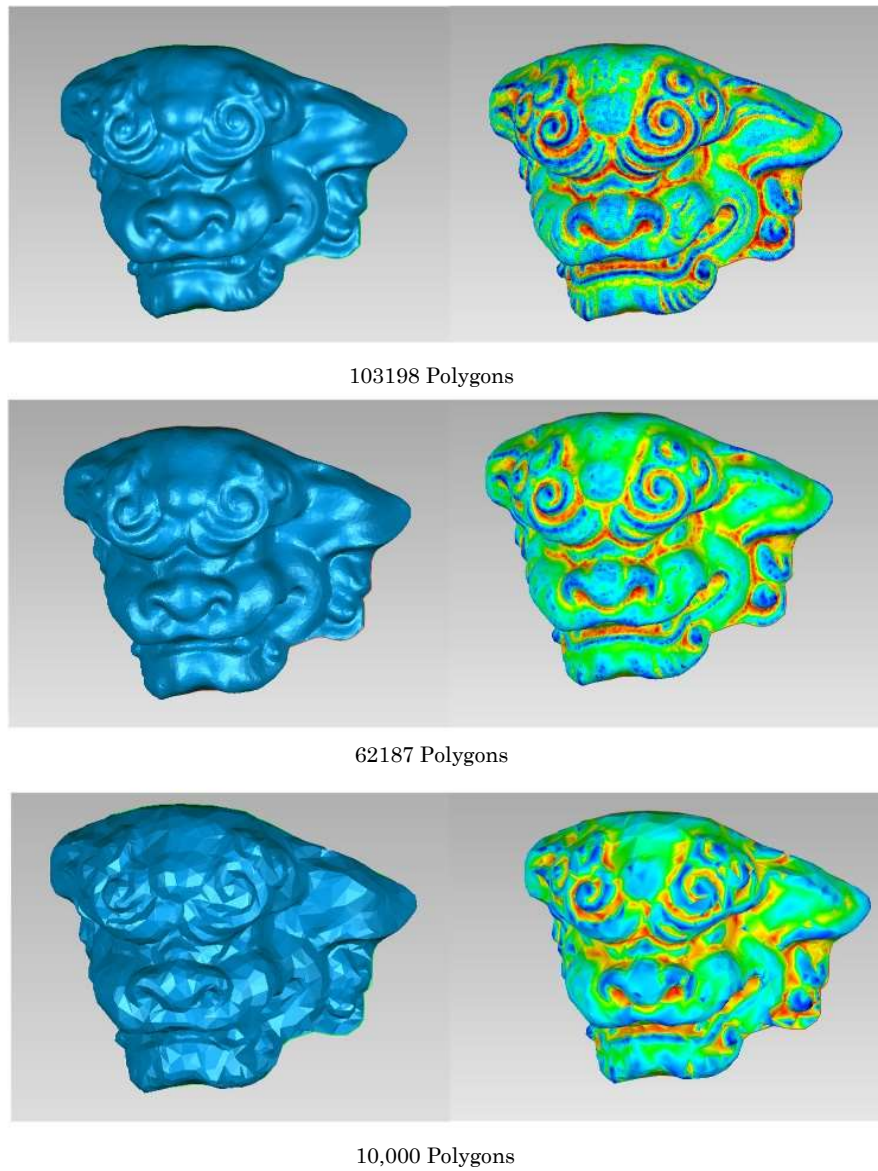
(a) Decimated Polygon Models　　　(b) Curvature Spectrum Maps

Figure 5-3. Curvature Spectrum of Yoshimitsu's Lion Face

Figure 5-3-4.

In Figure 5-3-1, a red area in high densities (Figure 5-3-1, pink frames) gradually became clear with the increase of parameter n over 20. The position of the red areas on the unit sphere are similar among the original, mid-poly and decimated models.

Since the original model has larger amount of polygons than the decimated models,

the boundary of the high-density area of the original model is larger than the other two models with the same parameter n. With the increase of n, the large high-density area of original model is divided by a larger amount of the small cubic spaces (the n^3 small cubic spaces used to count the density of the end points in n-dimensional histogram, introduced in section 4.2), and the differences of the end points between smaller areas within the red high- density area could be marked in gradation colors. Therefore, the boundary of the red area of the original model became smaller with the increase of the parameter n. In Figure 5-3-1 it could be found that the shape of the red area of original model with n = 120 became similar to the shapes of the red areas of mid-poly and decimated models with n = 100. (Figure 5-3-1, black arrows).

In Figure 5-3-2 it could be confirmed that the two high-density area (Figure 5-3-2, pink frame areas) retain in similar shapes with the same parameter n.

In Figure 5-3-3 it could be found that the two high-density areas marked with pink frames retains similar shapes in the same parameter n. With the increase of n, the boundary of the high-density areas decrease, but still with similar shapes.

In Figure 5-3-4, it could be confirmed that high density areas marked in pink frames retain in similar shapes with the same parameter n.

According to the comparison of the density distribution maps between the original, mid-poly, and decimated models, it was confirmed that the overall density of the end points on the unit sphere became more sparser with the decimation of the polygons from the result of Original models to decimated models, but the shapes of the distributions between the high, mid and decimated models with the same parameter n retain in similar shapes. This similarity certified that the distribution of the orientations of the main surfaces of the 3D model retained with the decimation of the polygon mesh. Therefore, the density distribution of decimated model could represent the main geometrical characteristics of the original form. The decimation of the

polygons deleted the small details on the main surfaces of the 3D model, which emphasized the main style characteristics of the form, and also reduced the heavy load of the computer calculation of the original data.

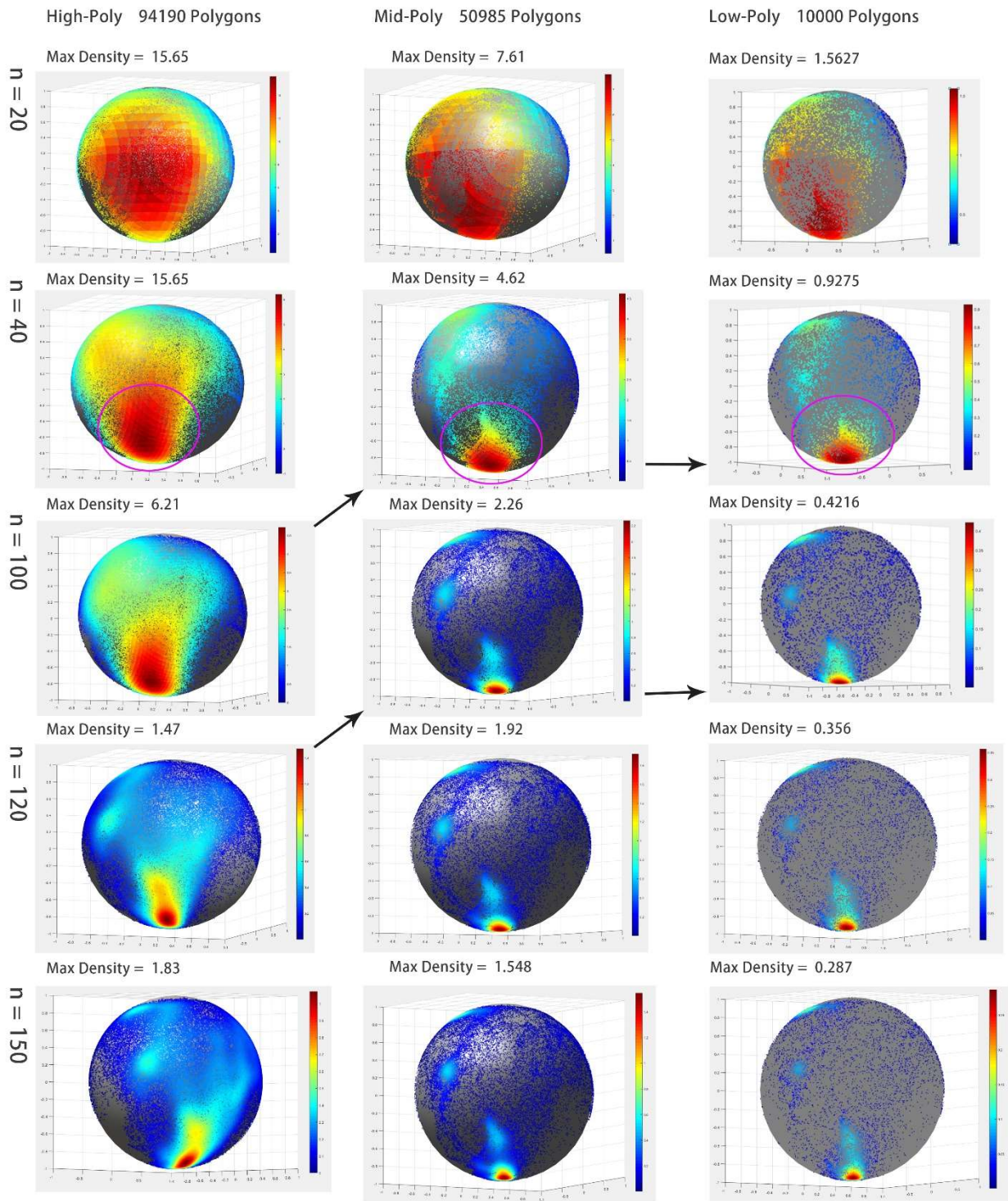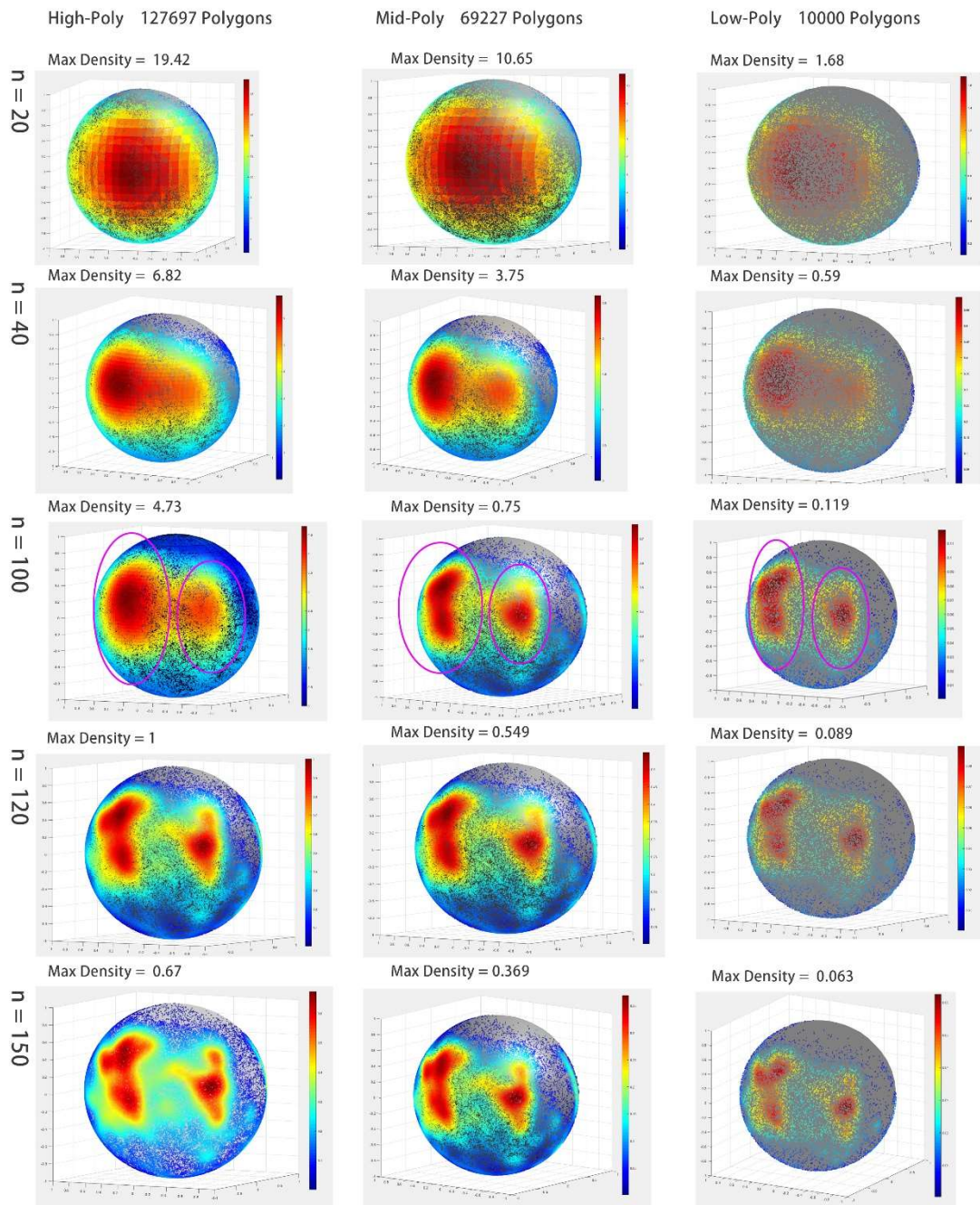Figure 5-3-1. Density Distributions in different parameter n and polygon numbers: Ihachi's wave

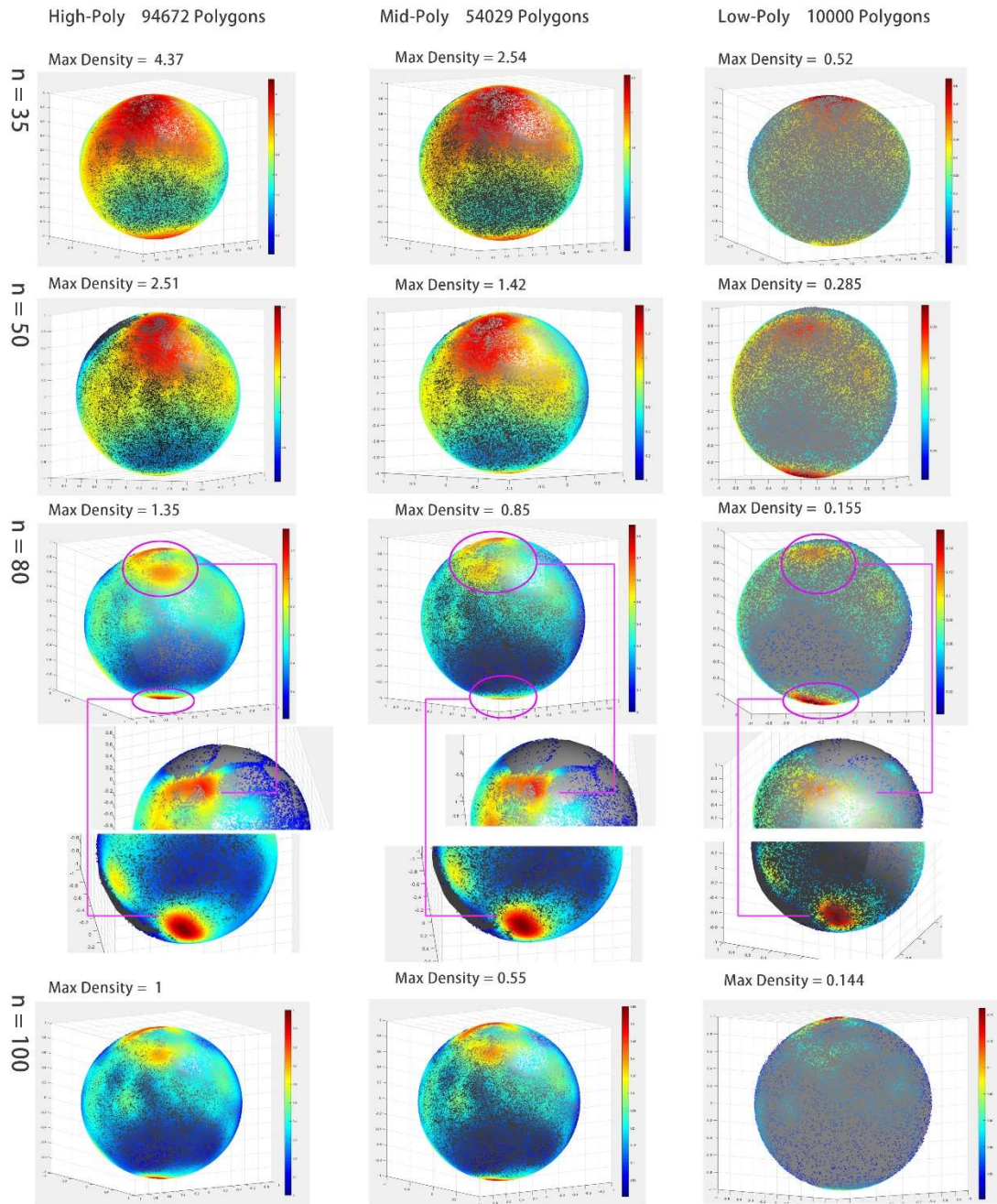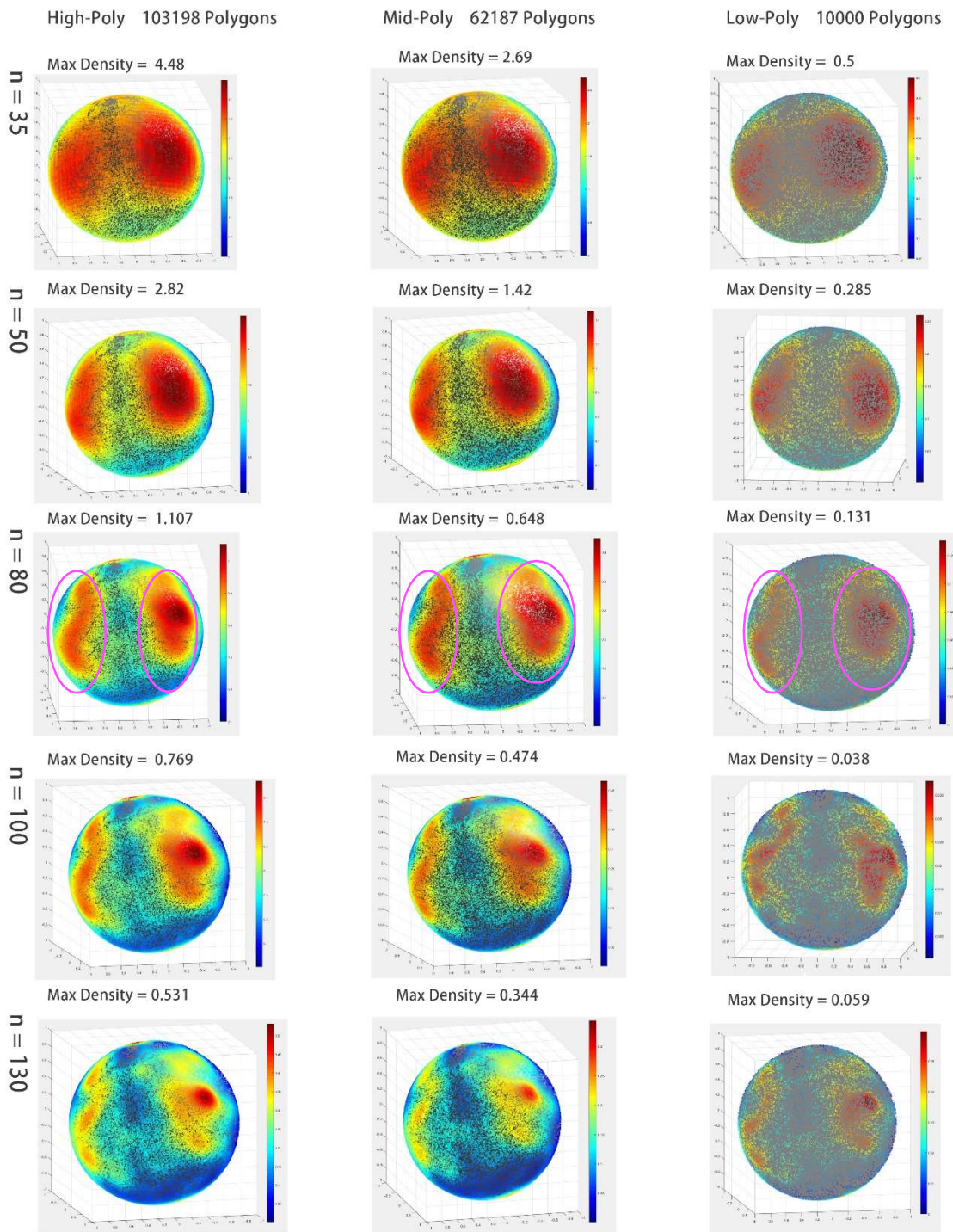Figure 5-3-2. Density Distributions in different parameter n and polygon numbers: Yoshimitsu's Dragon Tail

Figure 5-3-3. Density Distributions in different parameter n and polygon numbers: Yoshimitsu's Kibana Lion

Figure 5-3-4. Density Distributions in different parameter n and polygon numbers: Yoshimitsu 's Kibana Lion

5.2 Density Distributions with different parameter n

The results of the distribution on the unit sphere with different values of parameter n, from 10 to 600 were calculated. Some of the results showing a significant change in the color spectrum are presented in Figure 5-4 and Figure 5-5. The density distributions of the Ihachi sculptures are shown in the right column of Figures 5-4 and 5-5; the density distributions of the Yoshimitsu sculptures are shown in the left column. To compare the difference in the Ihachi and Yoshimitsu density distributions using the same parameter n directly with the same color spectrum standard, the color bar in Yoshimitsu's color spectrums was changed to the color bar of Ihachi's color spectrum. The new Yoshimitsu color spectrums are shown in the middle column. The results confirmed that the difference between the Ihachi and Yoshimitsu distributions on the unit sphere became more evident as the value of parameter n was increased. In the first set, comparing Ihachi's wave and Yoshimitsu's dragon tail, the difference in the distributions becomes apparent when the value of n is more than 40. Beyond that point, the maximum density of Ihachi's wave becomes much higher than the density of Yoshimitsu's dragon (Figure 5-4). In the second set, comparing Kibana lions, the difference in the distributions becomes evident when the value of n is approximately 80 to 100; here, the maximum density of Ihachi is roughly 1.5 times that of Yoshimitsu (Figure 5-5).

Based on the results, it was noted that the distributions and the maximum densities of the Ihachi and Yoshimitsu figures changed in different ways when the value of parameter n is increased. These different patterns of change could be used to confirm
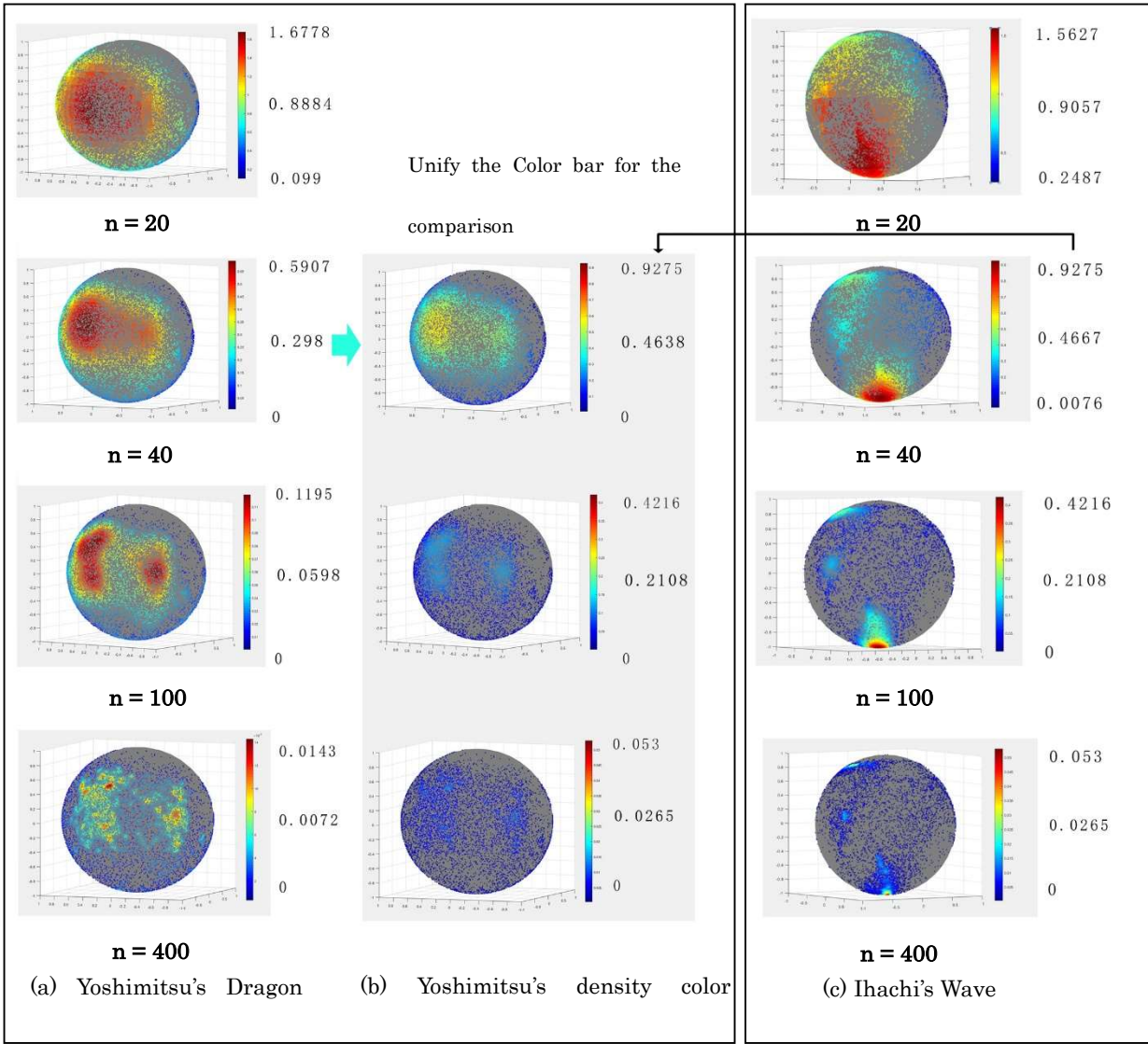
Figure 5-4. Density Distributions for different n values: Ihachi's Wave and Yoshimitsu's Dragon

the difference in the distributions of the orientations of the Ihachi and Yoshimitsu sculptures. Accordingly, the critical points where the difference in the distributions occurs as the value of parameter n were chose.
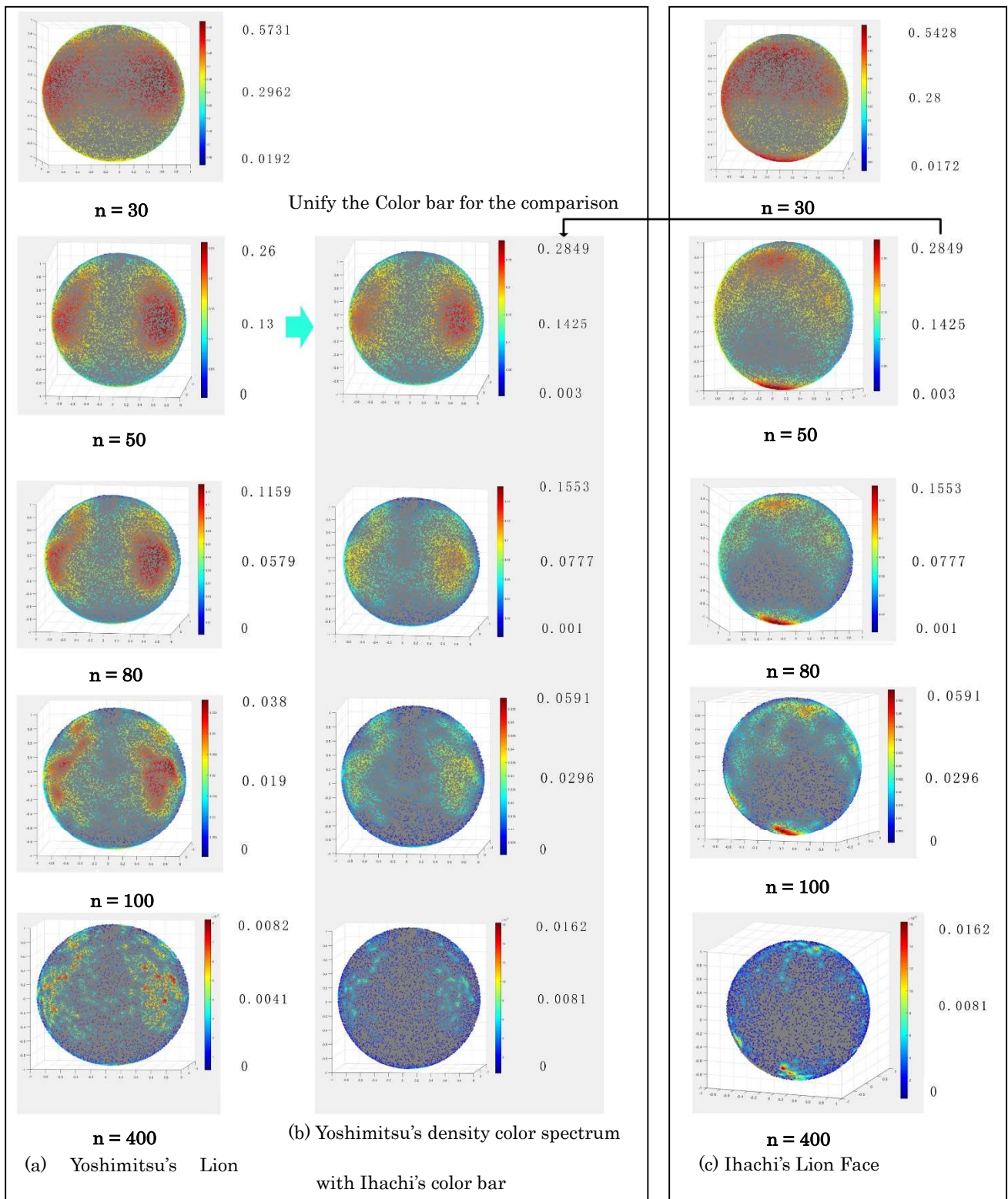
n = 30

Unify the Color bar for the comparison

n = 30

n = 50

n = 50

n = 80

n = 80

n = 100

n = 100

n = 400

n = 400

(a) Yoshimitsu's Lion

(b) Yoshimitsu's density color spectrum
with Ihachi's color bar

(c) Ihachi's Lion Face

Figure 5-5. Density Distributions for different n values: Ihachi's and Yoshimitsu's Lion faces

5.3 Comparison in the density spheres of Ihachi and Yoshimitsu's sculptures

5.3.1 Density Sphere of Ihachi's Wave and Yoshimitsu's Dragon Tail

From the color distribution on the density unit sphere, a significant red high-density area for Ihachi's wave was found. In contrast, for Yoshimitsu's dragon tail, there was no significant red-orange high-density area. In the large water blue area, the density distribution is relatively uniform. The highest density in the area approaches 0.25 of Ihachi's maximum density with the increase in parameter n.

5.3.2 Density Sphere of the Lion Faces of Ihachi and Yoshimitsu

Results for the lion's head comparisons are similar. As shown by the density unit sphere, there are two prominent red high-density areas and an orange area in Ihachi's lion's head form. In contrast, Yoshimitsu's lion head has no red high-density areas; however, there are two yellowish medium-density areas facing the x-y axis at 45 degrees and -45 degrees, respectively. The highest density in the area approaches half of Ihachi's maximum density with the increase in parameter n.
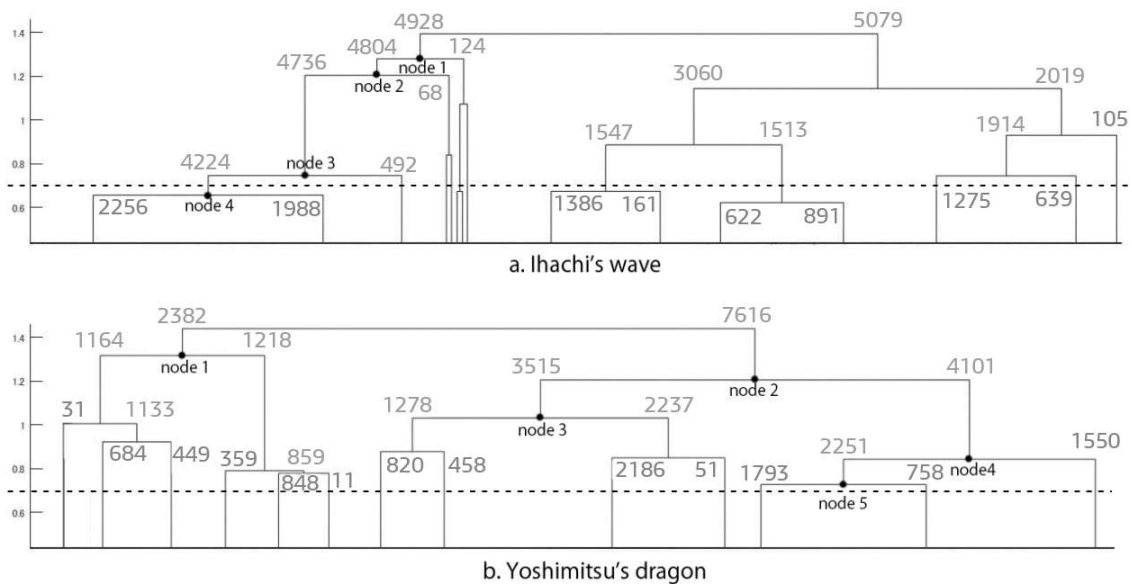

Figure 5-6. Dendrogram Trees of Ihachi's Wave and Yoshimitsu's Dragon

5.4 Linkage clustering analysis

Linkage clustering analysis on the forms for the comparison were applied to certify the accuracy of the results of density color spectrum. Dendrogram plot of hierarchical cluster trees was created daccording to the ward distance of the ending points of the unit normal vectors, and the ward distance between the clusters of the end points could be considered as an index to evaluate the degree of the concentration of the ending points. In the cluster tree, lateral axis stands for the number of cluster, and the height of vertical axis stands for the ward distance between two clusters being connected (Appendix1-5.4).

5.4.1 Linkage clusters in Ihachi's wave and Yoshimitsu's dragon

The dendrogram trees of the set of Ihachi's wave and Yoshimitsu's dragon are shown in Figure 5-6. It was confirmed that for Ihachi, the quantities of the endpoints in the two clusters connected to the leaf node 1, 2, 3 always have a notable difference over 1400, indicating the existence of a huge cluster of endpoint above the height of leaf node 3. According to the structure of the cluster tree, the cluster tree was cutted along y-axis of Ihachi and Yoshimitsu at the height of 0.7, which is approaching to
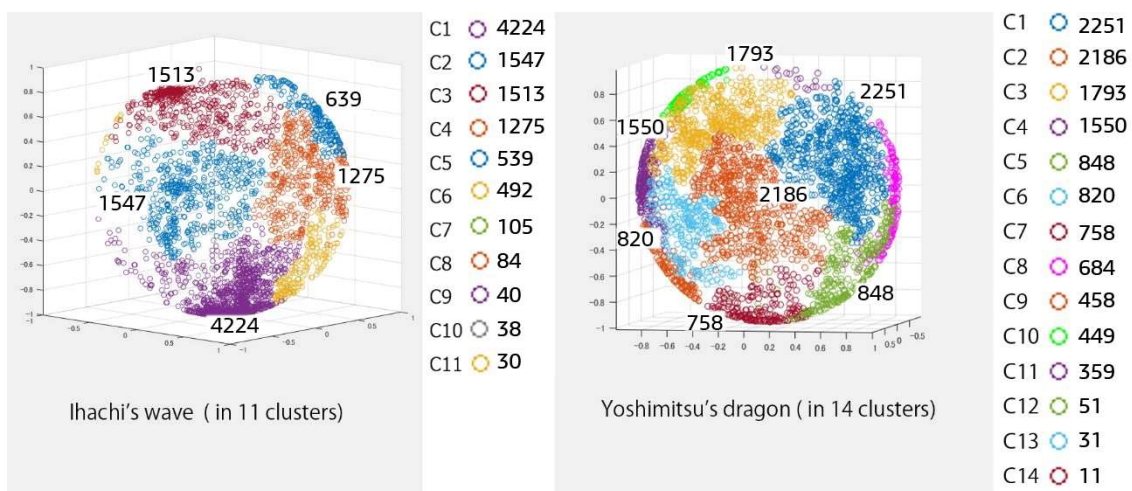

Figure 5-7. Linkage Clusters plotted on the Unit Normal Sphere

the height of node 3 of Ihachi. Then 11 clusters were generated and listed with quantities in descending order and plot the clusters on the unit sphere.

Among the 11 clusters, cluster 1 of Ihachi includes 1501 endpoints, which has an obvious quantity variance comparing with cluster 2 and cluster 3. And it was confirmed that the distribution of endpoints in cluster 1 fit the red and yellow fields (high density fields) well according to the density spectrum (Figure 5-4). This result shows that in the polygons of Ihachi's wave, 42.4% of the orientations of the normal vectors concentrate on the field of cluster 1, indicating the anisotropy of the normal orientations of the polygons.

In contrast for Yoshimitsu, difference between the numbers of the endpoints in the two clusters connected to the leaf node 1, 2,3,4,5 are not remarkable. The cluster tree was cutted at 0.7, which is in the same height of Ihachi and approaching to node 5. Then we got 14 clusters and plotted the clusters on the unit sphere (Figure 5-7). This result shows that the three clusters that contain a higher number of end points are less divergent and far fewer in number than the biggest cluster in Ihachi's wave.

### 5.4.2 Linkage clusters of Ihachi and Yoshimitsu's Kibana Lions

Since the two sculptures are in the same theme of Kibana lion, it became more difficult to find out the differences between the structures of the two dendrogram trees. Since the end points only distribute on the surface of the unit sphere, the Cartiesian coordinates (x,y,z)of the end points was transformed to the spherical coordinates(θ, ϕ ,r) to improve the accuracy of the calculation of the link distance between the linkage clusters. The dendrogram trees of the set of Ihachi and Yoshimitsu's Kibana lions and the numbers of the end points included in the clusters are shown in Figure 5-8. The x-axis shows the index of the clusters, and the y-axis stands for the distance of the two linked clusters.

According to the structures of the dendrogram trees, it was confirmed that in the
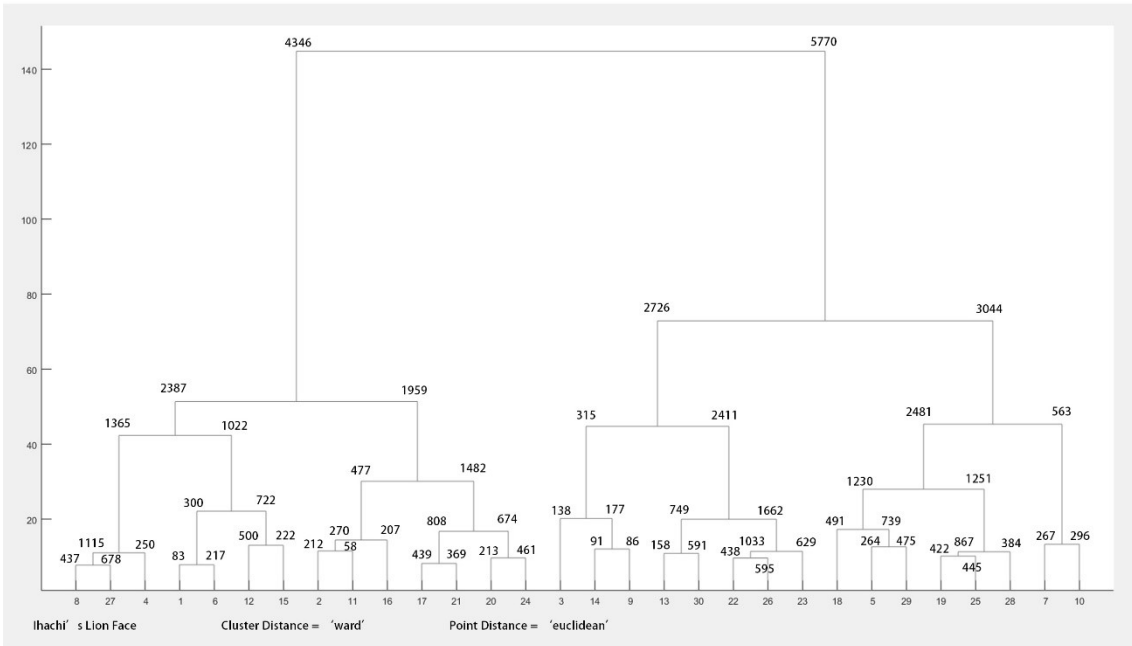
（ａ）Ihachi's Kibana lion dendrogram tree
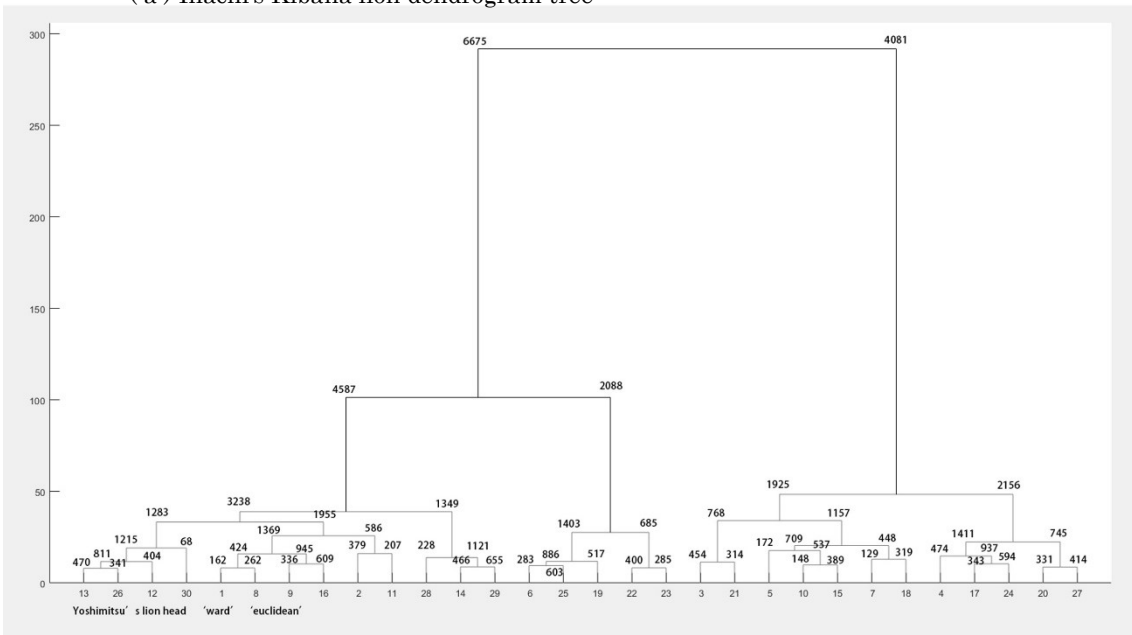
（ｂ）Yoshimitsu's Kibana lion dendrogram tree

Figure 5-8. Dendrogram Trees of Ihachi and Yoshimitsu's Kibana Lions

areas below the height of 20 in y-axis, the heights in y-axis of the nodes of Yoshimitsu appear to be relatively uniform and increased incrementally with a similar distance. Since the height of y-axis is the Euclidean distance between the centers of the two

connecting clusters, it shows that in the clusters with the link distance below 10, the distance between the end points in close proximity is similar, thus the facet normal vectors orient relatively equally to various directions.

While for Ihachi when the height in y-axis is below 10, the nodes have more significant disparity between the height in y-axis and the heights of the new nodes increase by different values. This result indicates that in the clusters with the link distance below 10, the distance between the end points in close proximity is not uniform. A part of the end points are in close distance, thus they connected into a cluster with a very low link distance, while for the next connection, they were merged
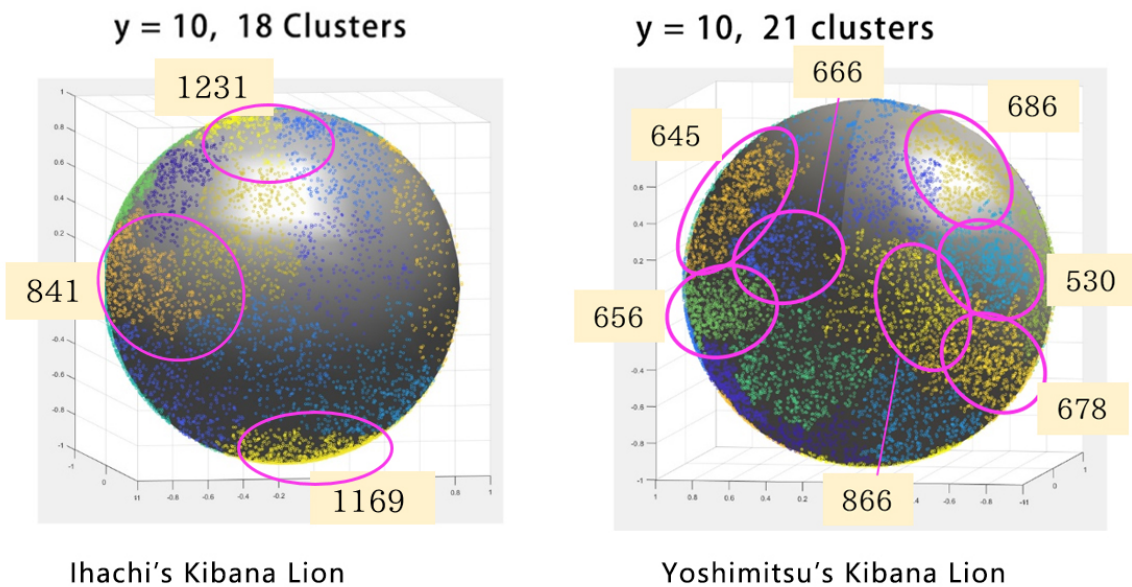
Figure 5-9 . Clusters with clustering distance over 10 of Ihachi's and Yoshimitsu's Kibana lions

into another cluster with a significantly further link distance. Therefore, this result indicates that there are several groups of end points gather in very close distance individually and also several groups of end points distributed sparsely, which represent the concentration of the orientations of the polygons on specific directions.

According to the structure of the dendrogram tree, the clusters with the clustering distance above 10 were calculated and plotted on the unit sphere in different colors

(Figure 5-9). By comparing the result between Ihachi and Yoshimitsu, it was confirmed that for Ihachi's Kibana lion, there are 3 big clusters including 841, 1169 and 1231 end points, and the position of the 3 clusters on the unit sphere is similar to the high-density areas on the density color map of Ihachi's Kibana lion. While for Yoshimitsu's Kibana lion, the numbers of the big clusters are significantly lower than Ihachi's result. The biggest cluster includes 868 end points and the other big clusters only includes similar number of end points, distributed on the areas similar to the high-density areas of the density color map of Yoshimitsu's Kibana lion.

For the clustering method, it became much easier to find the boundaries of the distributions of the ending points within a certain range of the number of ending points in a area on the unit sphere, which is more accurate than the density color map. While the density distribution color map could clearly visualize the transition of the distribution of end points and the location of the highest density points in a quicker and direct way than the linkage clustering.

5.5 Difference in the density distribution of Ihachi and Yoshimitsu

n = 40

n = 40

a.Ihachi's Wave

b. Yoshimitsu's Dragon Tail

n = 100

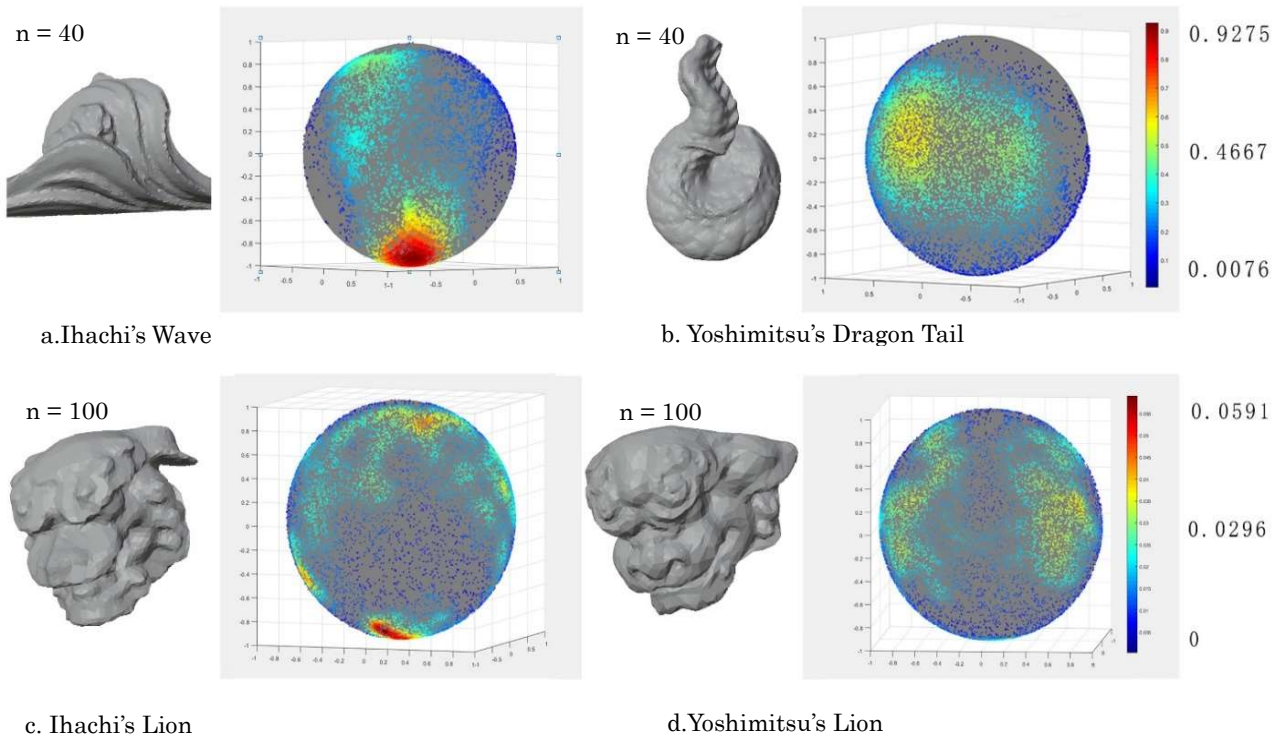n = 100

c. Ihachi's Lion

d.Yoshimitsu's Lion

Figure 5-10 . Distribution of Facet Normal Endpoints on the Unit Spheres of two groups of Ihachi and Yoshimitsu

Based on the density distribution of facet normal vectors on the unit sphere, differences in the density distributions of the works of the two carvers and a degree of similarity between the works of the same carver (Figure 5-10) were certified. Our findings were consistent with our direct observation, as reported in Chapter 2.

5.5.1 Density distribution of Ihachi's Sculptures

In section 2, Ihachi's wave form as "the lamination of wave plates," which gives the form a strong orientation in a specific direction was characterized. The red area of high density in the facet normal sphere of Ihachi's wave shows polygons concentrated in a specific direction—a finding that is highly consistent with our direct observation. In the case of Ihachi's Kibana lion, our direct observation of the lion's face led us to conclude that there was a distinct flatness in the form of the top of the head, the jaw, and the side faces, especially in the area around the mouth. The

presence of four red areas with a high density in the facet normal sphere of Ihachi's lion face showed a significant number of polygons in the overall form orienting towards the top, bottom and the left and right sides of the form, which is consistent with our direct observation. According to the distribution of the density of facet normal vectors of the two different thematic sculptures, the results reflect the distinctive specific orientation of the surfaces in the Ihachi form, which is manifested in the 2.5D form that tends to approach relief or the solid form with a hexahedral tendency.

5.5.2 Density distribution of Yoshimitu's Sculptures

As for Yoshimitsu's sculptures, in Chapter 3 the obvious composition of the spherical features observed both in the dragon tail form and the head form of the Kibana lion was noted. In the density distribution color map on the unit sphere of the dragon tail form, it is found that the overall density tended to be uniform and low, which is consistent with our direct observation. In the density distribution of the lion's head, although the overall density was relatively constant and low, there were two areas of medium density that were yellowish in color. These two regions are at an angle of 40-45° with the normal direction of the front view of the sculpture. This indicates the presence of oblique surfaces in the transition between the completely front-facing and completely side-facing faces in the model.

Chapter 6

Identification of the Carvings on the Arched Beams

Chapter 6. Identification of the Carvings on the Arched Beams

In this chapter, a trial of identifying the style characteristics of an anonymous wood carving on the arched beam of the shrine was implemented, which was considered that the sculptor might be Takeshi Ihachi by the researcher of the local museum. According to the method which was proposed in the former chapters, the high-resolution 3D scanning models of the anonymous beam carving and other four beam carvings in similar themes (two carvings of Takeshi Ihachi and two carvings of Goto Yoshimitsu) were collected. Then the color maps of the density distribution on the unit spheres to find out the similarities and differences between the beam carvings were generated and compared, which could be the hints of the style characteristics for the identification of the anonymous beam carving.

6.1 Direct observation and 3D data collection of the beam carvings

The Vivid 900 3D scanner and the Autodesk Recap were applied to create the original high resolution polygon models of the five beam carvings. The authorities of the two pairs of beam carvings made by Ihachi and Yoshimitsu were certified according to the inscriptions(刻銘) on the inner side of the wood carvings.

6.1.1 The anonymous beam carving of Shobunji Soshido

The anonymous beam carving (Figure. 6-1) is under the pent roof of Soshido(祖師堂) of Shobunji(正文寺) in Minami Bousou, Chiba. The theme of the beam carving is 'Wakaba Pattern(若葉文様)', which is a Japanese classical pattern with geometrically curved shapes of stems and fresh leafs that could usually observed on the beams of shrine and temples. According of the construction records of the temple, Takeshi Ihachi has participated in the manufacturing of the wood decorations. Also, the main shape of the beam carving appeared to be flat, focusing on the expression of

(a) Photo of the Beam Carving of Shobunji Soshidou
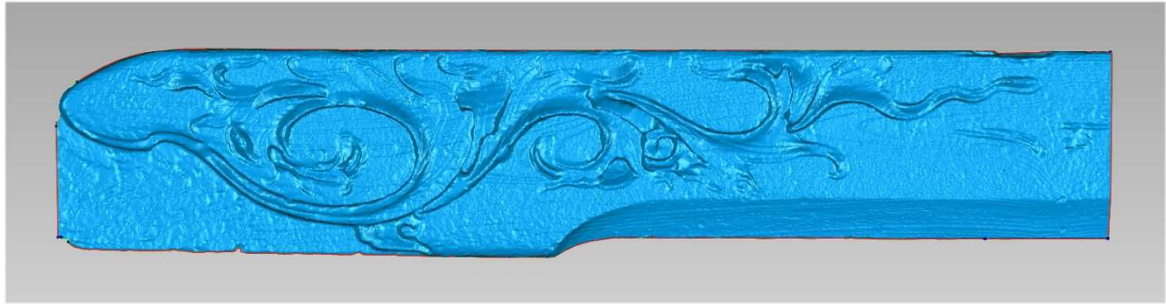
（b) Original Scanning model of the Beam Carving of Shobunji

Figure 6-1 The anonymous beam carving of Shobunji Soshidou

the geometrical curves and the shapes of the leafs tend to be limited to several special orientations of the surfaces. Therefore, the researcher of the local museum held an opinion that the beam carving might be sculpted by Takeshi Ihachi.

6.1.2 Two beam carvings made by Takeshi Ihachi

The two beam carvings are preserved in Oyamaji Fudodo（大山寺不動堂） and Shinkoji（真高寺） in Chiba. The shapes of the beam carvings are as shown in Figure 6-2 and Figure 6-3. The beam carving of Oyamaji is also in the 'Wakaba Pattern' with highly simplified curves. The beam carving of Shinkoji is located in the beam of the main gate of the temple(山門). The theme is the phoenix（鳳凰）pattern, and the shape appeared to be with a 2.5D style characteristic. The main shape of the phoenix tends to be flat, and the background around the phoenix was incised into a flat area with a lower depth.

6.1.3 Two beam carvings made by Goto Yoshimitsu

The two beam carvings are preserved in Myohonji（妙本寺） and Shozenji（勝
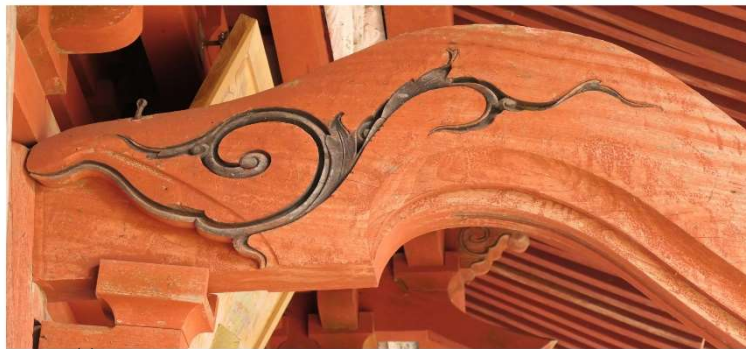
(a) Photo of the Beam Carving of Oyamaji Fudodo
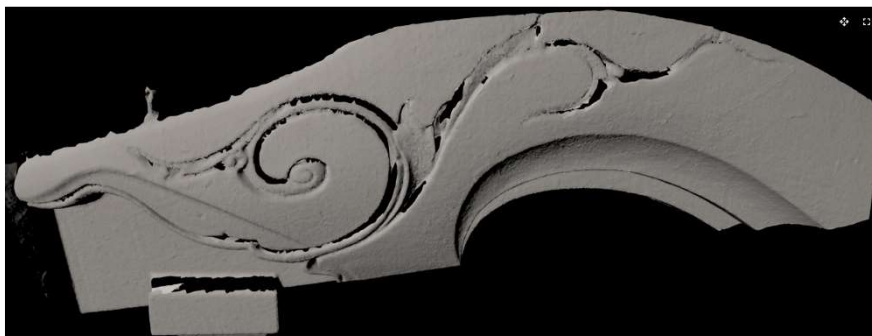
(b) Original Scanning model of the Beam Carving of Oyamaji Fudodo

Figure 6-2　Ihachi's beam carving of Oyamaji Fudodo

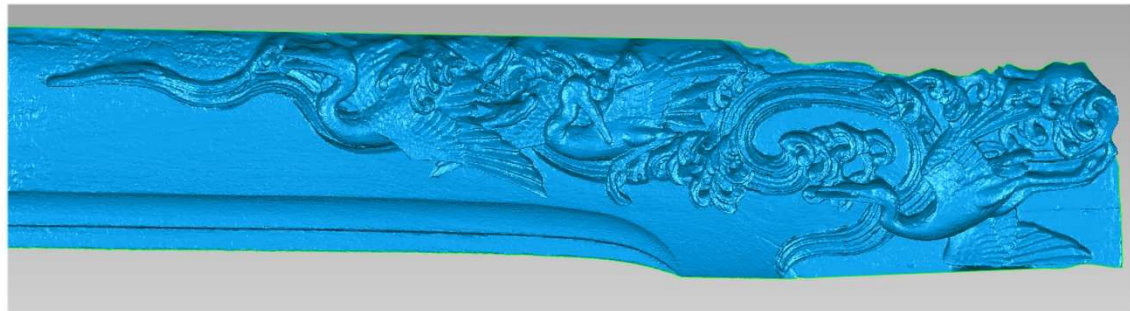(a) Photo of the Beam Carving of Shinkoji

(b) Original Scanning model of the Beam Carving of Shinkoji

Figure 6-3　Ihachi's beam carving of Shinkoji

善寺） in Chiba, shown in Figure 6-4 and Figure 6-5. The beam carving of Myohonji is in the theme of 'Crane and Wave（鶴と波）'. The shape of the wave is highly

(a) Photo of the Beam Carving of Myohonji

(b) Original Scanning model of the Beam Carving of Myohonji

Figure 6-4   Yoshimitsu 's beam carving of Myohonji

simplified into geometrical curved shapes, which is similar to the carved stems pattern. This type of simplification of stem and wave into curves in the traditional beam carving was common, which could also be seen in the old textbooks for the architect carvers in Meiji period, shown in Figure 6-6. The shapes of the cranes appeared to be more solid when comparing to the phoenix carving made by Ihachi. The shape of the body of the cranes shown the variation of the orientations of the surfaces.

The beam carving of the Shozenji is on the inner side under the pent roof. The theme is the pattern of 'Chrysanthemum and Stem（菊と若葉）', which is similar to the anonymous beam carving of 'Wakaba Pattern'. The shape of the stem was also highly simplified into the geometrical curves, but the shape of the chrysanthemum appeared to be solid.

(a) Photo of the Beam Carving of Shozenji
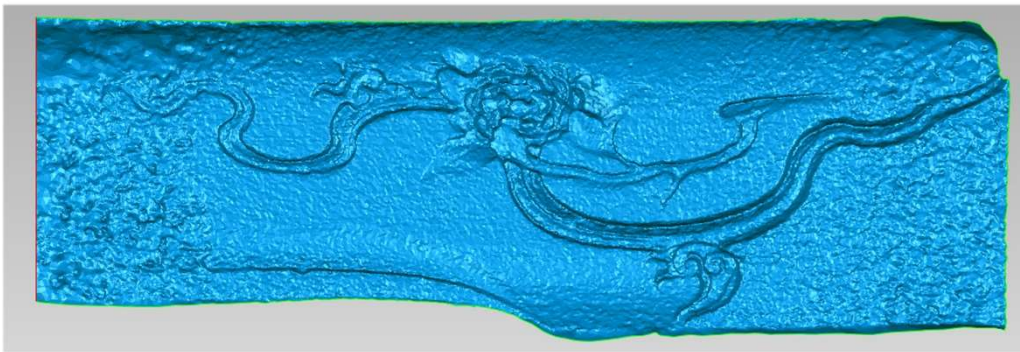
(b) Original Scanning model of the Beam Carving of Shozenji

Figure 6-5   Yoshimitsu 's beam carving of Shozenji

### 6.1.4 The technique of incised carving

Carvers usually used incised carving to gouge the geometrical curved grooves on the beam such as the 'Wakaba Pattern' that mentioned above. They used a U-shape chisel or a V-shape chisel (Figure 6-7) to gouge into the beam for multiple times along the curves that they drew on the beam, creating a curved groove with a U-shape cross section (Figure 6-8). With the incised carving, the concaved areas on the beam became the main shape of the wood carving.

6.2 Density maps of the anonymous beam carving

The curvature spectrum maps of the original high-solution model and decimated the number of the polygons were generated. By comparing the curvature spectrum
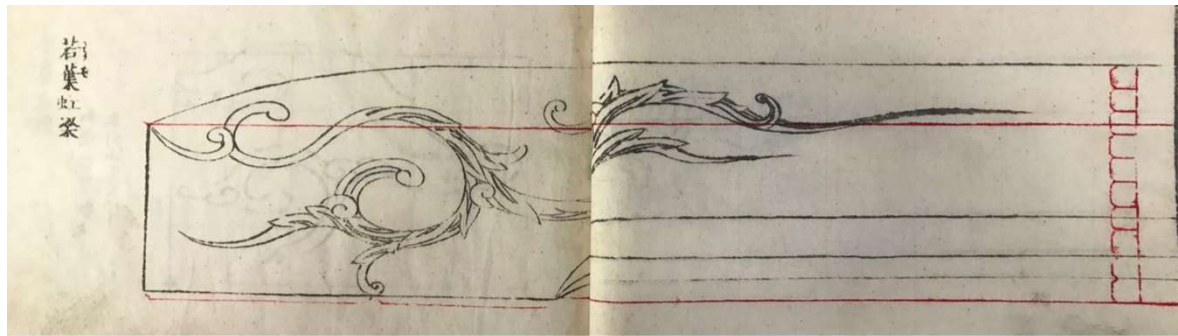
(a) Wakaba Pattern Design Sketch
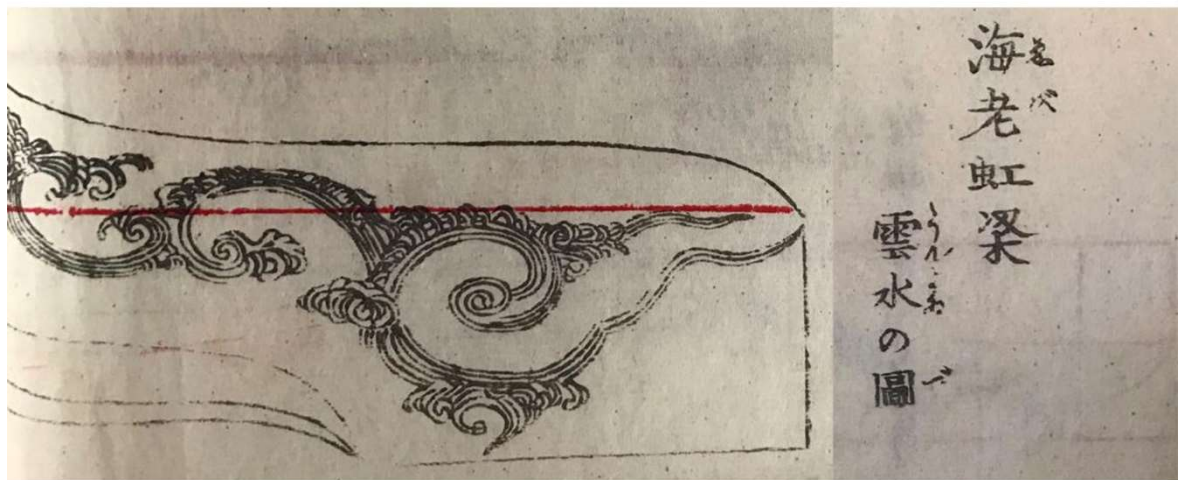
(b) Curved Wave and Cloud Pattern Design Sketch

Figure 6-6　Beam Carving Patterns Design Sketches in Carver's Textbook, Meiji

maps, the decimated model with about 30000 polygons was chosen as the decimated model (Figure 6-9).

According to the method of plotting the density of the end points of facet normal

Figure 6-7　Chisels for the incised carving

Figure 6-8　Cross-Section of the incised carving

vectors on the unit spheres that proposed in Chapter 4, the density distribution maps were generated with different parameter n (Figure 6-10).

Original Model   1407193 Polygons

Decimated Model   65000 Polygons

Decimated Model   30000 Polygons

Decimated Model   25000 Polygons
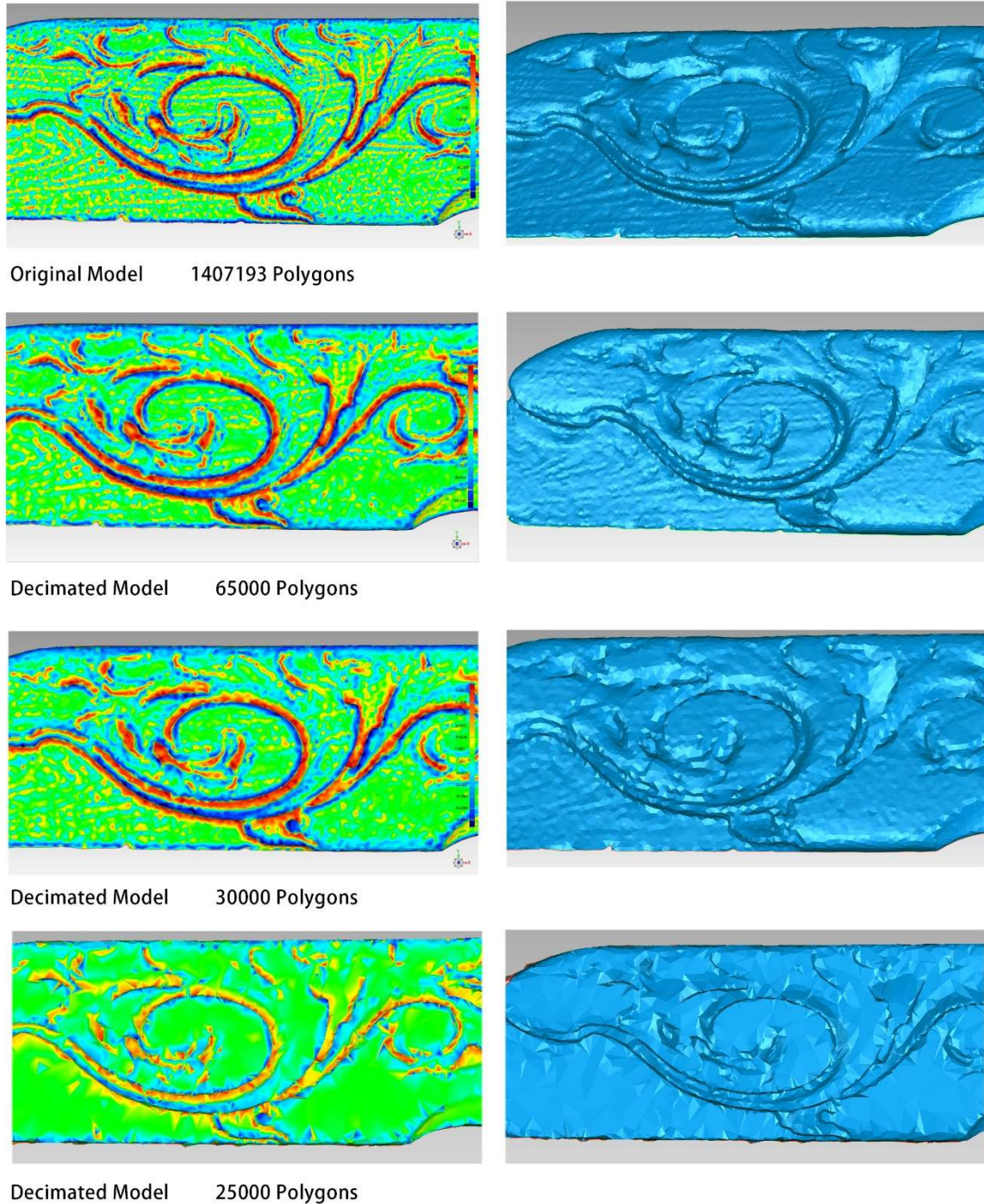
Figure 6-9   Curvature Mpas of Beam Carving of Shobunji with different polygon numbers
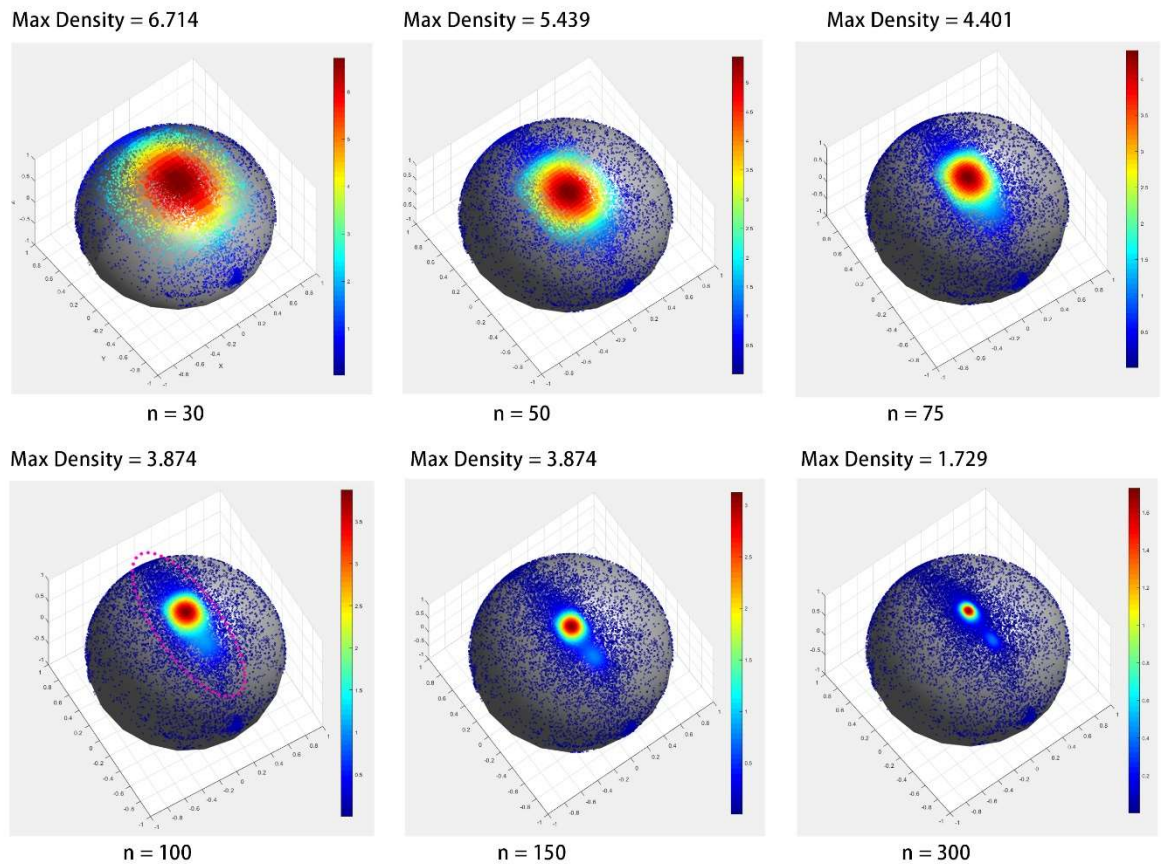
Figure 6-10　Density Distribution Color Map (Low-poly, 30000 Polygons) in different parameter n

According to the density distribution color maps, it was confirmed that a long and narrow shape of the distribution (Figure 6-10, points in the Pink frame) became more and more significant when parameter n is over about 100, with a red area with very high density in the center area. A new color bar of seven different color areas in repeating orders was used to analyze the density distribution map (Figure 6-11).
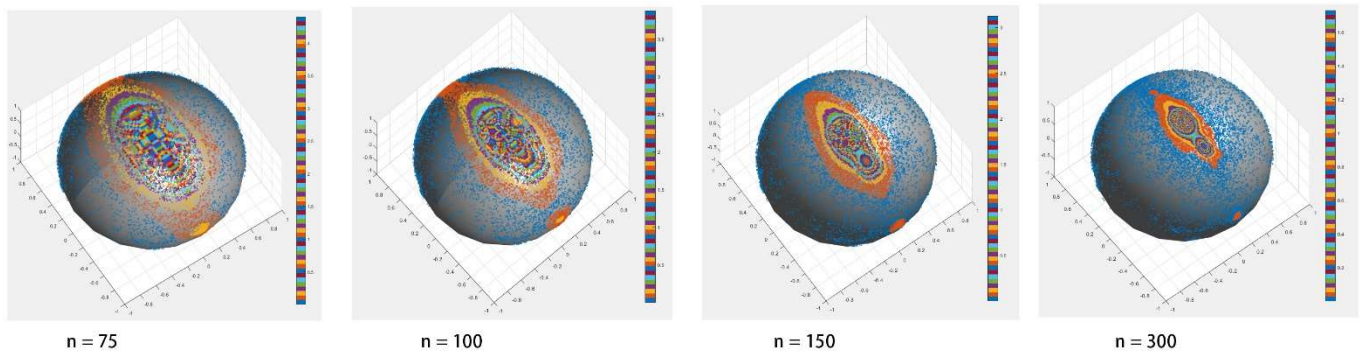
Figure 6-11　Density Distribution Color Map of repeating color orders
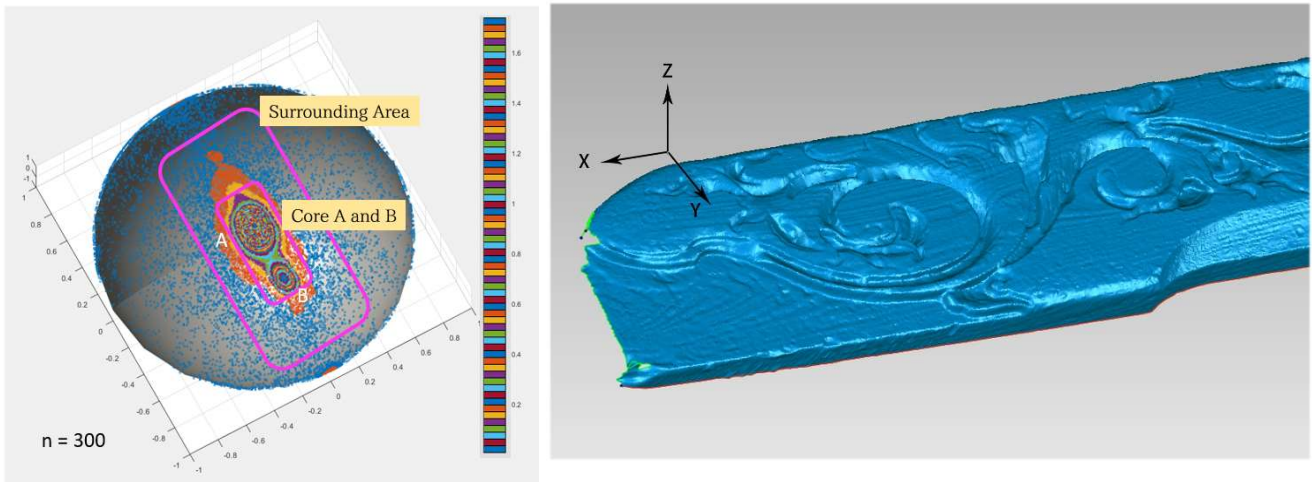
From the new density distribution maps of repeating color orders, it was found that the shape of the density distribution is close to rectangular shape, which has two basic parts: a long ellipse area with higher density in the center of the shape (Figure 6-12, Part 1) and the rectangular-shaped area surrounding the core (Figure 6-12, Core part).

The x-y-z directions of coordinate of the density distribution map and the 3D model is shown in Figure 6-12. Since the whole form of beam carving is close to a flat wood plate with the normal direction alone the z axis, the density in the core area (Area 1) in which a large amount of the end points belong to the polygons constructing the flat plane of the beam, is much higher than the other areas surrounding it. With the increase of the parameter n, while parameter n＞300，it was confirmed that there are two round core parts in the center area.

Since the core area is mainly consist of the normal vectors of the polygons on the
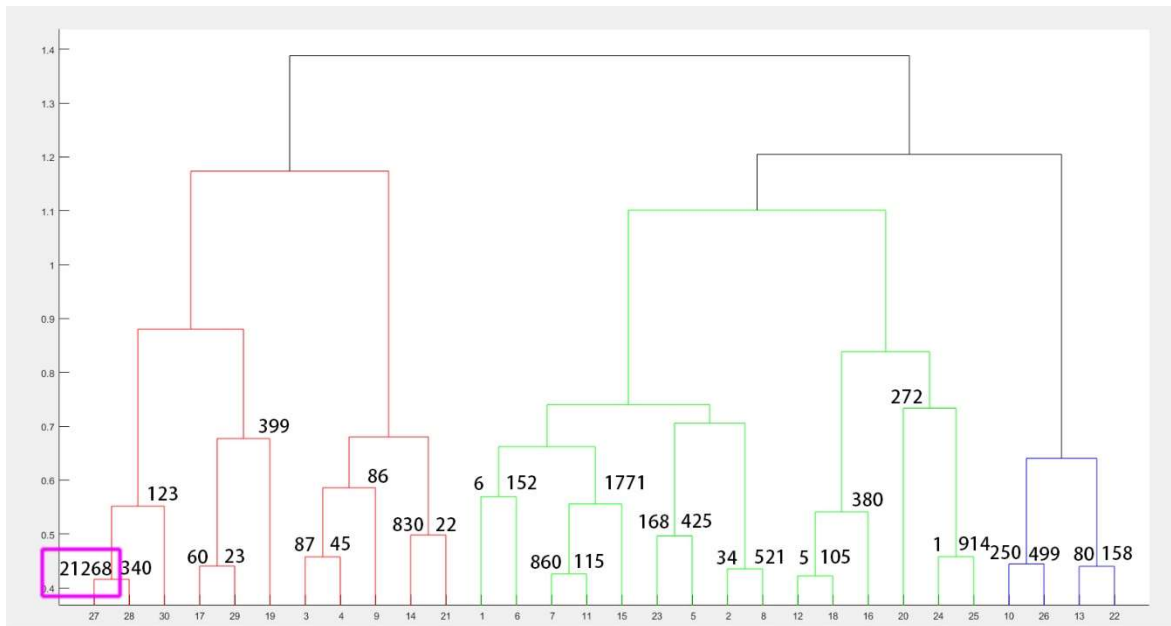
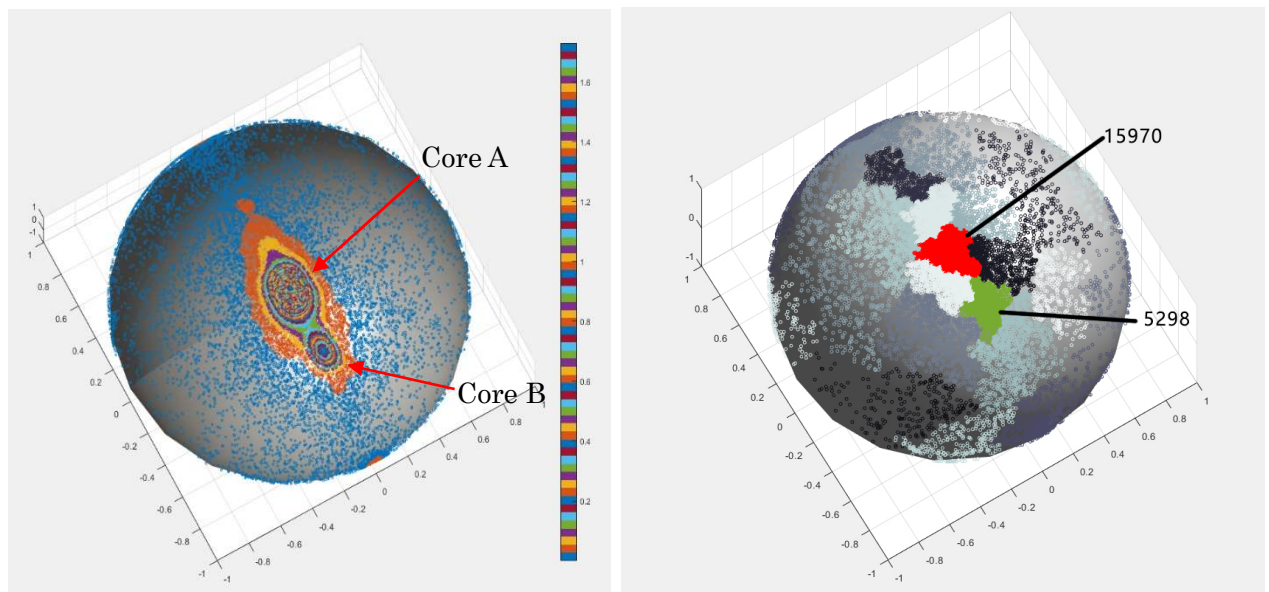Figure 6-13　Dendrogram tree of the end points in 30 clusters

Figure 6-14 Density Distribution of the rectangular area

flat plane, the linkage clustering was applied to the end points and generated the dendrogram tree to confirm the two core areas in the density distribution map. It was found that there is a huge cluster existing above the height of 0.4 in the y axis including 21268 end points (Figure 6-13). When the height of y axis goes below 0.4, the huge cluster 27 divided into two clusters including 15970 and 5298 end points.

The result of the linkage clustering is shown in Figure 6-14. The shapes of the boundaries and the locations of the two clusters are similar to the

6.3 Density maps of Ihachi's and Yoshimitsu's beam carvings

Density distribution color maps of Ihachi's and Yoshimitsu's beam carvings to confirm style characteristics with the same method in Section 6.2 were generated to confirm the similarity of Ihachi's beam carvings and the differences between the two carvers.

6.3.1 Density maps of Ihachi's beam carvings

The density distribution color maps of the beam carvings of Oyamaji Fudodo and Shinkoji are shown in Figure 6-15.

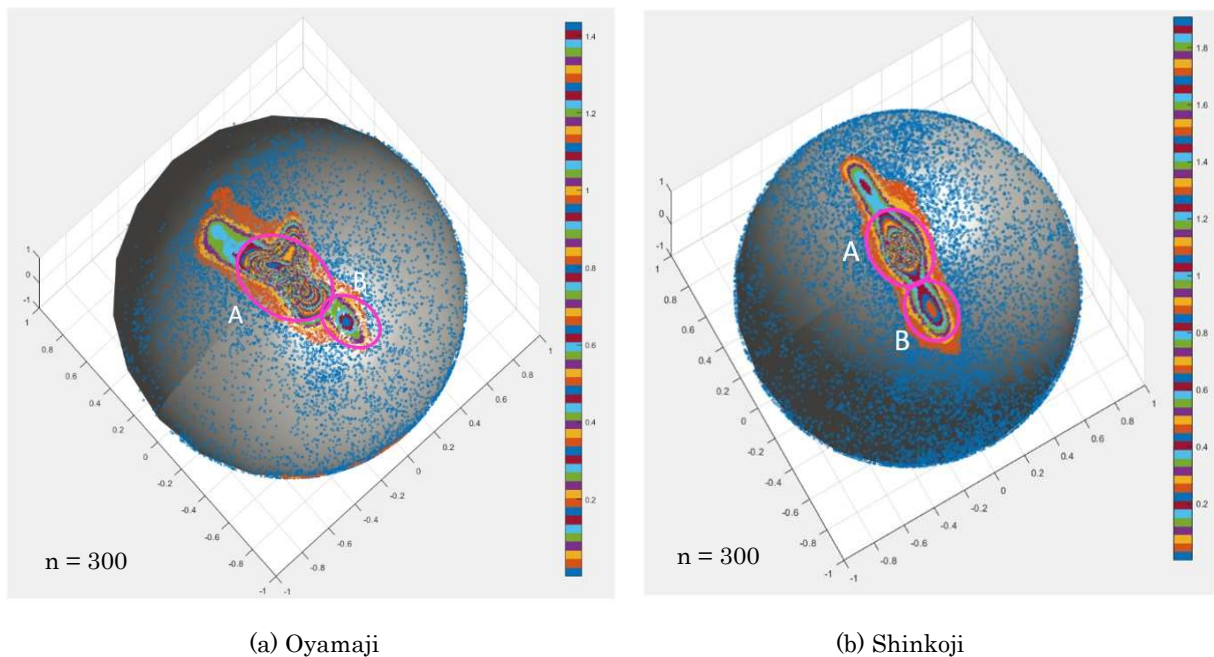(a) Oyamaji   (b) Shinkoji

Figure 6-15 Density Distribution of Ihachi's beam carving in Oyamaji and Shinkoji

From the density distribution maps it could be observed that in the center area of Oyamaji and Shinkoji, while parameter n＞300，two separated core areas could be observed, which is similar to the shape of the core area of Shobunji. The two

sepereated core areas indicate that the surfaces in Ihachi's beam carvings mainly orient to two directions: the normal vectors of core A concentrate on the normal direction of the flat plane of the beam, and normal vectors of core B concentrate on the direction tilting downward of about 30°.

6.3.2 Density maps of Yoshimitsu's beam carvings

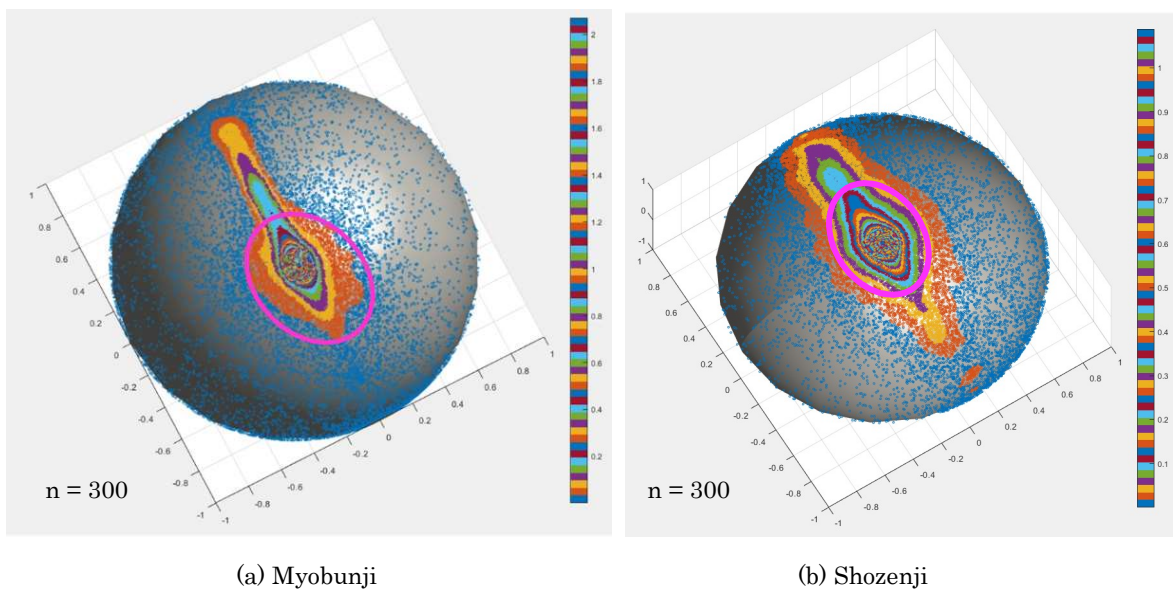The density distribution color maps of the beam carvings of Myobunji and Shosenji are shown in Figure 6-16.

(a) Myobunji   (b) Shozenji

Figure 6-17　Density Distribution of Yoshimitsu's beam carving in Myobunji

From the density distribution maps it was found that the whole shapes of Myobunji and Shosenji appeared to be unlike to the long rectangular shape of the density distribution maps of Ihachi's carvings. With the increase of parameter n, there is only one circle-shape core (Figure 6-17, pink frame) area in the density distribution maps of beam carvings of Myobunji and Shozenji, which are unlike to the shapes of the double core areas of Ihachi. This single core area and the concentric circles-shape areas surrounding the core area indicate that despite of the polygons of flat plane, the polygons of the incised carving areas such as the stem grooves, the crane forms in

Myobunji and the Chrysanthemum appear to be orienting to the directions in variety, which fitted the style characteristic of Yoshimitsu's dragon and Kibana lion that was confirmed in the former chapters.

6.4 Conclusion of the identification

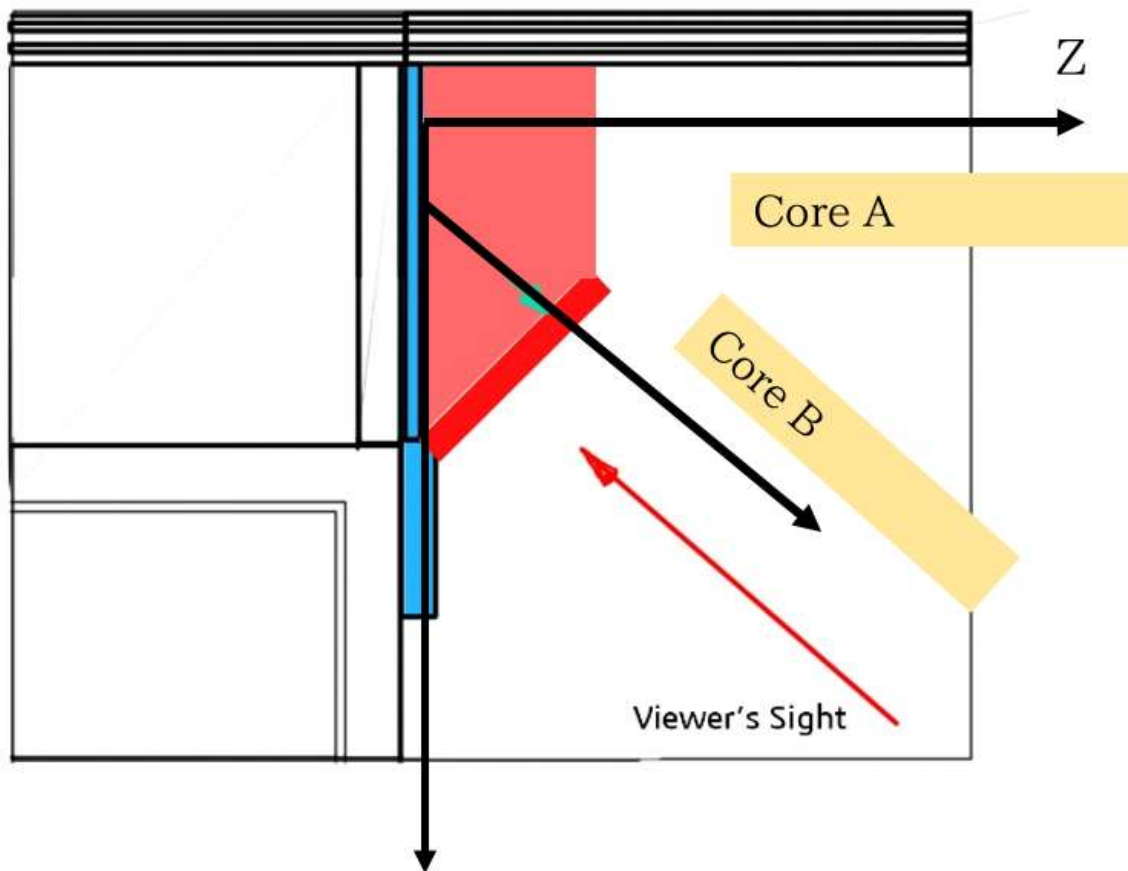By comparing the density distribution color maps, it was confirmed that the

Figure 6-18   Adjusting the orientation of the surfaces to match the viewer's sight

density map of the anonymous beam carving has similar characteristics of the shape of the distribution areas with Ihachi's beam carvings. In the density distribution of normal vectors of the anonymous beam carving and Ihachi's beam carvings, there are two round core areas of high density exist in the center part. This similar

characteristics indicates that the variation of the orientations of the surfaces in the anonymous beam carving and Ihachi's beam carvings mainly concentrate on two directions: the normal direction of the flat plane of the beam, and another direction with a downward slant of about 30 degrees. This special direction tilting downward is similar to the laminating direction of Ihachi's wave in Chapter 3, which was considered as the sculpting technique of adjusting the orientations of the surfaces of the form to the direction of the observer's sight (Figure 6-18), which could avoid the distortion of the form caused by the direction of the observer who stands at the downside of the beam carving [1].

While the silhouette of the density map of the anonymous beam carving is different from Yoshimitsu's density maps with concentric circles surrounding the core area, in which the surfaces orient to directions relatively equally with the directions represented by the end points in area surrounding the core in the density distribution map.

Chapter 7

The influence of the orientation distribution of Surfaces to the Sculptures

Chapter 7. The influence of the orientation distribution of Surfaces to the Sculptures

In Chapter 5, it was verified that the surfaces in Takeshi Ihachi's sculptures of the wave and the lion tend to concentrate toward several specific directions. While for Yoshimitsu, the orientation distribution of surfaces appeared to be more uniform. According to the observation and comparison of multiple sculptures by Takeshi Ihachi and Goto Yoshimitsu in Chapter 2, it was confirmed that seen in the two sculptors' other works. These characteristics are close to the sculptor's unique carving preference or style. Based on the basic theory of style design and the results of the analysis in the previous chapters, how the orientations of the surfaces might change
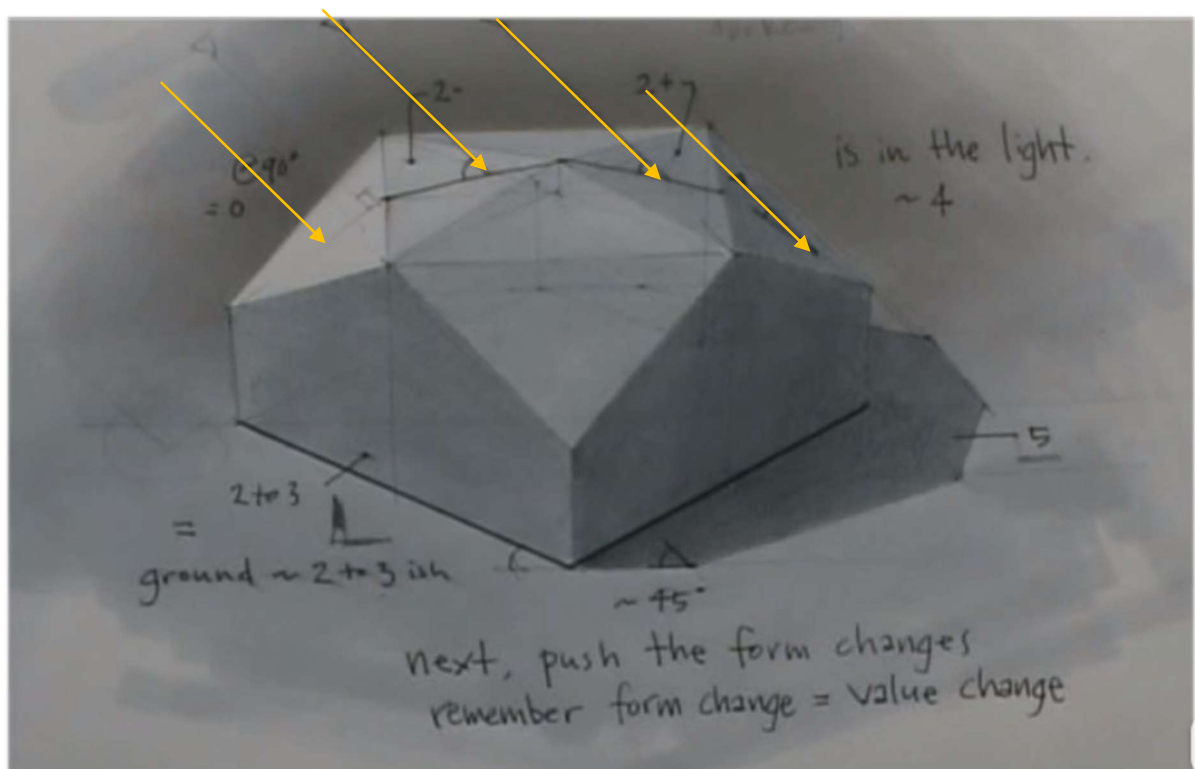

Figure 7-1. Brightness values of the surfaces change with the angles between the light

and the normal direction of the surfaces

the form of the sculpture and the reason why the two carvers chose their specific characteristics of the surface orientations to create the form was discussed.

The first important point that needs to be clarified is how the changes in the orientation of the surfaces in the sculpture might affect the sculpture. Surface, like the point or line, is a basic geometric element that consists of a three-dimensional shape. When light shines on an object with undulating surfaces, the light that hits each local surface will reflect at different angles according to the different orientations of the surfaces. Then the reflecting light is captured by the human eye at different values of brightness. The observer perceives the three-dimensional shape and volume of the object based on the difference in the brightness of the surfaces (Figure 7-1) [1]. In Camille Mauclair's document, the sculptor Rodin also talked about the relationship between the orientation of the surface and the mass.

"When you start a sculptural work, always think of the surfaces as the tips of the volume."

In the modernism sculptors' and the art educators' opinions, the variation and distribution of the orientations of the surfaces in the sculpture could be considered as an essential factor that determines the 3-dimensional volume of the forms. In the following section, the influence of the orientation of the surfaces in the forms of Takeshi Ihachi and Goto Yoshimitsu on the volume and the mass of their sculptures was discussed.

7.1 Similarity of Goto Yoshimitsu and the Western sculptural forms

7.1.1 Creating the mass with the variation of the orientations of surfaces

Art history researcher Rudolf Wittkower quoted the sculptor Rodin's description of his workflow [2] to explain how the distribution of the orientations of the surfaces in the sculpture may influence the form:

"When I start to sculpt a figure, first I look at the two sides of the figure: the front

and the back, and the left and right sides... The next thing I do is look at the profile from diagonal angles. I rotate the clay and the model alternately, comparing and tweaking the form... In this way, it gradually guided to make a complete circle around the figure ...."

" Always consider the geometrical forms from the original natural shapes. Create the form by contours in perspective depth. These are my criteria."

Wittkower also summarized that the effect of this technique is to create "the mass of the form", or "the vividness that radiates outward from the inner of the status".

Although the concept of "vividness" is mysterious, the concept of "the mass of form" in its description is relatively easy to understand. It could be considered as the three-dimensional sense of volume of form. In the early stage of Rodin's workflow, he consciously kept doing two things which were also applied in this research:

1. keep the clay model in the geometric polyhedral form

2. repeatedly confirmed the orientation relationship between each large surface from multiple angles.

In Rodin's explanation of his workflow, the reason for keeping the clay model in the geometric polyhedral form (the rough carving introduced in Chapter 4) in the early stage is that it allows for a quick and accurate grasp of the composition of the surfaces in different directions, as well as for quick modifications and adjustments without complex details. When adjusting the surfaces in the sculpture from each different angle, Rodin focused on shaping and adjusting in the direction that extends from the point of view of the angle through the surface to the interior of the sculpture.

With this method, he wrapped up the volume of the sculpture with the combination and correspondence of the surfaces in different orientations [3] so that the sculptural form could maintain a three-dimensional mass and volume from multiple viewing
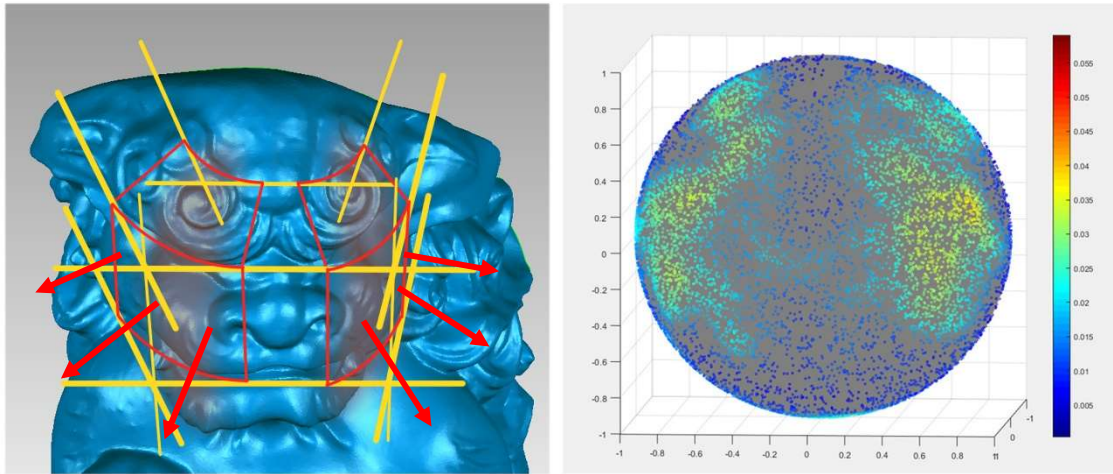
Figure 7-2. Transition Surfaces between the front and side surfaces

angles, which is similar to the style characteristic of connecting spheres extracted from the forms of Yoshimitsu's dragon tail and lion head. In Chapter 5, the end point density map of the form of the dragon tail and lion head were calculated. The overall density distribution is relatively uniform, with the end points distributed at an angle of approximately plus or minus 45 degrees from the frontal orientation of the model. This result indicates that in Goto Yoshimitsu's sculpture, the surfaces of each area of the model are consciously arranged to orient to different directions (Figure 7-2). This similarity in Rodin's sculpting concept of creating the mass from various viewpoints and the relatively uniform density distribution of the orientations of the polygons in the 3d model indicates the reason why Yoshimitsu's sculptures always have the style characteristics of connecting spheres: he aimed to create "the mass of the form" in his sculptures through this sculpting method.

7.1.2 Sculpting Practice of the mass and volume

In this section, a form analysis of a sculpting practice of the Venus head of Milos was used to explain the concept of creating the mass and volume of the sculpture by the variation of the orientations of the surfaces. The head sculpture was sculpted in

water clay by the author in the course of composition training and then remolded in plaster. Although the lack of experience and the understanding of the concept of volume in sculpture caused many problems in the reproduction of the head, it is appropriate to compare it with the original model. The differences between the practice and the original form could be the reference to understand the concept of creating the mass.

The main problems commented by the teacher in the course review are shown as below:

a. Insufficient mass and volume.

Compared to the original model, the practice work does not have enough volume and does not have a good understanding of the composition of the large blocks. Specifically, compared to the original model, the volume of the hair and the back of the head, which is covered by the hair, is obviously lacking in mass.

As shown in Figure 7-3-c, the lack of volume in the hair and the back of the head in the practice work can be observed in comparison with the original model. At the beginning of the creation of the head, it is necessary to sculpt the head from different angles while considering the overall three-dimensional structure of the head. At the same time, it is essential to sculpt the hair as a three-dimensional structure made of different materials with a certain volume covering the top of the head [4]. In the observation of the original form, it can be seen that there is a correspondence of two surfaces in the direction of the axis that passes through the imaginary center point inside the form [5]. For example, as shown in Figure 4, the bun hair of the backhead in the original form is not shaped in detail like the real human hair. In contrast, the surface of this area is relatively flat but not a fluffy sphere. The main surface of this area is oriented along the axis of the normal direction of the surface and passes through the interior of the sculpture to the flat surface of the forehead,

(a)   the practice form

● ORIGIN
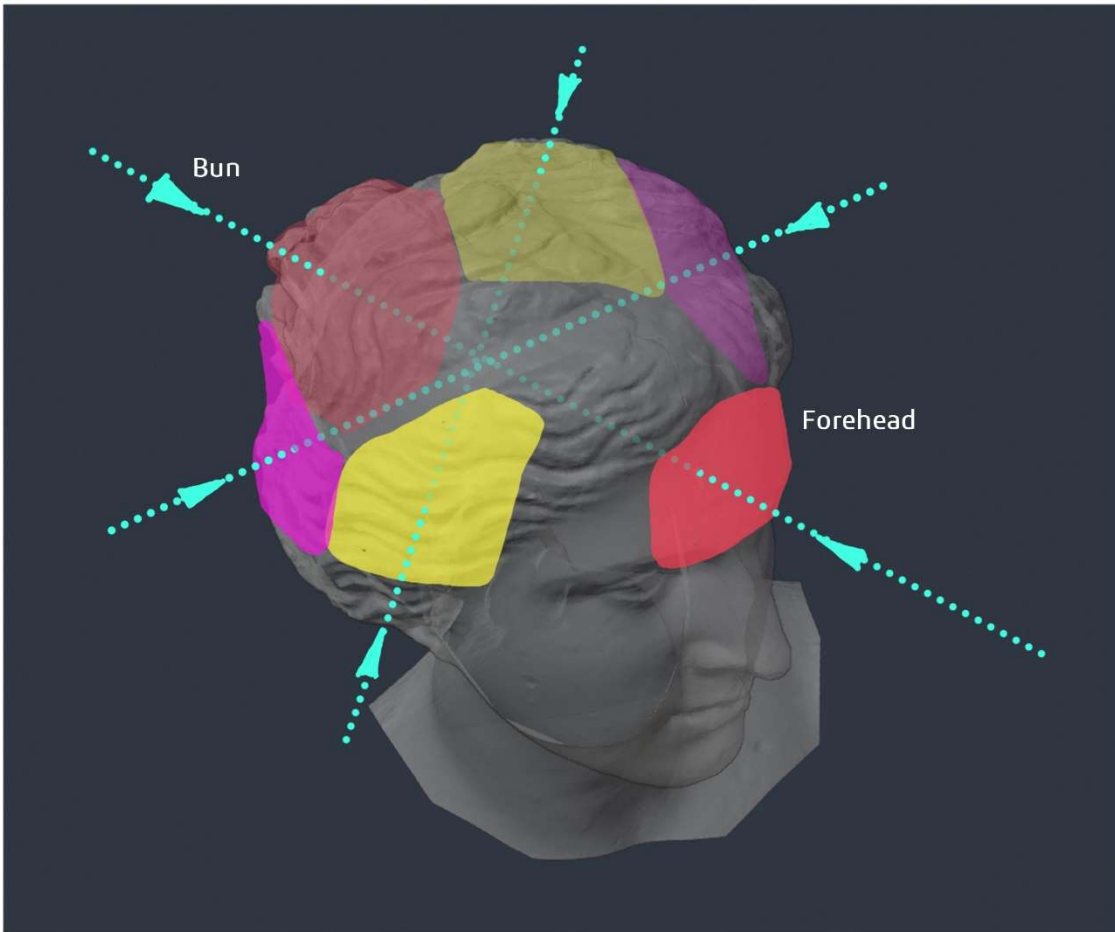● COPY

(b)   the origin form

A
C
B
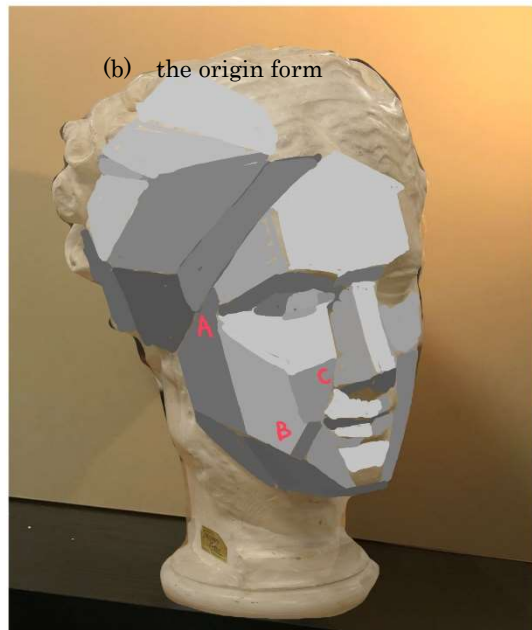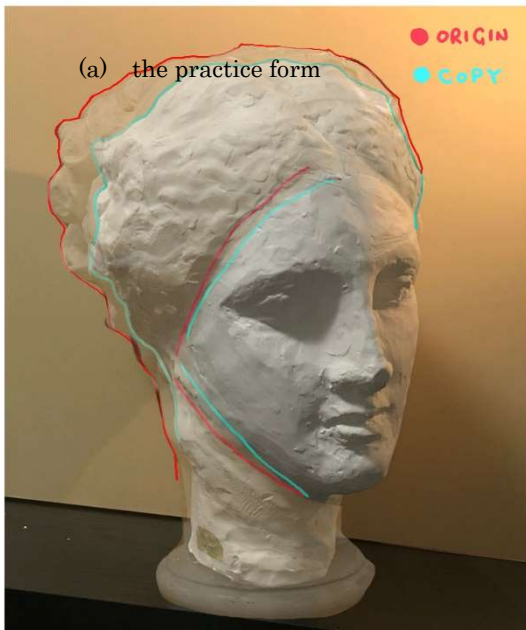
(c)   Volume Comparison

(d)   Abstracted Surfaces

Figure 7-3. Comparison of the Copy and the Origin Forms of Venus de Milo

(a) Surfaces of the original form in different angles

Bun

Forehead

(b) Corresponding surfaces marked in different colors

Figure 7-4. Corresponding relationship of the surfaces

which creates a correspondence in the composition of the form. With multiple sets of the corresponding surfaces at different angles, the sculptor could wrap up the mass and the volume of the sculpture with the surfaces surrounding the center of the form.

b. Insufficient transition between primary surfaces

The sculptor spent too much time on a specific angle and did not keep observing and modifying the transition between the primary surfaces from different angles during the sculpting process. The insufficient transition might also cause a lack of mass and the tensity of the form.

Compared with the original sculpture, the shape of the face in the practice work is not luscious enough. Surfaces of the cheek are too flat, and the front part of the cheek changes to the side part (A, B in Figure 7-3) in a sudden, and the transition surface(C in Figure 7-3) between the two is too small with the monotonous change in orientation [6].

Based on the analysis, the similarities between the modern Western sculptures represented by Rodin and Goto Yoshimitsu's sculptures. Yoshimitsu consciously arranged the orientation of each area in the wood sculpture, focusing on the transition between the front and the side, creating a real volume in the sculpture and making the shape have a strong three-dimensional sense of mass in multiple angles was analyzed. As described in Chapter 1, in the late Edo period, wood carvings for architectural decoration had already reached a high degree of completion in terms of realistic three-dimensional mass and volume. Goto's technique of creating realistic three-dimensionality by enriching the orientation of the surfaces in the sculptures could be regarded as one of the representative cases in that period.

7. 2 Takeshi Ihachi and the Japanese Relief

In Chapter 3, the stylistic features of the laminating layers in the wave form of Takeshi Ihachi and the cubic planar composition features of the Kibana lion form

were extracted. The quantitative analysis in Chapter 5 showed that in the wave form of the Takeshi Ihachi, surface orientations concentrated in the normal direction of the laminating layers, and in the cuboidal form of Kibana lion, the surface orientations are concentrated in the top, bottom, and left and right directions. In Chapter 2, the theory in the history of Japanese sculpture that "wood carving for architectural decoration was started from the three-dimensional expression of decorative architectural painting was introduced. According to this opinion, the evolution of architectural decorative wood carvings from the Momoyama period to the late Edo period can be interpreted as a process of 2.5D/3D transformation from screen paintings(屏障画) and gold lacquer(蒔絵) in the decorative buildings and temples of the Kamakura and Muromachi periods. The concept of "2.5D transformation" refers to the style characteristic that the reliefs based on 2D paintings have a three-dimensional shape in the frontal direction, but from other angles such as the side view, they have only increased in thickness and do not have a three-dimensional shape from that angle. This 2.5D three-dimensional technique might be considered as one of the reasons for the surfaces orienting in specific directions in Takeshi Ihachi's sculptures.

7.2.1 law of frontality in Takeshi Ihachi's sculptures

The sculpting technique of "2.5D transformation " could be widely seen in many ancient sculptures. Julius Lange, a 19th-century landscape painter and art historian, proposed the concept of "The law of frontality (sculpture 彫刻の正面性)" in his

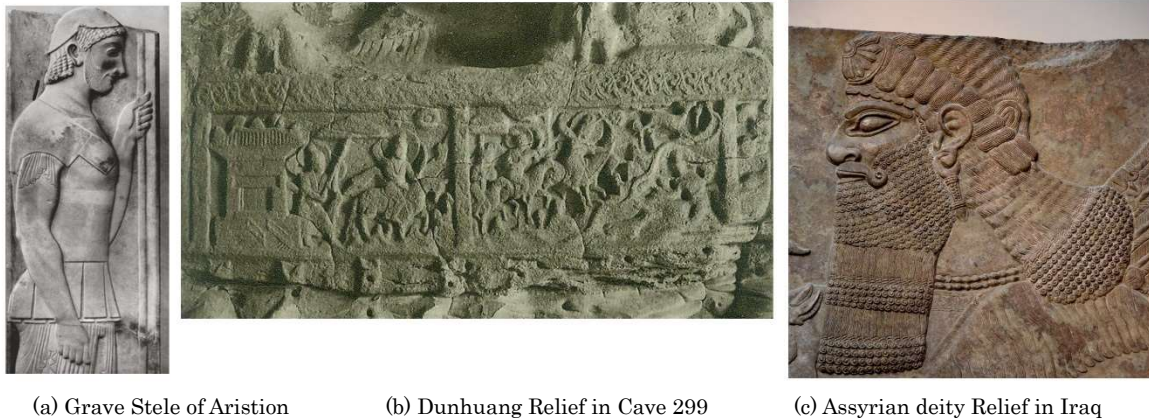(a) Grave Stele of Aristion   (b) Dunhuang Relief in Cave 299   (c) Assyrian deity Relief in Iraq

Figure 7-5. Ancient Reliefs following the law of frontality

study of the shallow reliefs of ancient Egypt. The concept of the frontality of sculpture indicates that in ancient relief carving, the form was shaped in a frontal direction toward the sculptor and the viewer [7]. This frontality could also be seen in ancient Greek sculptures such as the "Grave Stele of Aristion" from the 6th century B.C., a group of relief sculptures from the Bei Zhou(北周) period in Cave 299 at Dunhuang, China, and a 9th century B.C. shallow relief carving of an ancient Assyrian deity from Iraq (Figure 7-5). Although the paper for the sketch has not been invented in that period, the early sculptors might start their works from the rough chalk sketches on the rocks. These chalk sketches were considered as the 2D base of the reliefs [8].

This frontality also exists Takeshi Ihachi's reliefs. As shown in the figure below (Figure 7-6), it is a personal collection "Rhinoceros on the wave(波に犀)" by Ihachi. On the front side is a relief carving with a certain volume. Style characteristics of laminating layers could be observed in the wave form. On the backside, the composition is very similar to the relief in the front side, but the shape is close to a flat plane. According to the similarity of the composition, the three-dimensional relief on the front side can be interpreted as the result of the 2.5D transformation of the backside, along the vertical direction to the front.

(a) Frontside

(b) Backside

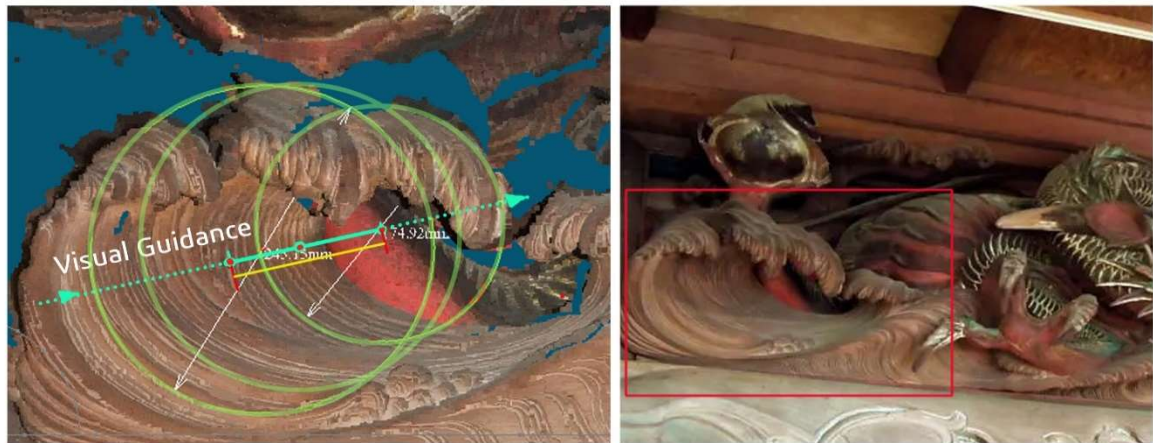Figure 7-6. Rhinoceros on the wave, personal collection of Ihachi's relief

Figure 7-7. Visual Guidance caused by the laminating Circle Features

However, a problem often existed in the three-dimensional expression of the ancient reliefs [8]. Due to the limitations of the thickness of the reliefs, it was difficult to express the perspective depth along the normal direction of the relief, which reduced the visual depth of the shape. This problem also existed in the wave carvings of other carvers in the same period with Takeshi Ichihachi. One of the reasons why the wave shape of Takeshi Ihachi has a better three-dimensional visual depth than the other carves' works is because of the style characteristic of laminating layers. As shown in Figure 7-7, in the wave form of Ihachi's relief of Chizoji Temple, multiple circle features were extracted from the laminating layers of the waves according to the method in Chapter 3. When the viewer watches the wave form, the viewer's sight might be visually guided by the repeated circular features hidden in the form. The distance that the viewer's sight moves along the center of the repeatedly arranged circular features(Yellow line, Figure 7-7) enhances the visual perspective depth of the form in the frontal direction. A similar method of expression to increase in perspective depth through overlapping layers could also be found in the Chinese ink painting of groups of mountains [10].

The density distribution of the polygon orientations of the wave sculpture in the

(a) from view's sight   (b) from the front sight   (c) density distribution
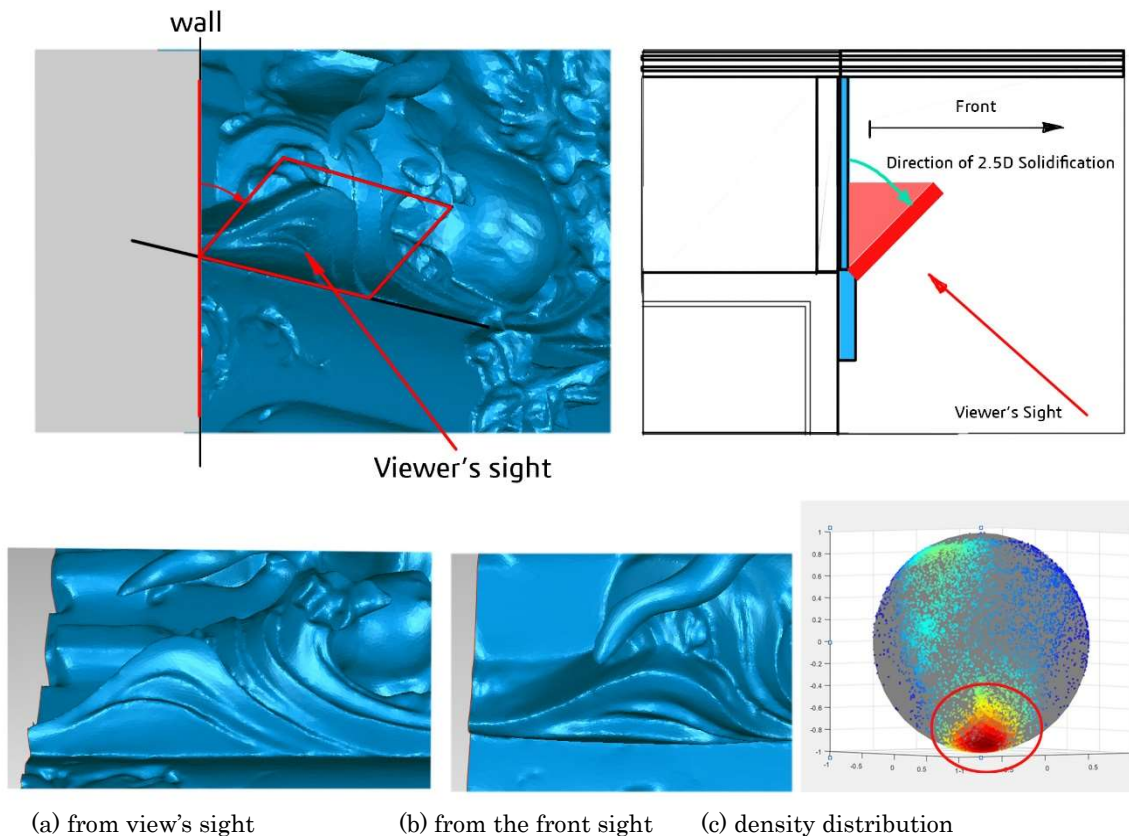
Figure 7-8. Adjusting the direction of 2.5D solidification to the view's sight

Fudodo Hall in Chapter 5 shows that 42.4% of the polygon in the wave form is oriented diagonally downward but not the directly front direction of the form. From a lateral perspective of the relief, the increased thickness of the 2.5D transformation has a triangular shape. Since the reliefs of the pent roof(向拝) and the Waki Shoji(脇障子) were usually placed on the high walls, the normal direction of laminating layers is modified due to the consideration of the viewers' sight when they look up to the relief from the downside of the pent roof [9]. The direction of the laminating layers was generally adjusted to an angle of about 45 degrees downward from the wall to prevent the sculptures from being deformed by the perspective of the viewer looking up from below (Figure 7-8).

Figure 7-9. Hard edges on the transection areas

7.2.2 Ihachi's Kibana and the Rough Sketch

Takeshi Ihachi's Kibana lion is a solid sculpture with real volume. However, according to the density spectrum of the surface orientations in Chapter 5, the density distribution of the Kibana lion is not uniform like Goto Yoshimitsu's Kibana lion. The orientations of the polygons concentrated on the top, bottom, and left and right directions. Therefore, the composition of Ihachi's Kibana lion is close to a group of cubics but not connecting spheres like Yoshimitsu.

Furthermore, geometrical curves could be observed in the contours of the facial areas and the edges of the mouth and jaw area (Figure 7-9). According to the workflow of sculpting a Kibana lion, the cubical form and the geometrical curves might be related to the three-view sketches (下図) used in the early carving stage. In
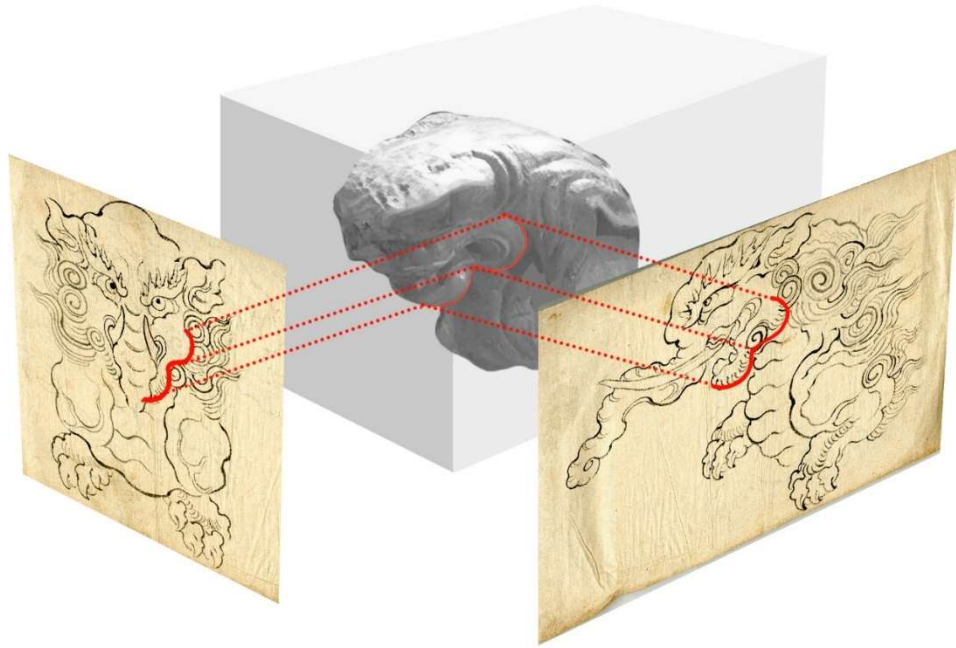
Figure 7-10. Mapping the 2d curve in the sketches into 3d edge on the sculpture

Chapter 3, the process to copy the three-view sketches of the front view and side view to the woodblock were introduced. In the early Edo period, the painters of Kano Style(狩野派) were invited to create reference sketches of reliefs for the carvers of the Nikko Toshogu Shrine. Later on, this type of sketches was widely used in the form design of the sculpture. It became an essential part of the workflow. The sketches are painted by a brush dipped in black ink on the rice paper. The sketch of relief is usually front-view. While for the solid sculptures, there are usually a front-view and a side-view, sometimes including a top-view. Figure 9 shows a front view and a side view of a Kibana Tapirus(獏). Before the rough carving begins, the carver would copy the two sketches onto woodblock as references for the contours and primary edges of the sculpture. Then the carver proceeds deeper into the wood in both the front and side directions to match the 2D curves on the front view and the side view into a 3D contour line of a solid form [11] (Figure.7-10). This process could be considered as a multiple 2.5D transforming proceeding along the front, side and top directions. The

Figure 7-11. Kibana Elephant of Komyoji Temple, Tokoname

forms of the 2.5D transforming finally intersected together into a solid form. Since there are only three directions that 2.5D transforming proceeds, the visual perspective depth mainly focused on three directions of the viewpoint: the front, the side, and the top. Therefore, this sculpting method might be one of the reasons why the forms of Takeshi Ihachi has geometric curves and cubical forms. An extreme example of this matching method is the Kibana Elephant of Komyoji Temple(光明寺) in Tokoname(常滑市), Aichi(Figure.7-11). However, the "line" in the sculpture is a geometric element that does not exist in the natural world but is created by subjective abstraction. Therefore, in sculpture, the sculptor usually eliminates the prismatic inflections between surfaces by adjusting the transition surfaces in multiple directions.

In this chapter, how the distributions of the orientations of the surfaces might influence the mass of the form were introduced. And the possible reasons for the difference in the style characteristics between Ihachi and Yoshimitsu's sculpture forms were discussed. Both of the style characteristics aim to increase the visual mass and volume of the sculpture. For Yoshimitsu, he chose the way of increasing the variation of the orientations of the surfaces to wrap up a real volume of the form, which is similar to the concept of western sculpting. While for Ihachi, he used the specific laminating layers to create a "fake" visual perspective depth of the relief, which is similar to the eastern painting skill, and this method also influenced his solid

sculptings such as the Kibana.

Reference

1. Scott Robertson，Scott Robertson's How to render, Design Studio, 18-19, 2013

2. Rudolf Wittkower，彫刻 その製作過程と原理，池上忠志 監訳，中央公論美術出版，平成六年

3.岩野勇三，彫刻――製作と技法の実際，日貿出版社，68，1982

4.岩野勇三，彫刻――製作と技法の実際，日貿出版社，80，1982

5.岩野勇三，彫刻――製作と技法の実際，日貿出版社，165，1982

6. https://www.perankhgroup.com/egyptian_art.htm

7. Wen c. Fong, Toward a structural analysis of Chinese landscape painting, Art Journal, 28, 388-397, 1969

8．伊東龍一，彫物大工の活動と工夫、彫物の未来（若林純，社寺の装飾彫刻・関東編下），日貿出版社，2015,8

9. Fukue, K., The formation of the concept of a solid in Sculpture, Journal of Graphic Science of Japan 42, 57-62, 2008

Chapter 8

Conclusion

Chapter 8 Conclusion

8.1 Style Characteristics in Ihachi's and Yoshimitsu's Sculptures

Starting from the geometrical features of the 2D and 3D composition relationships, the style characteristics in the four wood carving of the temple and shrine by Takeshi Ihachi and Goto Yoshimitsu were analyzed. In Group 1, the composition relationship of Ihachi's Wave sculpture showed the possibility of recomposition of the unique dynamic form of the Wave with multiple laminating flat layers. The style characteristic of the 'Connecting Spheres' in Yoshimitsu's Dragon sculpture shows the real mass and volume of muscle in the sculpture. By comparing the composition relationship between these two style characteristics, the differences in the representative forms of Ihachi and Yoshimitsu were examined.

Among the two Kibana lions in the second group, cubes constructed by flat plane features in Ihachi's form were extracted. For Yoshimitsu Goto, connecting spheres were extracted in the form, which is similar to the characteristic of the dragon tail. According to the stylistic features of the four sculptures, it was found that the style characteristics of Ihachi Takeshi's sculptures orient to specific directional. In contrast, the connected spheres of Yoshimitsu's sculptures have a relatively uniform distribution of orientations.

Based on the laminating layers and the connecting spheres extracted from the wave and the dragon tail, models were created to visualize and to explain the style characteristics of the two sculptures amd displayed them in an exhibition of sculptures by Takeshi Ihachi and Goto Yoshimitsu. According to the feedback from the viewers, 81% of them said that they understood Ihachi Takeshi's laminating layers and 49% of them understood Yoshimitsu Goto's connecting spheres.

8.2 Quantification and Visualization of the Orientation Distribution of the surfaces

To quantify and visualize the distribution of the orientations of the surfaces in the sculpture, the orientation of the surfaces that can influence the primary form of a sculpture were transformed into facet normal vectors of a polygon mesh, which can then be analyzed quantitatively and visualized by projecting the facet normal vector of the whole polygon model onto a unit sphere. The density of the facet normal vector endpoints distributed on the unit sphere indicates the degree of concentration in the orientation of the surfaces. Using this approach, it was confirmed differences in the orientation of faces in two sculptural forms carved by Ihachi Takeshi and Yoshimitsu Goto, as well as the similarity of such characteristics between different works of the same author. Both direct observation and the applied density analysis showed that the orientations of the surfaces in Ihachi's sculptures usually focus on several specific directions, especially for the sculptures with the style characteristic of laminating layers. At the same time, the concentration on the specific directions might also lead to a strong sense of a cubic form in which the transition of the faces is not round and natural. In contrast, the density distribution of Yoshimitsu's sculptures tends to be uniform, which clearly shows the importance that he attached to the changing transitions of surfaces in his forms and his awareness of creating a sense of volume by using different surfaces oriented in a variety of directions.

8.3 Identification of the anonymous beam carving

The density distribution color maps of the anonymous and Ihachi's beam carvings showed that there are two round core areas in the center part of the distribution. This characteristic of the shape of the density distribution of Ihachi shows that the orientations of the surfaces in Ihachi's beam carving concentrate on two specific

directions: the normal directions of flat plane of the beam and another direction tilting downward in about 30 degrees to match the viewer's sight. While in the density distribution color maps of Yoshimitsu's beam carvings, core area is in a round shape, surrounded by several concentric circle areas. This characteristic of the shape indicates that the surfaces in Yoshimitsu's beam carvings orients to directions in variation. According to the comparison of between the density distribution maps of beam carvings, the anonymous beam carving has a similar style characteristic to
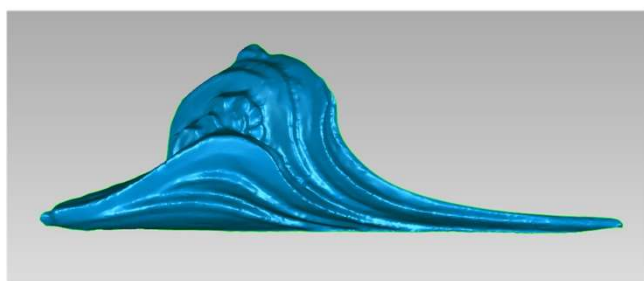
Wave Carving of Oyamaji
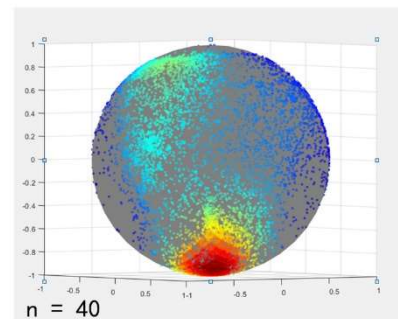
n = 40
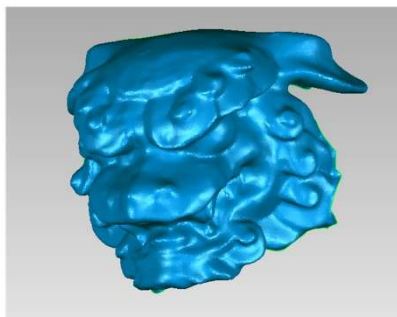
Kibana Lion of Oyamaji
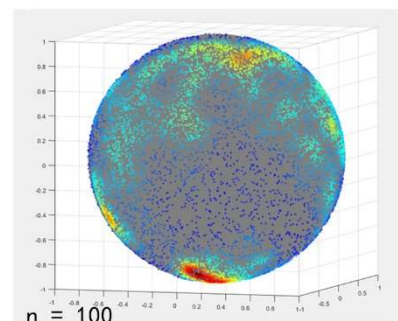
n = 100

Beam Carving of Shinkoji
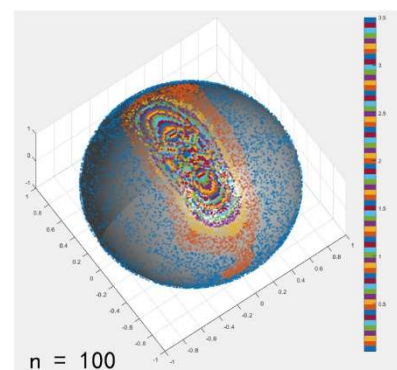
n = 100

Figure 8-1 Ihachi: Orientations of surfaces concentrating on specific directions
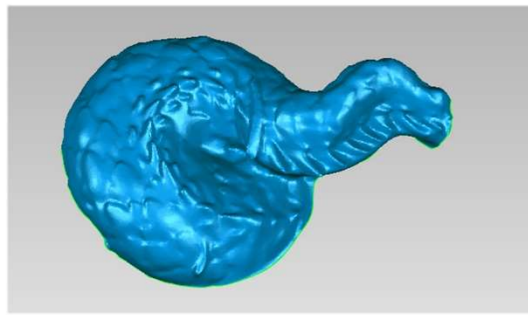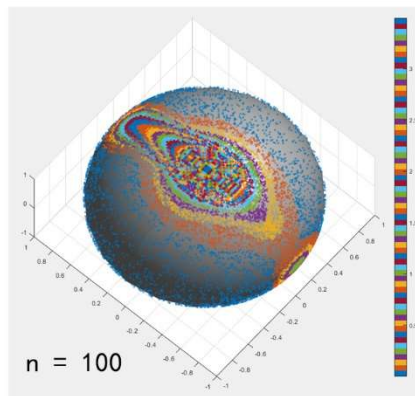
Dragon tail of Tsuruya Hachimangu   n = 40
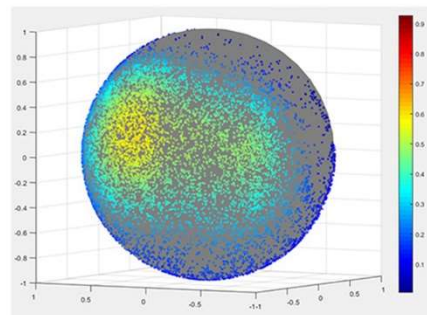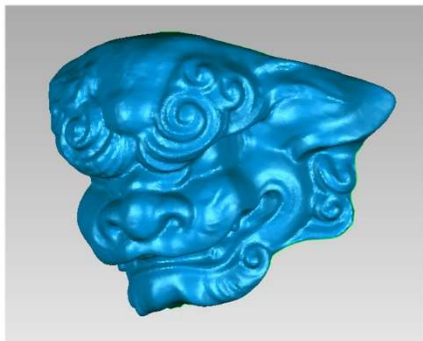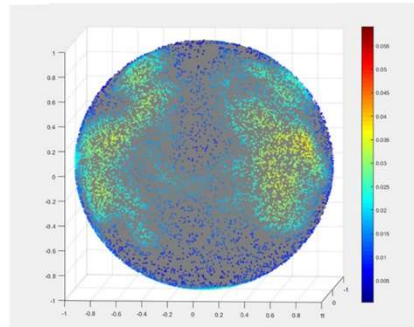
Kibana lion of Zenrinji   n = 100
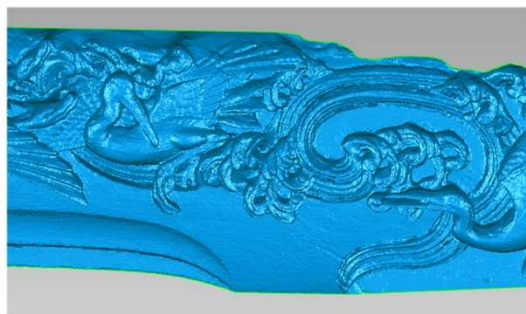
Beam Carving of Myohonji   n = 100

Figure 8-2 Yoshimitsu: Orientations of surfaces relatively equally in varieties

Ihachi rather than Yoshimitsu.

8.4 Style Characteristics of the surfaces' orientations of Ihachi and Yoshimitsu

According to the density distribution color maps and the results of the linkage clustering of the end points of the facet normal vectors of the polygons, it was confirmed that for Ihachi's sculptures, the orientations of the surfaces mainly

concentration on specific orientations, while for Yoshimitsu's sculptures, the orientations of the surfaces distribute to directions in varieties relatively equally. These two style characteristics could be found in different themes of the two carvers' works, including the carvings of the pent roofs(向拝彫刻), the Kibana and the beam carvings(Figure 8-1,8-2).

8.5 Reasons for the differences in orientation distributions in the sculptures of Ihachi and Yoshimitsu

The distribution of the orientations of the surfaces might influence the mass and the volume of the sculpture. In the wave form of Ihachi Takeshi, the concentration in specific direction is caused by his sculpting technique of 2.5D laminating layers proceeding along the normal direction of the relief. In the 2.5D transforming process, Ihachi enhanced the visual depth of perspective by the laminating layers. In Ihachi's Kibana lion, the concentration of the directions of the surfaces towards the top, bottom, and left and right sides could also be considered as the result of 2.5D transformation based on the three-view sketches of the woodblock. In contrast, Yoshimitsu Goto's sculpting method is similar to the concept of mass and volume in Western sculpting. He consciously adjusts the overall sculpture from multiple angles to create the real mass and volume of the sculpture.

8.6 Future works

During the field survey of Ihachi and Yoshimitsu's works, there were usually difficulties during the identification of the anonymous works, even accompanied by specialists in art history and folklore. In the general methods of identification of temple and shrine sculptures as the 'theory of style' and the iconography, it is usually difficult to quantify the similarity and the difference of the style characteristics between the different sculptures. In the future study, more quantification and

visualization analysis will applied to the identification of the anonymous works as an assistance technique. And other geometrical elements such as curves for the new form analysis of the style characteristics will analyzed as the new index to evaluate the style characteristics of the forms of the historical artifacts.

Acknowledgment

Appendices

## Appendix 1.   Manual of the quantification of the style characteristics

1. Repair the original model and generate the Curvature Map (Geomagic Studio 2013)

Before starting quantitative analysis of the original model, it is recommended to apply the
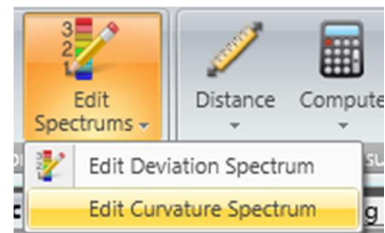

automatic repair by [Mesh Doctor] under 'Polygon' column to fix the geometrical errors such as spikes, holes and self-intersections.

After the geometrical repair by Mesh Doctor, either [Exact Surfacing] under 'Exact
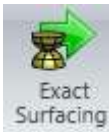
Surface' column or [Parametric Surfacing] under

'Parametric Surface' column could

activate the [Edit Spectrums]-[Edit Curvature Spectrums] under Analysis column. The curvature spectrum map could be generated by the [Edit Curvature Spectrums] (Figure A-1).

Click [Convert to Polygons] under 'Exact/Parametric Surface' column could quit the Surfacing model and reactivate the functions under 'Polygon' column.
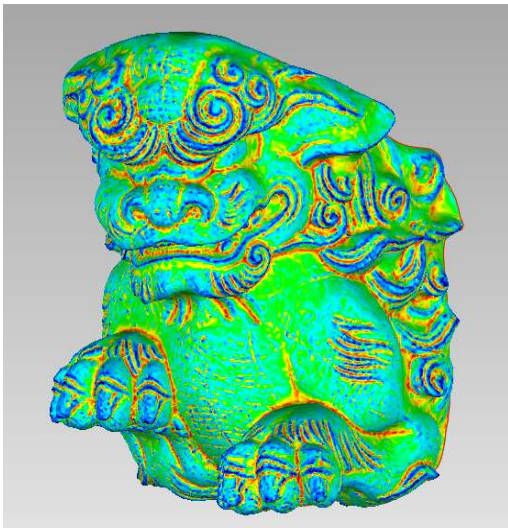

Figure A-1 Color Spectrum Map of Yoshimitu's lion

2. Cut out the Style Characteristic Part from the Model(Geomagic Studio 2013)

The part of the form with style characteristics could be cut out by [**Trim**] under 'Polygon' Column with planes, curves and sheets.

The form is basically cut along the concave/convex areas with high curvatures, which are marked in red and blue in the curvature spectrum map(Figure A-2). Since the curvature map could not be checked in the edit mode of [**Trim**], the result of the curvature map should be saved in various angles as the reference of cutting.

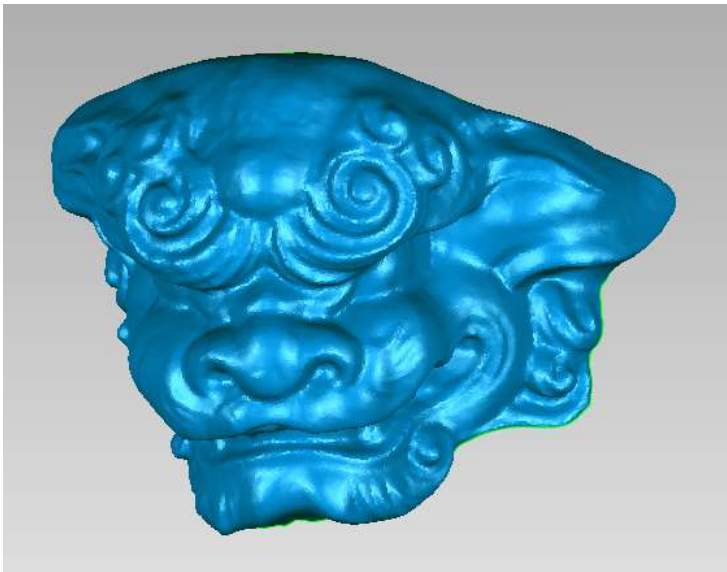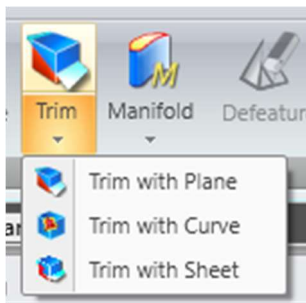The cut-out form should be saved as 'STL(ASCII)' format.

Figure A-2 Cut-out form of Yoshimitu's lion

3. Decimate the polygon number and Unify the shape of polygon(Geomagic 2013)

[**Refine-Remesh**] under 'Polygon' column provides the decimation and unification functions of original polygons to regular triangle with same edge length to the original high-resolution polygon model.

The proper percentage of the decimation of the polygon number should be determined according to the result of [**Deviation**] under 'Analysis' column. The [Deviation] function calculates the Average Deviation and the RMS (Root Mean Square) estimate of the shortest distance from the vertex on the decimated model (target) to any point on the surface of the original model (reference). Average Deviation and RMS of various percentage of the decimation could be plotted in Matlab or Excel to confirm the change of the deviation with the variation of the decimation percentage (Figure A-3).

Since decimation percentage could not be defined in the edit mode of [Remesh], the polygon number of the original model should be confirmed at the left-bottom side of the
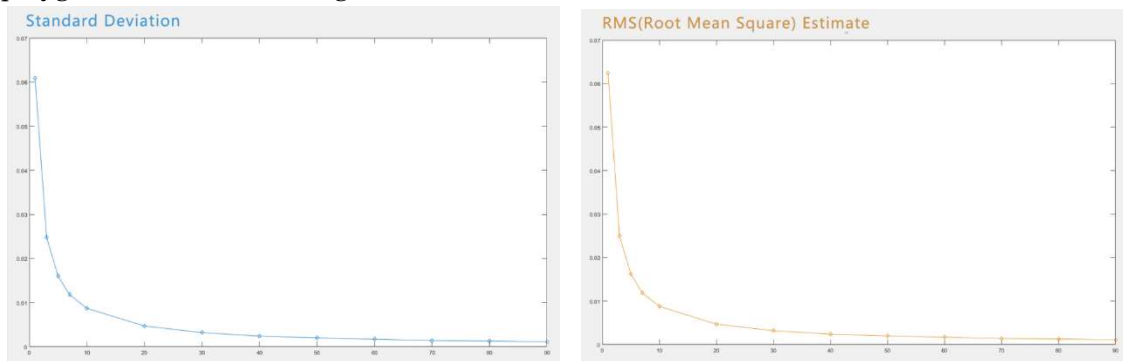

Figure A-3 Standard Deviation and RMS estimate of the decimated model

workspace in Geomagic Studio 2013, and the polygon number of a selected decimation percentage should be calculated. Then various values of the 'Target Edge Length' are tested to reach the polygon number of the selected percentage (Figure A-4).

129
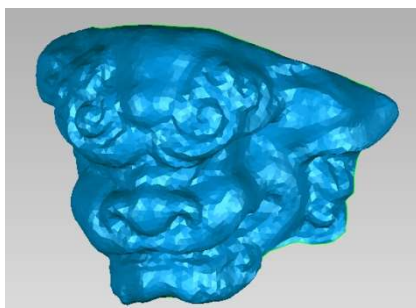
Figure A-4 Decimated Model of 10000 polygons

4. Extract the End points of facet normal vectors of the polygons (R-Studio)

According to the structure of STL (ASCII) format, the Euclidean coordinates of the End points of facet normal vectors could be extracted in R-Studio with codes below:

```
STLEDP<-read.delim("STLEDP.txt", header=F,sep=" ",
                    as.is=c(TRUE,TRUE),strip.white=FALSE,fileEncoding="UTF-8")
out<-data.frame("name","p1","p2","p3")
names(out)<-c("name","p1","p2","p3")
for(i in 1:dim(STLEDP)[2]){
  STLEDP[,i]<-as.character(STLEDP[,i])
}
for(i in 1:dim(STLEDP)[1]){
  if(STLEDP[i,1]=="facet"){
    out<-rbind(out,data.frame(name="facet",p1=STLEDP[i,3],p2=STLEDP[i,4],p3=STLEDP[i,5]))
  }
}
write.csv(out,"STLEDP.csv")


#--------------------------------------------------------------------
Groupcsv<-read.csv("budongtangyiba.csv")
for(i in 1:dim(Groupcsv)[2]){Groupcsv[,i]<-as.character(Groupcsv[,i])}


Fullstl<-read.delim("youmubi-head ihachi-simp.txt", header=F,sep=" ",
                    as.is=c(TRUE,TRUE),strip.white=FALSE,fileEncoding="UTF-8")
#class(Fullstl[3,3])
#substr("abcdef", 2, 4)
```

```
#----------------------------------------------------------------------

indexstl<-data.frame("i","p1")

for(i in 1:dim(indexstl)[2]){indexstl[,i]<-as.character(indexstl[,i])}

for(i in 1:10024){indexstl[i,1]<-as.character(7*i-5)

indexstl[i,2]<-paste(substr(Fullstl[7*i-5,3],1,8),substr(Fullstl[7*i-5,4],1,8),substr(Fullstl[7*i-5,5],1,8))

#indexstl[i,2]<-substr(Fullstl[7*i-5,3],1,8)

#indexstl[i,3]<-substr(Fullstl[7*i-5,4],1,8)

#indexstl[i,4]<-substr(Fullstl[7*i-5,5],1,8)

}

#length(unique(indexstl[,2]))==length(indexstl[,2])

#indexstl[,2][duplicated(indexstl[,2])]

#----------------------------------------------------------------------

label<-c("22")

tem<-c("")

temtable<-Groupcsv[Groupcsv[,6]==label,]

temtable<-temtable[c(3,4,5)]

tem<-as.character(c(1:(dim(temtable)[1]-1)))

for(i in 1:length(tem)){tem[i]<-

paste(substr(temtable[i+1,1],1,8),substr(temtable[i+1,2],1,8),substr(temtable[i+1,3],1,8))}


length(unique(tem))

outstl<-data.frame("Y1","Y2","Y3","Y4","Y5")

for(i in 1:dim(outstl)[2]){outstl[,i]<-as.character(outstl[,i])}

outstl[1,]<-c("solid", "WRAP","","","")

tem2<-data.frame("Z1","Z2","Z3","Z4","Z5")
```

```
for(i in 1:length(tem)){

  temIndex<-as.numeric(indexstl[indexstl[,2]==tem[i],1])

  if(!identical(temIndex,numeric(0))){

  tem2<-Fullstl[c(temIndex:(temIndex+6)),]

  names(tem2)<-names(outstl)

  outstl<-rbind(outstl,tem2)}

}

outstl<-rbind(outstl,c("endsolid","WRAP","","",""))


write.table(outstl,file = paste("stlgroup",label,"-",i,".stl", sep=""), quote = FALSE, row.names = FALSE,

col.names = FALSE)
```

Process:

1) Before the extraction, it is recommended to build a new folder with alphabet directions only (No Kanji or Hiragana / Katakana) and an empty txt file named STLEDP. Open the STL file of the decimated model and copy the contents to the new empty txt file.

2) Set the Working Directory to the new folder in 'Session-Set Working Directory-Choose Directory'
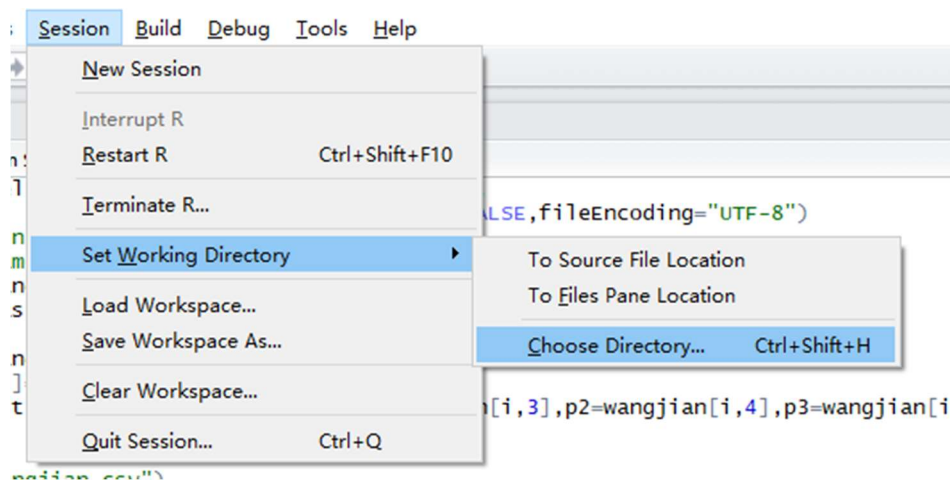
3) Select Row 1-2 of the code and click 'Run' to import the STL file.


```
1  STLEDP<-read.delim("STLEDP.txt", header=F,sep=" ",
2                     as.is=c(TRUE,TRUE),strip.white=FALSE,fileEncoding="UTF-8")
```

When the import of the data finished, select Row 1-13

(Row 13 should be 'write.csv(out,STLEDP.csv")') and click 'Run' again.

It will take some time, which is according to the size of the STL file.

4) When finished, the Console Workspace in the left-down side of R-studio will show the hint 'write.csv(out,STLEDP.csv")'.

A new csv-format file with all Euclidean coordinates of End points should be generated

	A	B	C	D	E
		Yoshilionface10000			
	VarName1	name	p1	p2	p3
	数値　▼	分類　▼	数値　▼	数値　▼	数値　▼
1		name	p1	p2	p3
2	1	name	p1	p2	p3
3	2	facet	-0.843413...	-0.285211...	0.4553102...
4	3	facet	-0.478462...	-0.070918...	-0.875239...
5	4	facet	-0.349803...	0.6294853...	0.6938196...
6	5	facet	-0.054510...	0.3676062...	-0.928382...
7	6	facet	-0.486458...	0.4352672...	-0.757561...
8	7	facet	-0.577784...	0.4997761...	0.6452824...

Figure A-5 csv-format Euclidean coordinates of End points

5. Plot the end points distributed on unit sphere (Matlab)

5.1 Plot the non-colored distribution of the end points

Import the csv-format file with [Import Data] in 'Matrix' mode in Matlab, select the three columns of x-y-z coordinates of the end points and import. It should be seen on the right side of the workspace. Rename the matrix as 'X'.

Plotting code is shown as below:

```
scatter3(X(:,1),X(:,2),X(:,3),5)

hold on;

sphere;

camlight,lighting gouraud;
```

This code plots the distribution of the end points with non-color marked and adds a unit sphere as reference (Figure A-6).
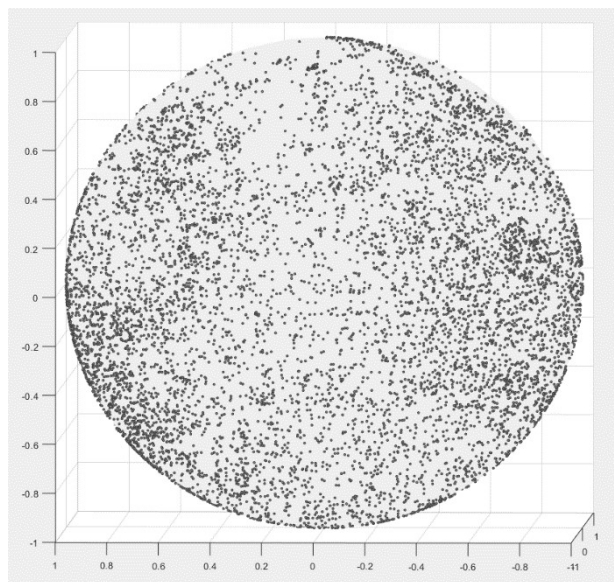

Figure A-6 Distribution of End points of Yoshimitu's lion face (non-colored)

5.2 Generate the reference points with equal intervals on the unit sphere (Python)
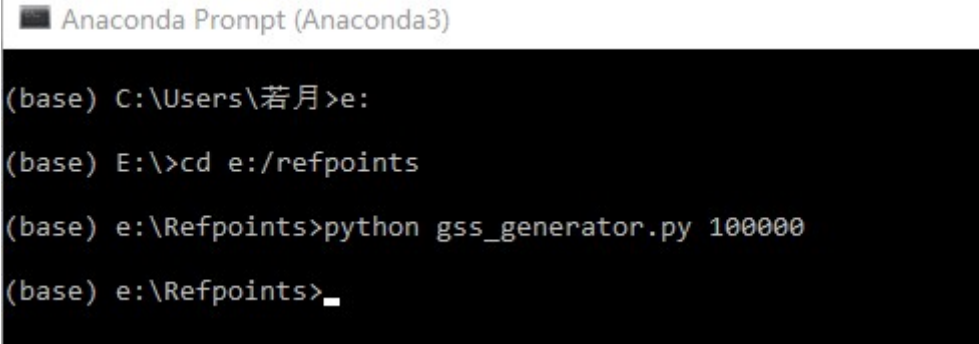
Based on Atsushi Yamaji's GSS Generator code in pas-format, the code to generate the reference points with equal intervals on the unit sphere in Python by Jakalada on github.

The coordinates of the reference points could be directly generated in Python in Linux OS, while for the Windows OS users, the generating process is shown as below:

1) Install Python for Windows and Anaconda 3

2) Open Anaconda Prompt (Anaconda 3) and copy the Python file with the code contents of GSS generator above to the folder that you want to save the reference points file. For example, here we create a new folder 'Refpoints' under E:/

The Python file could be named gss_generator (or anything you like, whatever)

Use commend 'E:' and then 'cd E:/Refpoints' to jump to the new folder in Anaconda Prompt.

3) Type in 'python gss_generator n' to run the generating program in Python, n is the number of the reference end points that you want.

4) Wait for a few minutes and the Euclidean coordinates and Spherical coordinates of the reference end points saved in CSV-format will be generated in E:/Refpoints folder, which

could be import directly into Matlab.

5.3 Plot the distribution color map according to the kernel estimated density (Matlab)

Import the x-y-z coordinates of the end points of the decimated form and the reference points from the .csv files in Matlab. Name the matrix of decimated form as 'X' and the reference points as 'Y'. Then Open 'histcnd.m' in Matlab to activate the N-dimensional histogram algorism.

The code to plot the distribution color map according to the kernel estimated density revised by the reference points with equal intervals is shown as below:

```
edge = linspace(-1,1,n); % change here to your need;

[county, ~, ~, loc] = histcn(Y,edge,edge,edge);

[countx, ~, ~, loc] = histcn(X,edge,edge,edge);

count = countx./county;

count(find(isnan(count)==1)) = 0

count(find(count==inf))=0;

kernel = exp(-linspace(-1,1,20).^2);

K = 1;
```

```
for k=1:3

    K = K(:)*kernel;

end

K = reshape(K,length(kernel)+[0 0 0 ]);

K = K/sum(K(:));

count = convn(count, K,'same');


density= zeros(size(X,1),1);

valid = all(loc,2);

loc = loc(valid,:);

density(valid) = count(sub2ind(size(count),loc(:,1),loc(:,2),loc(:,3)));


scatter3(X(:,1),X(:,2),X(:,3),5,density)

colormap(jet)

colorbar

hold on;
```

In Row 1, parameter n marked in red is the number of the bins+1 that you determined.
The Bandwidth of the bin = 2 / (n-1).

After the distribution color map is generated, the max estimated density could be
confirmed in the edit mode of the color bar.

Right click the max density value in the edit mode of the color bar, and switch to the
workspace of Matlab, type

```
sphere;

camlight,lighting gouraud;
```

(This process keeps the max density of end points without being changed by adding a unit

sphere.) And the distribution color map is shown as below (Figure A-7):
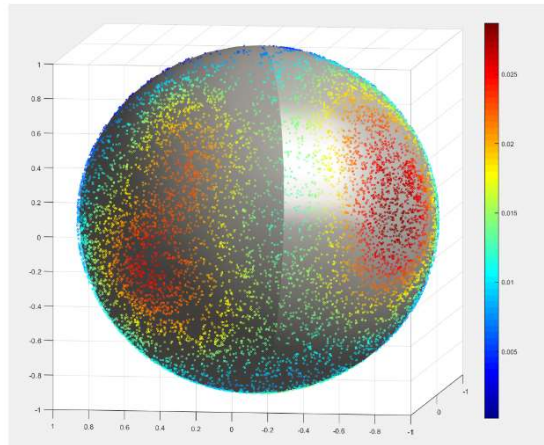
Figure A-7 Distribution color map of End points of Yoshimitsu's lion face

Codes to check the errors in the data are listed as below:

```
X(all(X==0,2),:) = [];          %remove the empty row in matrix 'X'

X(all(X==0,1),:) = [];          %remove the empty column in matrix 'X'

count(find(isnan(count)==1)) = 0;     %replace the 'Nan' elements in matrix 'count' to '0'

count(find(count==inf))=0;               % replace the 'Inf' elements in the matrix 'count' to '0'

max(max(count));                         %find the maximum element in matrix 'count'

min(min(count));                         %find the minimum element in matrix 'count'

sum(count(:)==inf);          %find the number of inf element in matrix 'count'

[i,j,z]=ind2sub(size(count),find(count==inf)); %find the locations of inf elements in 'count'
```

Code to calculate the variation of non-zero numbers of all Bin (model)/Bin (ref)

```
edge = linspace(-1,1,10); % change here to your need;

[county, ~, ~, loc] = histcn(Y,edge,edge,edge);

[countx, ~, ~, loc] = histcn(X,edge,edge,edge);

count = countx./county;

count(find(isnan(count)==1)) = 0

count(find(count==inf))=0;

count(count==0) = NaN;

b = count(:)

c = nonzeros(b);

d =  (c(1,:)-mean(c)).^2

var=sum(d)/length(c)
```

5.4 Linkage clustering of the coordinates of End points of facet normal vectors (Matlab)

Code to generate the index of each element and clusters in the dendrogram tree is shown as below:

1) For matrix 'X' (3 columns) is the Euclidean coordinates of the end points of facet normal vectors.

```
Z = linkage(X,'ward','euclidean');
```

'ward' and 'euclidean' could be changed to other method, which could be checked in the introduction of 'Linkage' commend in Matlab.

2) For matrix 'C' (3 columns) is the Spherical coordinates of matrix 'X'

Code to transform 'X' to 'C' and generate index 'Z' is as below:

```
x = X(:,1);

y = X(:,2);

z = X(:,3);

[azimuth,elevation,r] = cart2sph(x,y,z);

C = [azimuth,elevation,r];

Z = linkage(C,'ward','euclidean');
```

3) The structure of index 'Z'

According to the explanation of 'Linkage' commend in Matlab, Z is a matrix of 3 columns(Figure A-8). The first and second columns shows the index of the end points and the clusters in the dendrogram. For a point cloud with n points, the index of the points is from 1 to n, and the clusters connected by these points are marked as n+k. The third column shows the distance between the two points/clusters with index in the same row.

Figure A-8 Structure of Index 'Z'

4) **Cut the Dendrogram and generate the dendrogram tree**.

After Z is generated, the code to cut the dendrogram tree and mark the points which cluster it belongs to is shown as below.

a. Cut the tree above a determined distance between two clusters (the height of Y axis, for example: 1).

T = cluster(Z,'cutoff',1,'Criterion','distance');

b. Cut the tree at a determined number of clusters (for example: 30).

T = cluster(Z,'maxclust',30);

Either of these two methods will generate a one-column matrix 'T', which shows the index of the cluster that the point belongs to. The dendrogram tree could be generated by code shown below:
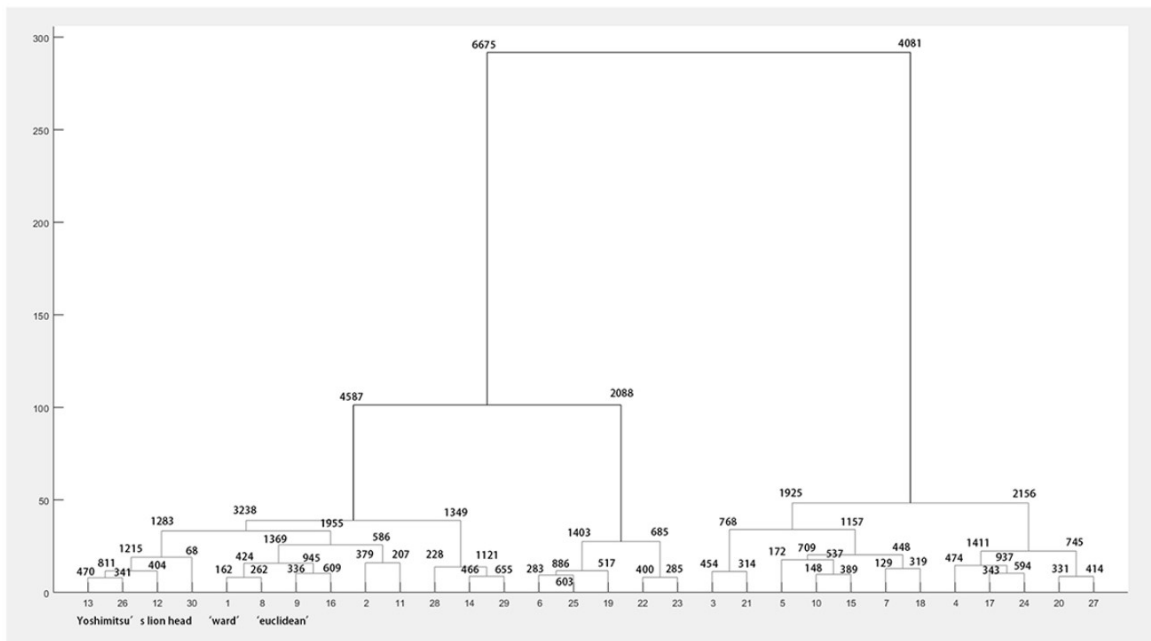
Figure A-9   Dendrogram Tree of cluster distance above 1 of Yoshimitsu's lion face

a. at certain distance(Figure A-9)

confirm the clusters at the certain distance and use code of b.

b. with a determined number of clusters

```
dendrogram(Z,30)
```

5) Plot the result of linkage clustering according to the Cut distance/Determined Cluster number (Shown by matrix 'T')

Code to plot the distribution with colors is shown as below (Figure A-10):

```
scatter3(X(:,1),X(:,2),X(:,3),10,T);

hold on;

sphere;
```

camlight,lighting gouraud;
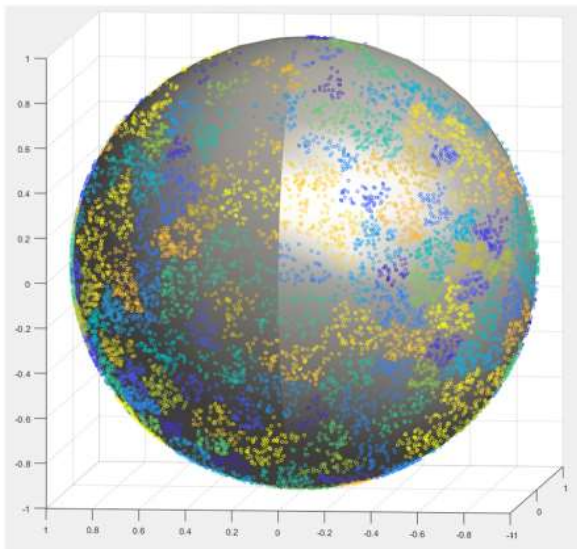
Figure A-10   Distribution color map with Cluster-distance above 1 of Yoshimitsu's lion face

Code to check the number of the points in each cluster according to the result of 'T'

If matrix 'T' is generated according to a certain number of clusters or a certain cluster-distance, the code to check the number of the points in each cluster is shown as below:

```
M = [X T];

groupIndexes = findgroups(T)

% Make clusters as a cell array because every group might have a different number of members.

for k = 1 : max(groupIndexes)

        thisGroupRows = groupIndexes == k;

        groupValues{k} = M(thisGroupRows, 2);

end

celldisp(groupValues)
```

Python Code of GSS by Jakalada on github

```python
#!/usr/bin/env python
# coding: utf-8


'''参考文献に記載されている Delphi のコードの移植版


Notes
-----
参考文献: 多数の点を球面上に一様分布させるソフトウェア GSS Generator
https://www.jstage.jst.go.jp/article/geoinformatics/12/1/12_1_3/_article/-char/ja/


Examples
--------
# 600 個の点を生成
$ python gss_generator.py 160
'''


from __future__ import division, absolute_import, print_function


import csv
import sys


import numpy as np
import matplotlib.pyplot as plt
from mpl_toolkits.mplot3d import Axes3D
```

```python
def generate_gss(n):
    '''一般化螺旋集合を生成する

    Parameters
    ----------
    n : int
        生成する一般化螺旋集合の点数

    Returns
    -------
    ndarray
        一般化螺旋集合
        生成された天底の点から天頂の点までの球面座標の配列
    '''
    # [[colatitude, longitude], ...]
    gss = np.zeros((n, 2))

    # 天底の点の座標を代入
    gss[0][0] = np.pi
    gss[0][1] = 0.0

    # 天底-天頂間に含まれる点の座標を順に算出
    for index in range(1, n - 1):
        # 参考資料に記載の Delphi のコードでは計算式における k を
```

```
    # そのまま配列インデックスとして使用するため,
    # 配列サイズを+1 として先頭要素は使用せず他関数でも無視されている.
    # 紛らわしいため, このコードでは配列インデックスと k を区別する.
    k = index + 1


    # 参考資料 第(1)式
    # 第(2)式と第(3)式が依存しているパラメータの算出
    hk = -1.0 + 2.0 * (k - 1.0) / (n - 1.0)


    # 参考資料 第(2)式
    # 余緯度の算出
    gss[index][0] = np.arccos(hk)


    # 参考資料 第(3)式
    # 経度の算出
    prev_lon = gss[index - 1][1]
    lon = prev_lon + 3.6 / np.sqrt(n) / np.sqrt(1.0 - hk * hk)
    # 参考資料に記載の Delphi のコードでは経度の値は
    # 増加するままとしているが点数が増えた場合の浮動小数点数の精度に
    # 不安があるため丸め込む
    gss[index][1] = lon % (np.pi * 2)


# 天頂の点の座標を代入
gss[n - 1][0] = 0.0
gss[n - 1][1] = 0.0
```

```python
        return gss


def spherical2cartesian(coord):
    '''球面座標を直交座標に変換する


    Parameters
    ----------
    spherical_coord : array_like
        天底の点から天頂の点までの球面座標の配列


    Returns
    -------
    cartesian_coord : ndarray
        直交座標(x, y, z)
    '''
    col = coord[0]
    lon = coord[1]
    x = np.sin(col) * np.cos(lon)
    y = np.sin(col) * np.sin(lon)
    z = np.cos(col)
    return np.array([x, y, z])


def cartesian2spherical(coord):
    '''直交行座標を直交座標に変換する
```

Parameters

----

cartesian_coord：array_like

　　直交座標(x, y, z)

Returns

----

spherical_coord：ndarray

　　球面座標(余緯度, 経度)

"""

x = coord[0]

y = coord[1]

z = coord[2]

colat = np.arccos(z / np.sqrt(x * x + y * y + z * z))

lon = np.arctan2(y, x)

return np.array([colat, lon])

def relocate(gss):

　　"""天頂と天底の点の座標を一様性が増すように調整する

　　Parameters

　　----------

　　gss：array_like

　　　　一般化螺旋集合

Returns

----

relocated_gss：ndarray

　　天頂と天底の点の座標が調整された一般化螺旋集合

'''

```
# 資料に第(4)式と第(5)式に当たるが 5 での除算が
# 資料に記載の Delphi のコードでは行われておらず単なる総和になっている.
# ただし, 5 での除算を加えて平均の結果を確認したところ
# 5 点の直交座標の平均と総和の結果は異なるが,
# それらを球面座標に変換した結果は同じなので問題ない.
n = len(gss)
relocated_gss = np.array(gss)


# 天頂と天底の周囲の 5 点の座標の配列インデックス
index_of_five_points = np.array([1, 2, 4, 5, 6])


# 天底の点の座標を調整
spherical_coords_for_nadir = gss[index_of_five_points]
cartesian_coords_for_nadir = np.array(
    [spherical2cartesian(c) for c in spherical_coords_for_nadir])
cartesian_coords_mean_for_nadir = cartesian_coords_for_nadir.sum(axis=0)
relocated_gss[0] = cartesian2spherical(cartesian_coords_mean_for_nadir)


# 天頂の点の座標を調整
spherical_coords_for_zenith = gss[n - (index_of_five_points + 1)]
```

```python
    cartesian_coords_for_zenith = np.array(

        [spherical2cartesian(c) for c in spherical_coords_for_zenith])

    cartesian_coords_mean_for_zenith = cartesian_coords_for_zenith.sum(axis=0)

    relocated_gss[-1] = cartesian2spherical(cartesian_coords_mean_for_zenith)


    return relocated_gss



def save_scatter2d(gss, filename):
    # 下半球に含まれる点のみを抽出

    n = 0

    for coord in gss:

        if coord[0] <= np.pi * 0.5:

            n += 1

    gss_of_hemisphere = gss[0:n]


    # 直交座標に変換

    cartesian_coords = np.array(

        [spherical2cartesian(c) for c in gss_of_hemisphere])


    # グラフを作成

    plt.figure(figsize=(6, 6))


    # 値の範囲

    plt.xlim((-1.1, 1.1))

    plt.ylim((-1.1, 1.1))
```

```python
    # 散布図を描画

    plt.scatter(

        x=cartesian_coords.T[1],

        y=cartesian_coords.T[0],

        c='k',

        s=3)


    # 散布図を画像ファイルとして保存

    plt.savefig(filename)

    plt.close()



def save_scatter3d(gss, filename):

    # 直交座標に変換

    cartesian_coords = np.array(

        [spherical2cartesian(c) for c in gss])


    # グラフを作成

    figure = plt.figure(figsize=(6, 6))

    ax = Axes3D(figure)


    # 値の範囲

    ax.set_xlim(-1.1, 1.1)

    ax.set_ylim(-1.1, 1.1)

    ax.set_zlim(-1.1, 1.1)
```

```python
    # 3D の散布図を描画
    ax.scatter3D(
        cartesian_coords.T[0],
        cartesian_coords.T[1],
        cartesian_coords.T[2])


    # 3D の散布図を画像ファイルとして保存
    plt.savefig(filename)
    plt.close()



def save_cartesian(gss, filename):
    # 直交座標に変換
    cartesian_coords = np.array([spherical2cartesian(c) for c in gss])
    with open(filename, 'w') as f:
        writer = csv.writer(f)
        for coord in cartesian_coords:
            writer.writerow(coord)



def save_spherical(gss, filename):
    with open(filename, 'w') as f:
        writer = csv.writer(f)
        for coord in gss:
            writer.writerow(coord)
```

```python
if __name__ == '__main__':

    if len(sys.argv) < 2:

        sys.stderr.write('n argment is required\n')

        sys.exit(1)


    try:

        n = int(sys.argv[1])

    except ValueError:

        sys.stderr.write('%s is illegal argment\n' % sys.argv[1])

        sys.exit(1)


    if (n < 20):

        sys.stderr.write('%s is lower than 20\n' % sys.argv[1])

        sys.exit(1)


    # 一般化螺旋集合を生成

    gss = generate_gss(n)


    # 天頂と天底の座標を調整した一般化螺旋集合を生成

    relocated_gss = relocate(gss)


    # 2D の散布図を画像ファイルとして保存

    # 下半球を天底方向から眺めた様子

    save_scatter2d(gss, 'gss.png')
```

```
save_scatter2d(relocated_gss, 'relocated_gss.png')


# 3D の散布図を画像ファイルとして保存
# 球全体を眺めた様子
save_scatter3d(gss, 'gss_3d.png')

save_scatter3d(relocated_gss, 'relocated_gss_3d.png')


# すべての点の球面座標を CSV ファイルとして保存
save_spherical(gss, 'gss_spherical_coords.csv')

save_spherical(relocated_gss, 'relocated_gss_spherical_coords.csv')


# すべての点の直交座標を CSV ファイルとして保存
save_cartesian(gss, 'gss_cartesian_coords.csv')

save_cartesian(relocated_gss, 'relocated_gss_cartesian_coords.csv')
```

Appendix 2. Words and phrases in English and Japanese

Unlike the field of engineering and computer graphics, the words and phrases of the styling design sometimes are not defined in specific names, and the terms of the Japanese historical people, places, books might be hard to understand in the spelling of the pronunciation by alphabets. To avoid the misunderstanding of the phrases in this paper, a part of the terms of the styling design and sculpting are listed below as the reference. And the Kanji are attached to the specific Japanese words in the paper.

Styling design	造形デザイン
Style Characteristics	形態特徴
Three-dimensional sense	立体感
3D composition	立体構成
2D composition	平面構成
Carver	彫物大工
Tensity of the form	造形の張り（緊張感）